TIM 2023 Los Alamos Workshop on Time Integration for Multiphysics

Adaptive time integration procedures for solving PDEs

UFJF
Universidade Federal de Juiz de Fora

Prof. Delfim Soares Jr.
Structural Engineering Department
Federal University of Juiz de Fora

Objectives

This presentation aims to report and discuss some explicit, implicit, explicit/explicit, explicit/implicit, semi-explicit/explicit time integration procedures to numerically analyse large scale problems that are governed by space-time partial differential equations.

The time integration procedures that are discussed here are adaptive, locally adjusting themselves according to the physical properties of the model, the adopted spatial discretization, the adopted time-step value, and the evolution of the computed responses.

These solution procedures are also entirely automated, automatically dividing the spatial domain of the model into different subdomains, at which different solution strategies are applied, as well as automatically computing the time-step values of the analyses for optimal computational performance.

Illustration of a time integration procedure adapting itself according to the properties of the discretized model and its computed responses

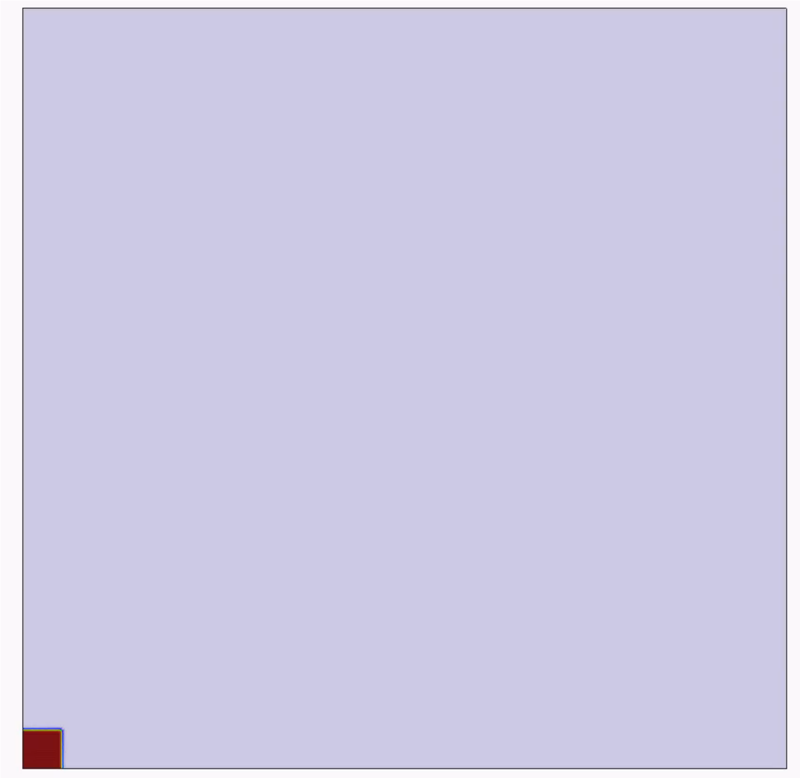

Computed solution

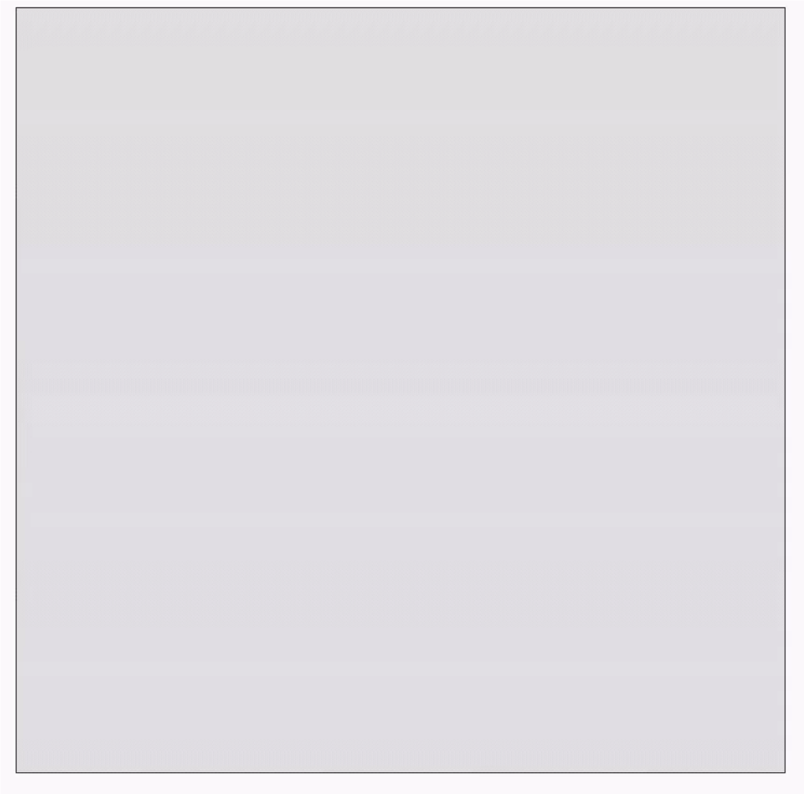

Time integration parameters

Illustration of automated subdivisions of a model for the application of different time integration strategies

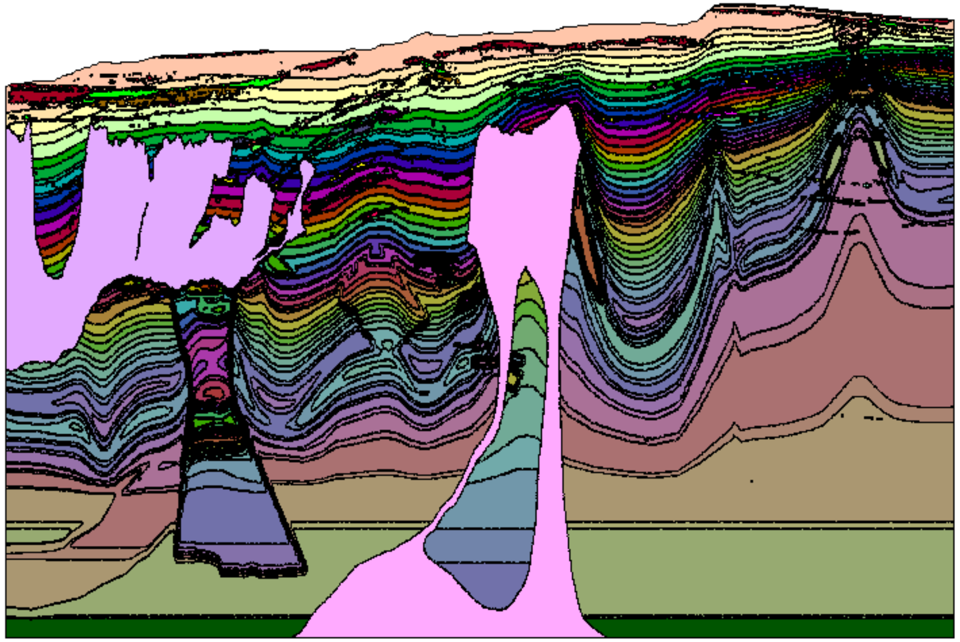

Model with different physical properties

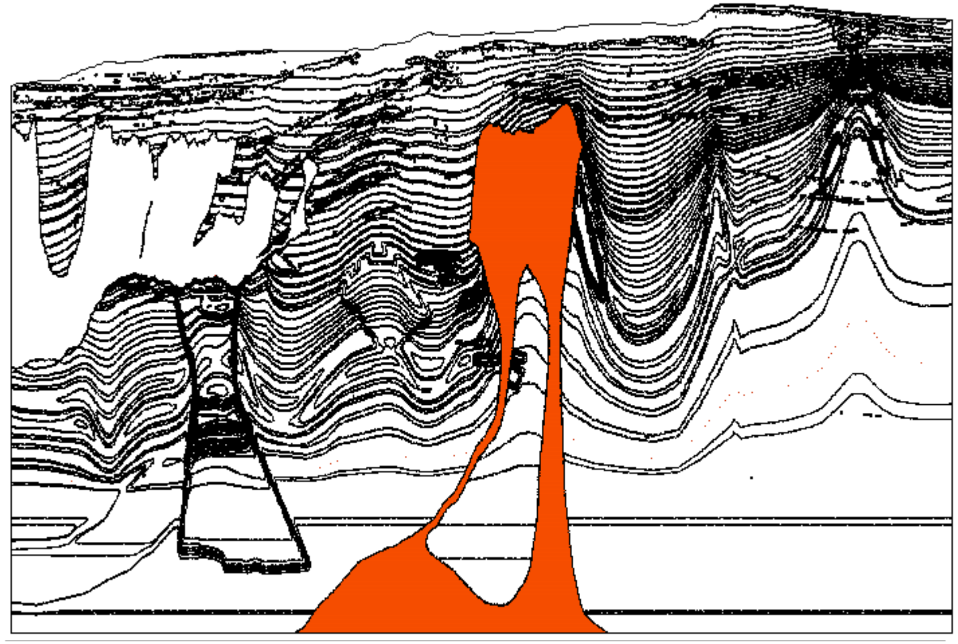

Subdivision for explicit/implicit analyses
Subdivision for explicit/explicit analyses

Discussion concerning time-stepping algorithms

When numerically solving space-time PDEs, the adopted time integration procedure should become consonant with the adopted spatial discretization methodology, so that their errors may be properly counterbalanced.

A proper “adaptation” of the applied time integration procedure to the employed spatial discretization may provide much better results than more elaborated and/or higher-order time-domain formulations.

Discussion concerning time-stepping algorithms

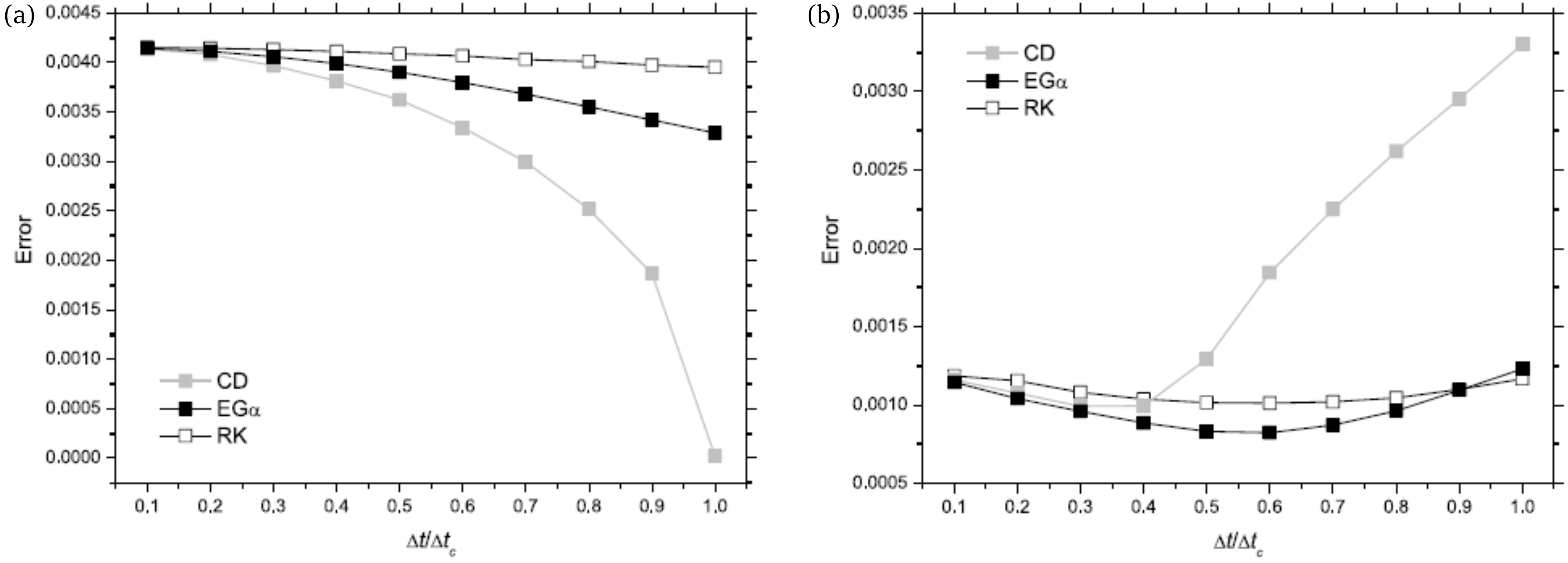

Convergence curves for a simple 1D wave propagation analysis considering a regular finite element mesh and three standard explicit time-marching techniques: (a) adopting linear finite elements; (b) adopting quadratic finite elements.

Basic framework to introduce some adaptive time integration procedures

Once a spatial discretization technique is applied, the governing PDEs of a problem may be numerically treated to become a semi-discrete system of equations. In order to discuss the use of the referred adaptive time integration procedures, the following hyperbolic system of equations is here initially considered, which may be obtained once wave propagation models are discretized considering the Finite Element Method (FEM).

PDEs for some wave propagation models:
(with index notation)

Acoustic models

$$(Kp_{,i})_{,i} - \rho \ddot{p} - \xi \dot{p} + S = 0$$

+ boundary and initial conditions

Elastodynamic models

$$\sigma_{ij,j} - \rho \ddot{u}_i - \rho \zeta \dot{u}_i + \rho b_i = 0$$

$$\sigma_{ij} = \lambda \delta_{ij} \varepsilon_{kk} + 2\mu \varepsilon_{ij}$$

$$\varepsilon_{ij} = (u_{i,j} + u_{j,i})/2$$

+ boundary and initial conditions

By applying the FEM for spatial discretization: $\mathbf{M}\ddot{\mathbf{U}}(t) + \mathbf{C}\dot{\mathbf{U}}(t) + \mathbf{K}\mathbf{U}(t) = \mathbf{F}(t)$

where: $\mathbf{M}_e = \int_{\Omega_e} \mathbf{N}_e^T \rho_e \mathbf{N}_e d\Omega$ $\mathbf{C}_e = \int_{\Omega_e} \mathbf{N}_e^T \xi_e \mathbf{N}_e d\Omega$ $\mathbf{K}_e = \int_{\Omega_e} \mathbf{B}_e^T \mathbf{D}_e \mathbf{B}_e d\Omega$ ... $\int \mathbf{N}_e^T \mathbf{b}_e(t) d\Omega$

Basic framework to introduce some adaptive time integration procedures

By time integrating the referred semi-discrete matrix equation, at an element level (subscript e), considering a time-step Δt ($t^{n+1} = t^n + \Delta t$), the following expression can be established:

$$\mathbf{M}_e \int_{t^n}^{t^{n+1}} \ddot{\mathbf{U}}_e(t)dt + \mathbf{C}_e \int_{t^n}^{t^{n+1}} \dot{\mathbf{U}}_e(t)dt + \mathbf{K}_e \int_{t^n}^{t^{n+1}} \mathbf{U}_e(t)dt = \int_{t^n}^{t^{n+1}} \mathbf{F}_e(t)dt$$

whose integrals may be evaluated as:

$$\int_{t^n}^{t^{n+1}} \ddot{\mathbf{U}}_e(t)dt = \dot{\mathbf{U}}_e^{n+1} - \dot{\mathbf{U}}_e^n$$

$$\int_{t^n}^{t^{n+1}} \dot{\mathbf{U}}_e(t)dt = \mathbf{U}_e^{n+1} - \mathbf{U}_e^n$$

$$\int_{t^n}^{t^{n+1}} \mathbf{U}_e(t)dt = \Delta t\, \mathbf{U}_e^n + \tfrac{1}{2}\alpha_e^n \Delta t^2 \dot{\mathbf{U}}_e^n + \tfrac{1}{2}\gamma_e^n \Delta t^2 \dot{\mathbf{U}}_e^{n+1}$$

$$\overline{\mathbf{F}}_e = \int_{t^n}^{t^{n+1}} \mathbf{F}_e(t)dt$$

Basic framework to introduce some adaptive time integration procedures

By considering the previous integral definitions and the following relation:

$$\mathbf{U}^{n+1} = \mathbf{U}^n + \tfrac{1}{2}\Delta t\dot{\mathbf{U}}^n + \tfrac{1}{2}\Delta t\dot{\mathbf{U}}^{n+1}$$

the previously described, locally-defined, integral equation may be rewritten as:

$$(\mathbf{M}_e + \tfrac{1}{2}\Delta t\mathbf{C}_e + \tfrac{1}{2}\gamma_e^n\Delta t^2\mathbf{K}_e)\dot{\mathbf{U}}_e^{n+1} = \overline{\mathbf{F}}_e + (\mathbf{M}_e - \tfrac{1}{2}\Delta t\mathbf{C}_e)\dot{\mathbf{U}}_e^n - \Delta t\mathbf{K}_e(\mathbf{U}_e^n + \tfrac{1}{2}\alpha_e^n\Delta t\,\dot{\mathbf{U}}_e^n)$$

These equations allow to compute $\dot{\mathbf{U}}^{n+1}$, once assembling is considered, and $\mathbf{U}^{n+1}$, defining the recurrence relationships for a simple, single-step, truly self-starting, time-marching procedure.

Basic framework to introduce some adaptive time integration procedures

The basic properties of the method can be studied considering the features of its amplification matrix, regarding a SDOF model.

SDOF model:

$$\ddot{u}(t) + 2\xi w\,\dot{u}(t) + w^2 u(t) = f(t),$$

Recurrence relationship for the time-integration method:

$$\begin{bmatrix} u^{n+1} \\ \dot{u}^{n+1} \end{bmatrix} = \begin{bmatrix} A_{11} & A_{12} \\ A_{21} & A_{22} \end{bmatrix} \begin{bmatrix} u^{n} \\ \dot{u}^{n} \end{bmatrix} + \begin{bmatrix} L_{11} & L_{12} \\ L_{21} & L_{22} \end{bmatrix} \begin{bmatrix} f^{n} \\ f^{n+1} \end{bmatrix} = \mathbf{A} \begin{bmatrix} u^{n} \\ \dot{u}^{n} \end{bmatrix} + \mathbf{L} \begin{bmatrix} f^{n} \\ f^{n+1} \end{bmatrix}$$

Amplification matrix and load operator vector:

$$A_{11} = \left[1 + \xi w \Delta t + \frac{1}{2}(\gamma - 1) w^2 \Delta t^2\right] / A_0$$

$$A_{12} = \left[1 + \frac{1}{4}(\gamma - \alpha) w^2 \Delta t^2\right] \Delta t / A_0$$

$$A_{21} = \left[-w^2 \Delta t^2\right] (1/\Delta t) / A_0$$

$$A_{22} = \left[1 - \xi w \Delta t - \frac{1}{2}\alpha w^2 \Delta t^2\right] / A_0,$$

$$L_{11} = \frac{1}{2}\beta_1\, \Delta t^2 / A_0$$

$$L_{12} = \frac{1}{2}\beta_2\, \Delta t^2 / A_0$$

$$L_{21} = \beta_1 \Delta t / A_0$$

$$L_{22} = \beta_2\, \Delta t / A_0,$$

$$A_0 = 1 + \xi w \Delta t + \tfrac{1}{2}\gamma w^2 \Delta t^2$$

Basic framework to introduce some adaptive time integration procedures

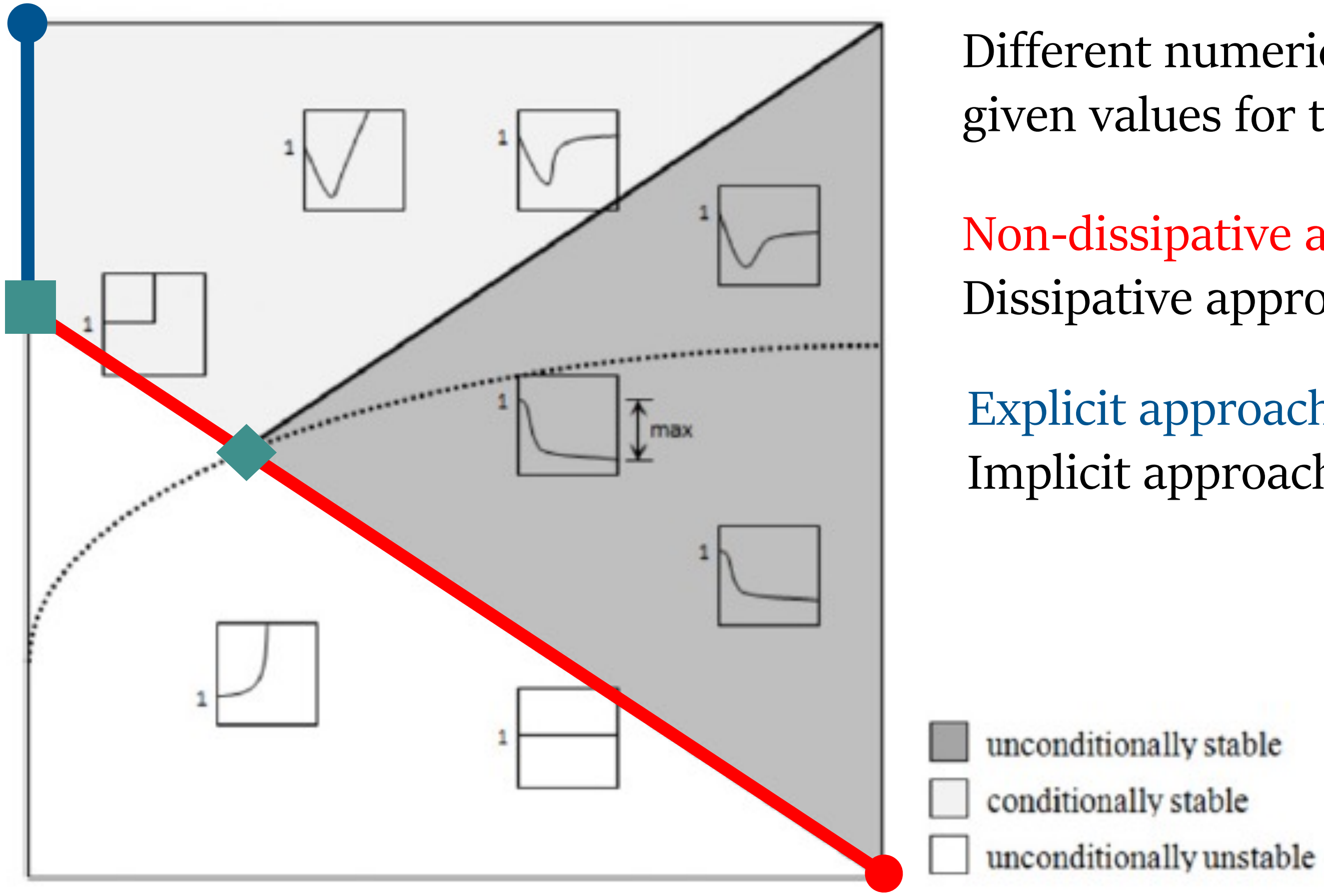

Spectral radius behaviour and regions of stability for the γ–α plane

Different numerical properties are provided according to the given values for the referred time integration parameters

Non-dissipative approach: α=1-γ
Dissipative approach: α>1-γ

Explicit approach: γ=0
Implicit approach: γ>0

Central difference method (α=1; γ=0)

Trapezoidal rule (α=1/2; γ=1/2)

Basic framework to introduce some adaptive time integration procedures

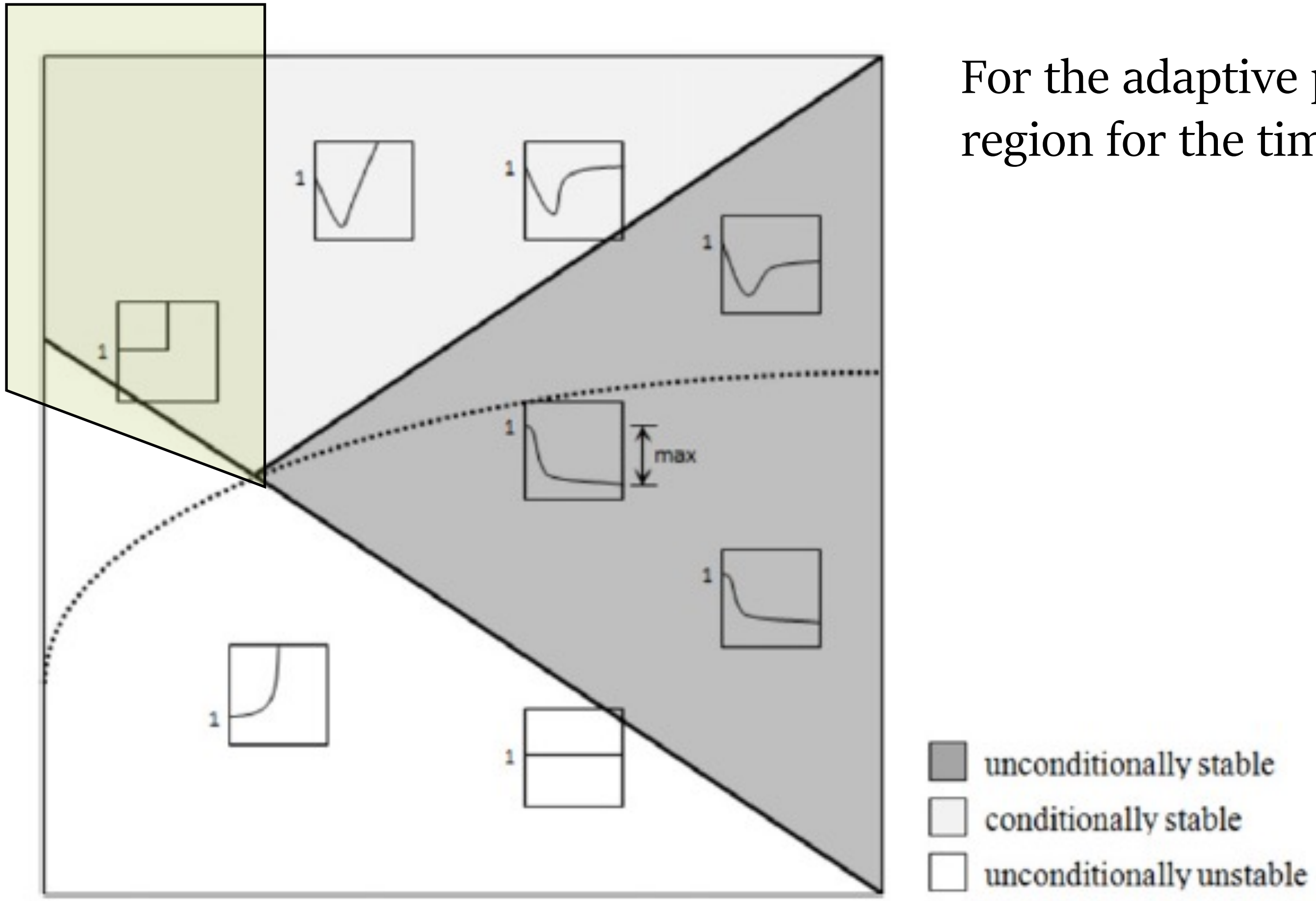

Spectral radius behaviour and regions of stability for the γ–α plane

For the adaptive procedures discussed here, the following region for the time integration parameters is focused:

$$0 \leq \gamma \leq \tfrac{1}{2}$$
$$\alpha \geq 1 - \gamma$$

Adaptive approach

In the adopted adaptive approach, the time integration parameters of the method are locally computed as function of the maximal sampling frequency of the element $\Omega_e^{\max} = \omega_e^{\max}\Delta t$, where $\omega_e^{\max}$ stands for the element maximal natural frequency, which is evaluated as the square root of its highest eigenvalue, considering the generalized eigenvalue problem of local matrices $\mathbf{M}_e$ and $\mathbf{K}_e$:

$$\omega_e^{\max 2} = \lambda_e^{\max} = \max(\text{eigenvalues}(\mathbf{M}_e, \mathbf{K}_e))$$

Thus, the time integration procedure may adapt to the local properties of the model and to its adopted spatial and temporal discretizations.

Adaptive approach

It may also adapt to the computed responses. In this case, the time integration parameters may be locally evaluated introducing numerical dissipation when and where it is necessary, activating or not dissipative elements along the analysis.

This idea can be automatically carried out based on an oscillatory criterion. In this sense, if the computed response of a degree of freedom of the model oscillates along time, the α parameters of the elements surrounding this degree of freedom are modified, locally introducing numerical dissipation into the analysis.

$$\varphi_e^n = \sum_{i=1}^{n_e} \left| \left| u_i^n - u_i^{n-2} \right| - \left| u_i^n - u_i^{n-1} \right| - \left| u_i^{n-1} - u_i^{n-2} \right| \right|$$

$$\text{If} \left(\underset{j=n-m}{\overset{n}{or}} (\varphi_e^j = 0) \right), \ \alpha_e^n = 1 - \gamma_e^n$$

$$\text{If} \left(\underset{j=n-m}{\overset{n}{and}} (\varphi_e^j \neq 0) \right), \ \alpha_e^n = \overline{\alpha}_e^n \ \ (\overline{\alpha}_e^n \geq 1 - \gamma_e^n)$$

Adaptive explicit/implicit time integration procedure

For the discussed explicit/implicit formulation, the following local parameters are defined:

If $\Omega_e^{\max} \le 2$, $\gamma_e^n = 0$ ⟶ Explicit element

If $\Omega_e^{\max} > 2$, $\gamma_e^n = \frac{1}{2}\tanh(\frac{1}{4}\Omega_e^{\max})$ ⟶ Implicit element

which, as illustrated below, automatically allows to define the explicit (white colour) and implicit (orange colour) subdomains of the model, for the analysis:

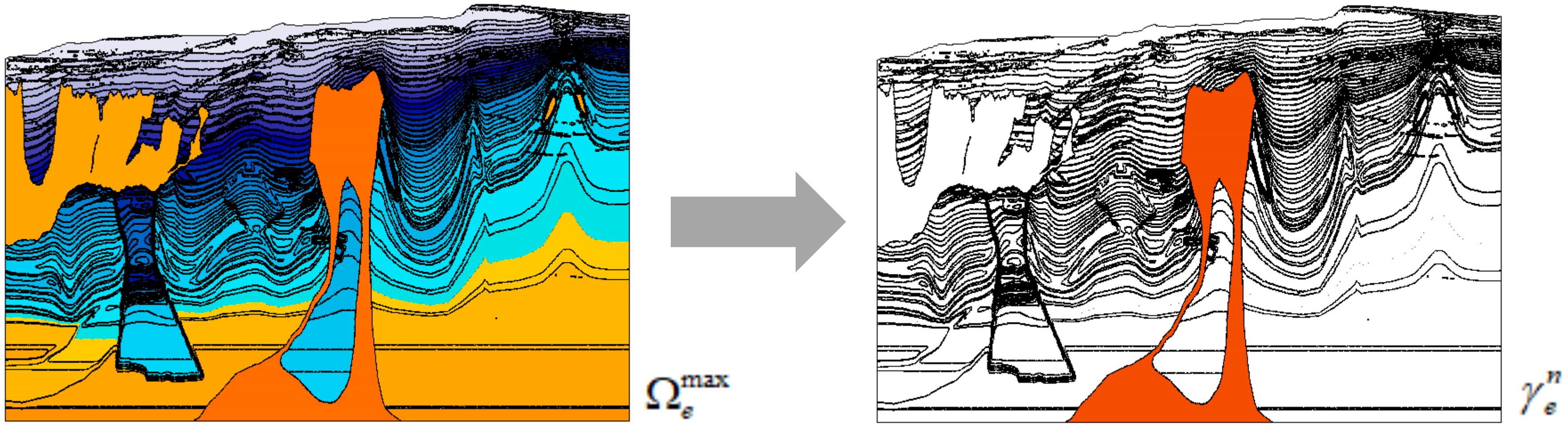

Adaptive explicit/implicit time integration procedure

For the discussed explicit/implicit formulation, the following local parameters are defined:

If $\Omega_e^{\max} \leq 2$, $\gamma_e^n = 0$

If $\Omega_e^{\max} > 2$, $\gamma_e^n = \frac{1}{2}\tanh(\frac{1}{4}\Omega_e^{\max})$

This expression is established so that:

(i) Stability is guaranteed (i.e., $\Omega_c \geq \Omega_e^{\max}$);

(ii) Low dispersion errors are provided.

The proposed implicit non-dissipative formulation is always more accurate than the trapezoidal rule, which is “the second-order accurate A-stable linear multistep method with the smallest error constant” (Dahlquist’s theorem).

Adaptive explicit/implicit time integration procedure

For the discussed explicit/implicit formulation, the following local parameters are defined:

$$\overline{\alpha}_e^n = 2\left[2\gamma_e^n + \left(1+\frac{\varsigma_e \Delta t}{2\rho_e}\right)\left(\frac{2}{\Omega_e^{\max}}\right)^2\right]^{\frac{1}{2}} - 1 - \gamma_e^n - \frac{\varsigma_e \Delta t}{2\rho_e}\left(\frac{2}{\Omega_e^{\max}}\right)^2$$

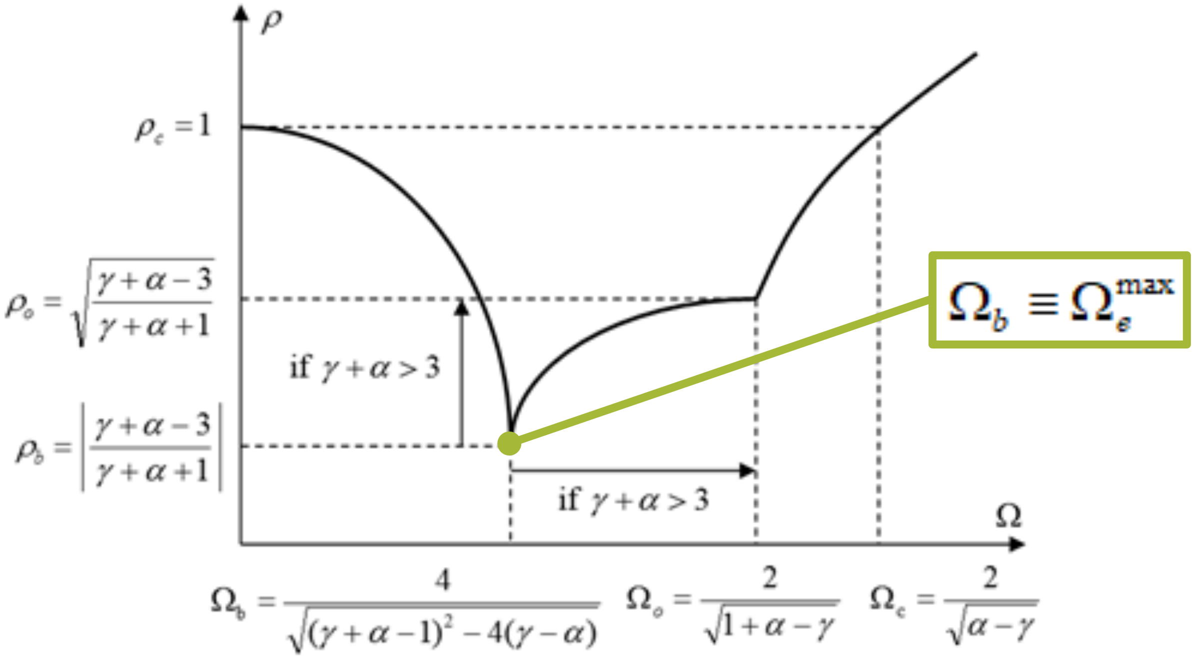

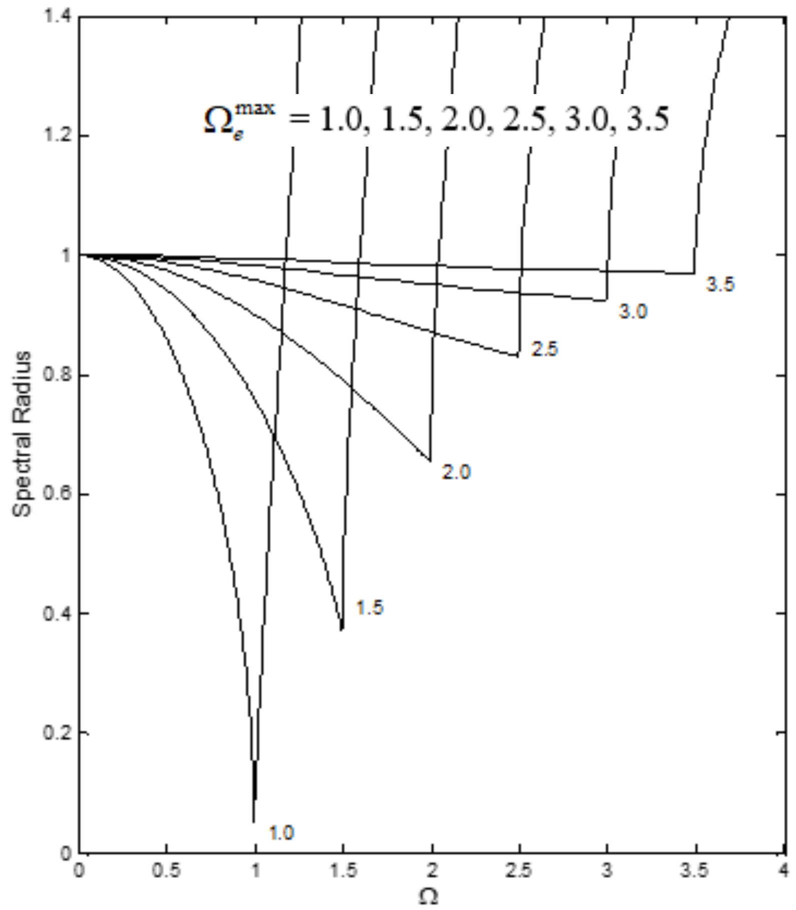

Adaptive explicit/implicit time integration procedure

In automated explicit/implicit analyses, by increasing the adopted Δt value, less time steps are necessary for solution, which is beneficial for efficiency; however, simultaneously, by enlarging Δt, more implicit elements may be activated, increasing the solver computational effort. Thus, an optimization algorithm may be applied to compute an optimal Δt value, so that maximal efficiency is provided.

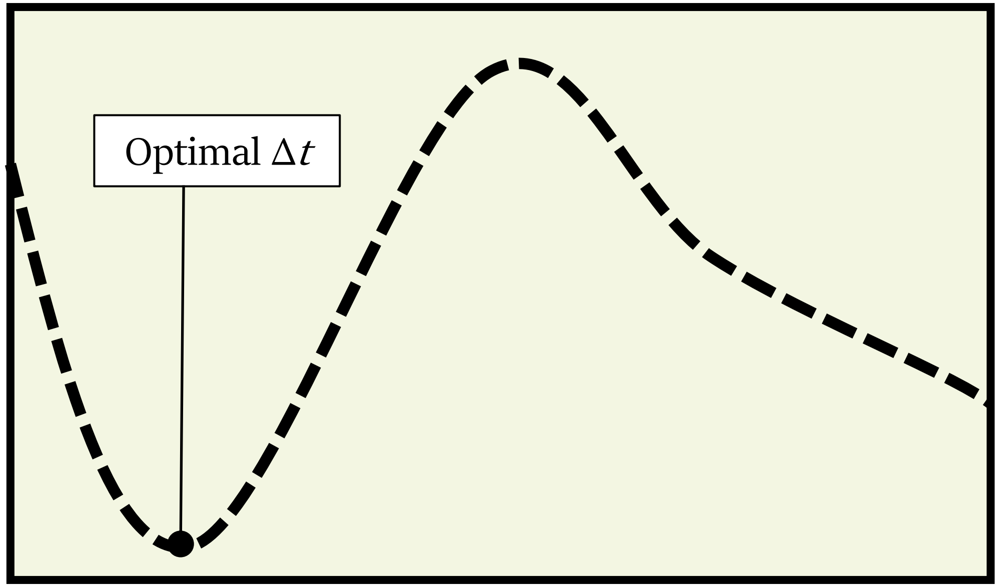

Evolution of the expected number of operations in the analysis vs. the adopted time-step value

Adaptive explicit/explicit time integration procedure

As previously remarked, for an explicit formulation, $\gamma_e^n = 0$ is considered.

In this case, explicit/explicit analyses may be carried out dividing the discrete model into groups of explicit elements that may have the same Δt assigned, respecting their stability limit.

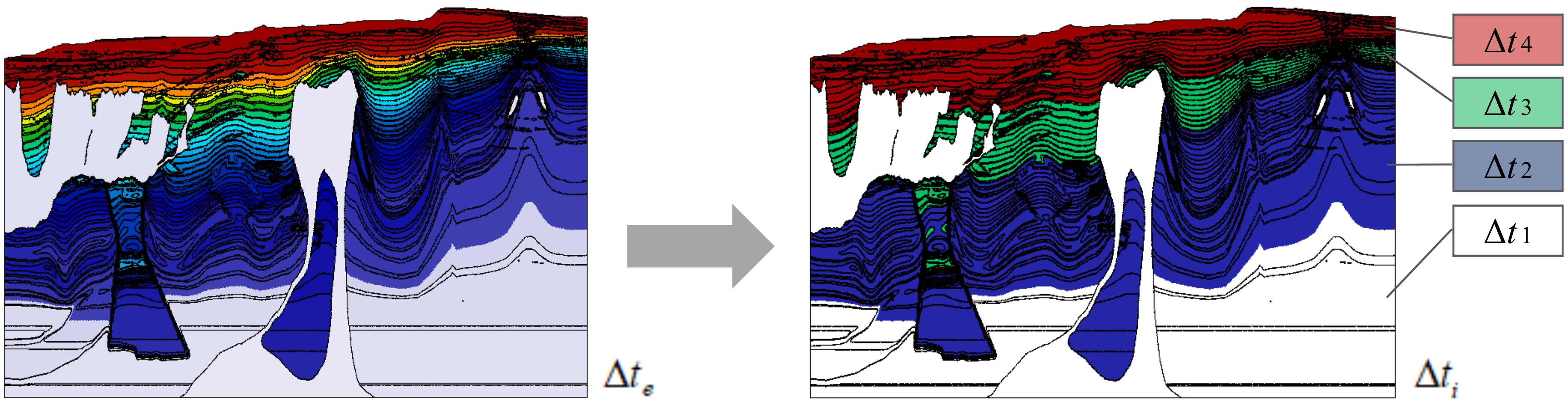

Adaptive explicit/explicit time integration procedure

To provide this subdivision, the following algorithm may be followed:

(i) calculate the limiting time-steps of all elements (e.g., $\Delta t_e = 2/\omega_e^{max}$), and find the smalles Δt_e of the model (i.e., $\Delta t_e^{min} = \min(\Delta t_e)$), which is the basic time-step for the proposed controlled subdivision of the domain;

(ii) with Δt_e^{min} defined, calculate subsequent time-step values as multiple of the power of 2 of this minimal time-step value (i.e., calculate $\Delta t_i = 2^{(i-1)} \Delta t_e^{min}$);

(iii) associate each element to a computed time-step value (i.e., to Δt_i, where $\Delta t_i \leq \Delta t_e < \Delta t_{i+1}$ and i indicates the subdomain of that element);

(iv) associate a time-step value (i.e., associate a subdomain) to each degree of freedom of the model considering the lowest time-step value of its surrounding elements.

Adaptive explicit/explicit time integration procedure

Once this subdomain division is considered, a sub-cycling algorithm may be followed, in which values close to the boundaries of these time-step subdomains may need to be interpolated. In this case, the following equations may be considered, which are consistent with the adopted approximations of the referred time marching technique:

$$\mathbf{U}(t) = \frac{1}{2\Delta t}\left(\dot{\mathbf{U}}^{n+1} - \dot{\mathbf{U}}^{n}\right)t^2 + \dot{\mathbf{U}}^{n}t + \mathbf{U}^{n}$$

$$\dot{\mathbf{U}}(t) = \frac{1}{\Delta t}\left(\dot{\mathbf{U}}^{n+1} - \dot{\mathbf{U}}^{n}\right)t + \dot{\mathbf{U}}^{n}$$

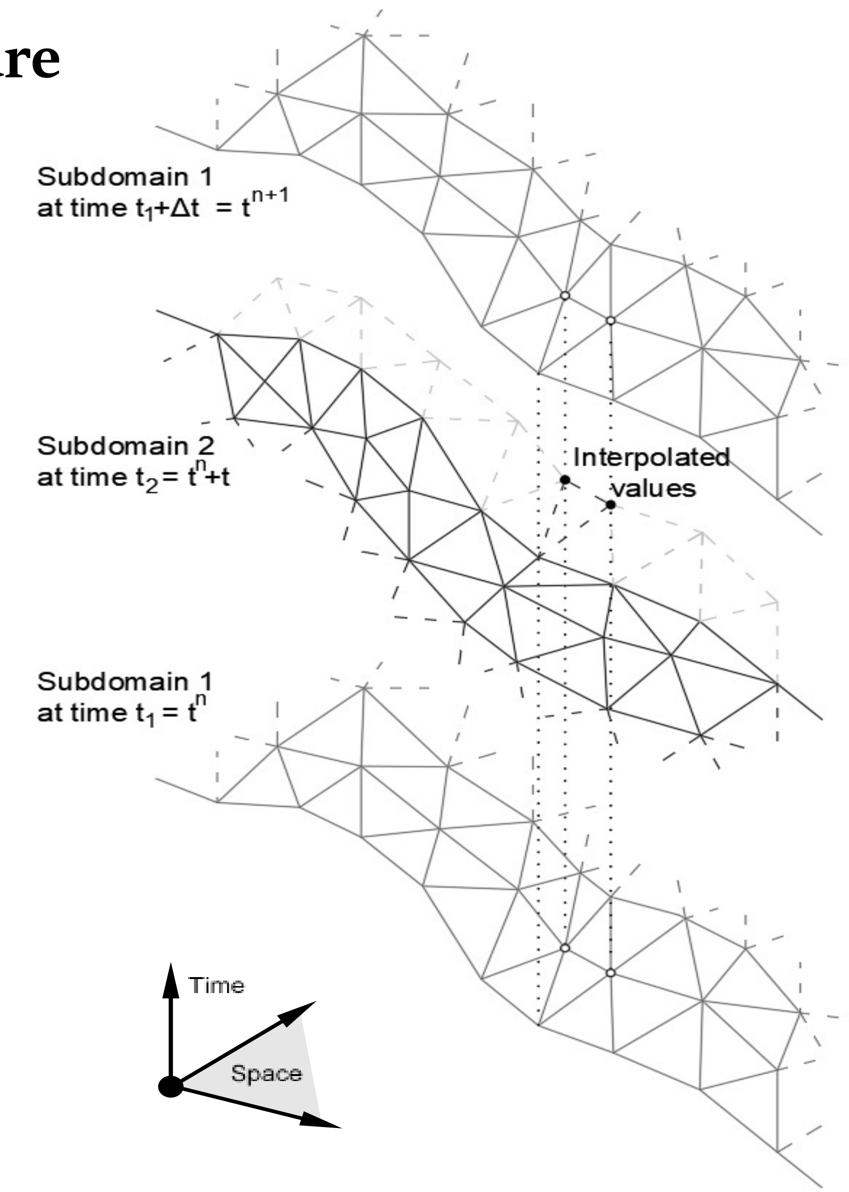

Numerical applications considering explicit/implicit and explicit/explicit analyses

Initially, an acoustic infinite-domain model, submitted to an impulsive source, is analysed. For this model, analytical answers are known (Green's functions), allowing to analyse the accuracy of the considered time integration techniques. The discussed explicit/implicit and explicit/explicit formulations, as well as standard explicit methodologies, are here applied to analyse this model. Four FEM meshes, which consider refinement towards the applied source position, are regarded for the analyses, and Perfectly Matched Layers (PMLs) are employed to simulate the infinite domain.

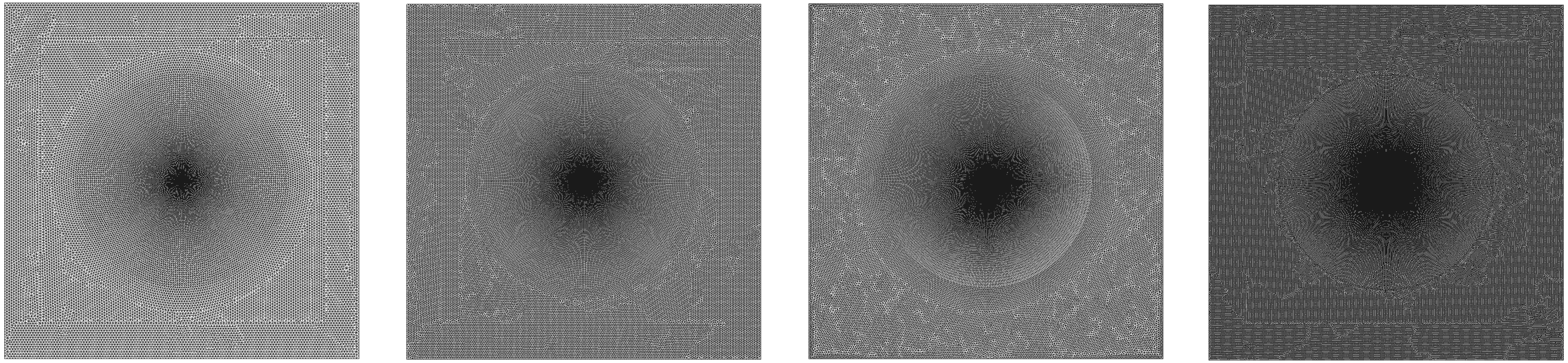

50k 100k 150k 200k

Numerical applications considering explicit/implicit and explicit/explicit analyses

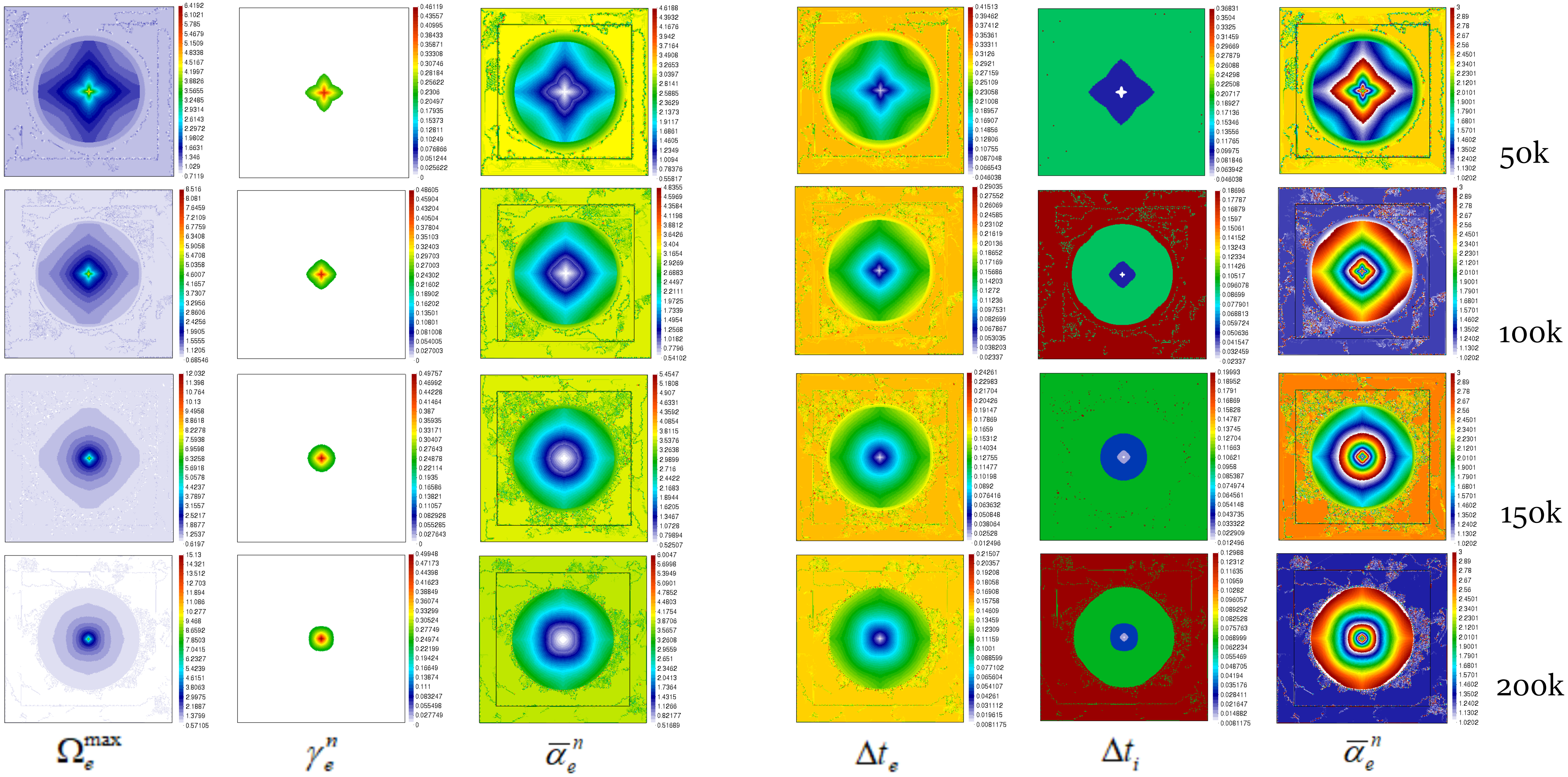

Mesh	Method	Δt (max) (s)	Relative value	Error	Relative value	CPU time (s)	Relative value
50k	CD	0.046038233	1.109548341	0.798011132	2.137210316	14.46070892	1.668798343
	EGα	0.041492769	1	0.785386795	2.103400182	15.98963547	1.845239906
	NB	0.08620727	2.077645625	0.790874715	2.118097771	16.12635803	1.861017997
	Exp	0.046038233	1.109548341	0.52417599	1.403832966	14.00488853	1.616195645
	Exp/Exp	0.368305864	8.876386727	0.373389145	1	8.665342331	1
	Imp/Exp	0.149255845	3.597153169	0.419698571	1.124024564	9.451831818	1.090762656

Method	Type	Percentage of elements (%)
Exp/Exp	Δt_1 = 0.046038233	1.525323910
	Δt_2 = 0.092076466	18.125245386
	Δt_3 = 0.184152932	80.325873576
	Δt_4 = 0.368305864	0.031409501
Imp/Exp	Explicit	90.357283078
	Implicit	9.642716921

Mesh	Method	Δt (max) (s)	Relative value	Error	Relative value	CPU time (s)	Relative value
100k	CD	0.023370401	1.109548333	0.762614821	2.568889242	22.88965607	2.117798866
	EGα	0.021062986	1	0.738738373	2.488460763	24.23314095	2.242100898
	NB	0.043761421	2.077645639	0.75148604	2.531401632	28.92198372	2.675922441
	Exp	0.023370401	1.109548333	0.509066418	1.714804391	22.65373993	2.095971412
	Exp/Exp	0.186963208	8.876386662	0.29686559	1	10.80822945	1
	Imp/Exp	0.100516273	4.772175866	0.346039766	1.165644578	11.24567986	1.040473827

Method	Type	Percentage of elements (%)
Exp/Exp	Δt_1 = 0.023370401	0.730778433
	Δt_2 = 0.046740802	7.119357154
	Δt_3 = 0.093481604	35.181049609
	Δt_4 = 0.186963208	56.972802679
Imp/Exp	Explicit	90.780028712
	Implicit	9.219971287

Mesh	Method	Δt (max) (s)	Relative value	Error	Relative value	CPU time (s)	Relative value
150k	CD	0.012495648	1.109548441	0.703323192	3.318572702	50.01919365	2.326550697
	EGα	0.011261922	1	0.672640998	3.173801292	57.37683296	2.668777742
	NB	0.023398284	2.077645716	0.692457897	3.267305699	64.78535271	3.013371398
	Exp	0.012495648	1.109548441	0.456617029	2.154509941	50.21524048	2.335669454
	Exp/Exp	0.199930368	17.75277506	0.211935448	1	26.38242531	1.227129938
	Imp/Exp	0.075932135	6.742377996	0.260082924	1.227179912	21.49929237	1

Method	Type	Percentage of elements (%)
Exp/Exp	Δt_1 = 0.012495648	0.455137404
	Δt_2 = 0.024991296	4.282278211
	Δt_3 = 0.049982592	14.694626056
	Δt_4 = 0.099965184	80.363312602
	Δt_5 = 0.199930368	0.207967894
Imp/Exp	Explicit	88.715250093
	Implicit	11.284749906

Mesh	Method	Δt (max) (s)	Relative value	Error	Relative value	CPU time (s)	Relative value
200k	CD	0.008117472	1.109548451	0.666377456	3.836889795	88.7935276	2.139639558
	EGα	0.007316014	1	0.637917567	3.673022517	114.932354	2.769501536
	NB	0.015200085	2.077645696	0.659035903	3.794618363	126.7395802	3.054017862
	Exp	0.008117472	1.109548451	0.417648945	2.404752683	89.03837395	2.145539571
	Exp/Exp	0.129879552	17.75277521	0.173676465	1	49.48914909	1.192529951
	Imp/Exp	0.062027565	8.478327836	0.219533683	1.264038184	41.49929237	1

Method	Type	Percentage of elements (%)
Exp/Exp	Δt_1 = 0.008117472	0.335567123
	Δt_2 = 0.016234944	3.056004308
	Δt_3 = 0.032469888	9.350505594
	Δt_4 = 0.064939776	30.706635553
	Δt_5 = 0.129879552	56.553780490
Imp/Exp	Explicit	88.456092064
	Implicit	11.543907935

Numerical applications considering explicit/implicit and explicit/explicit analyses

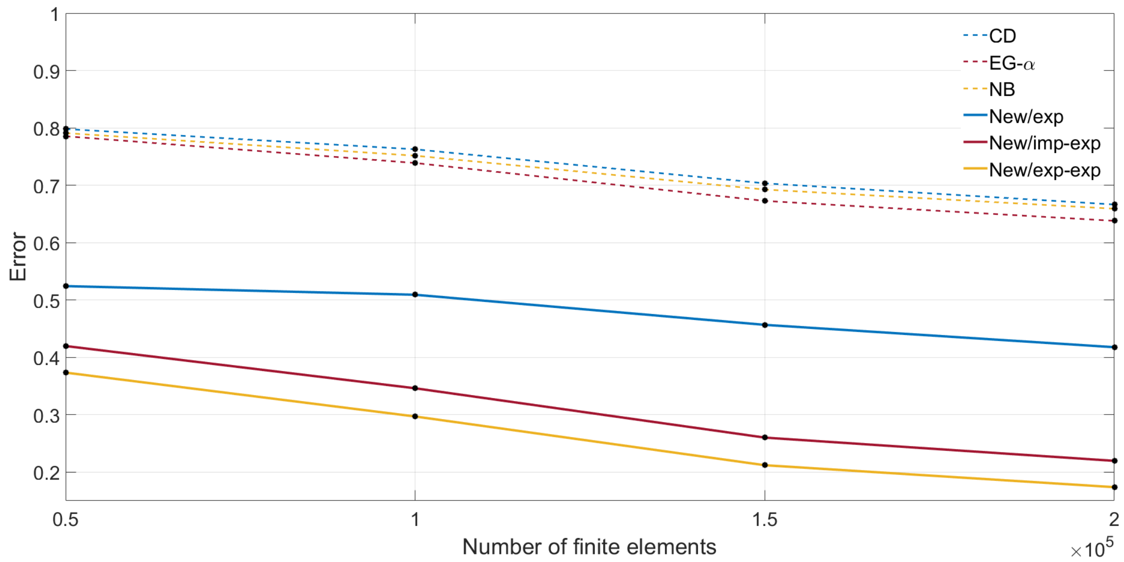

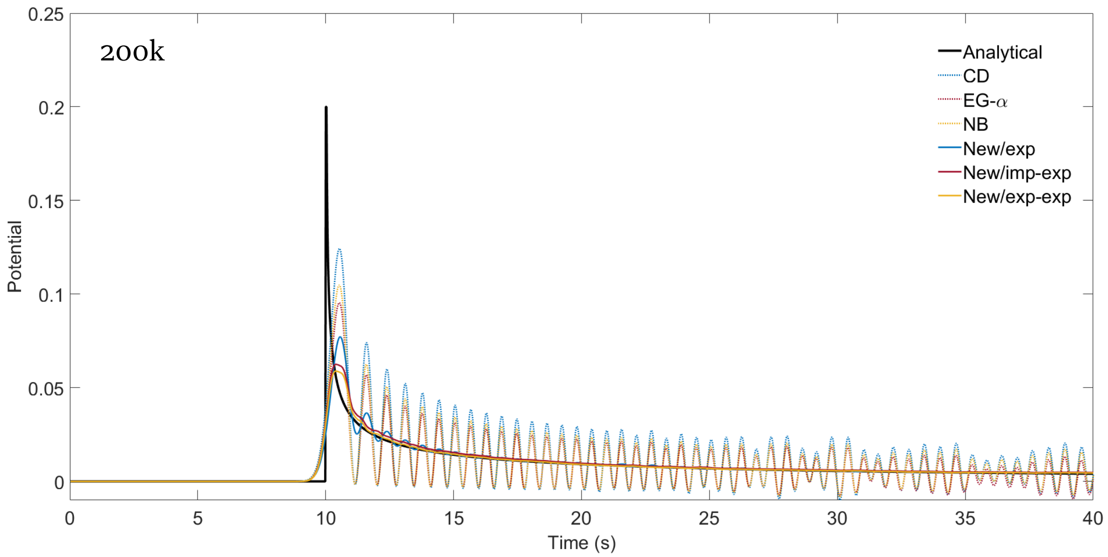

Numerical applications considering explicit/implicit and explicit/explicit analyses

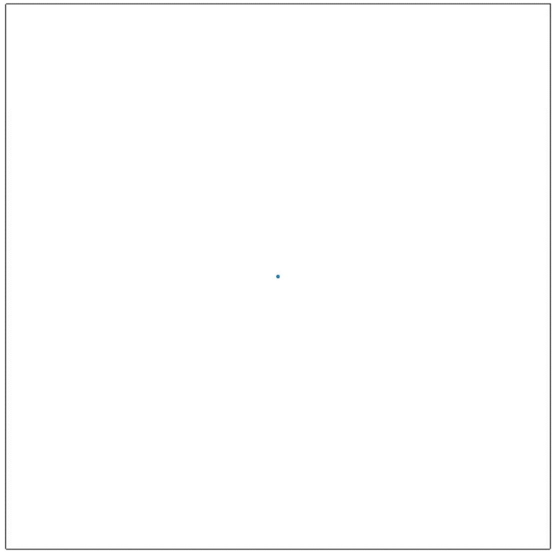

Analytical

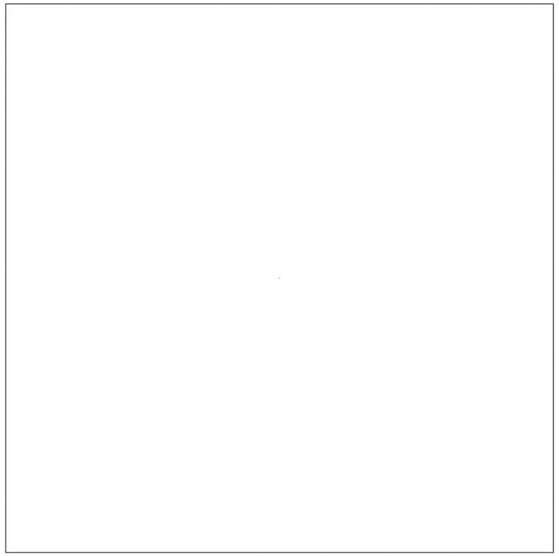

EG-α

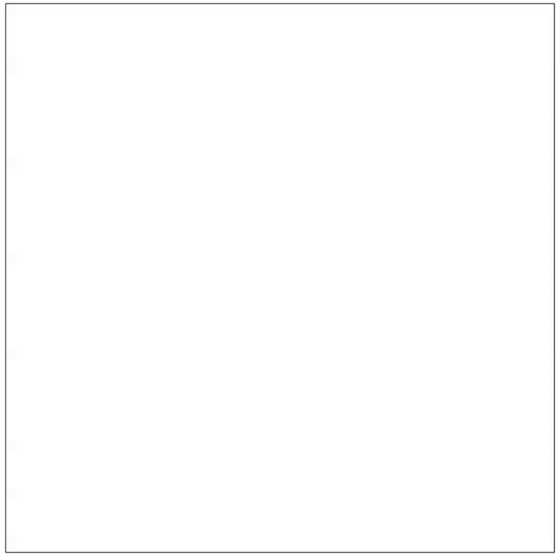

Imp/Exp

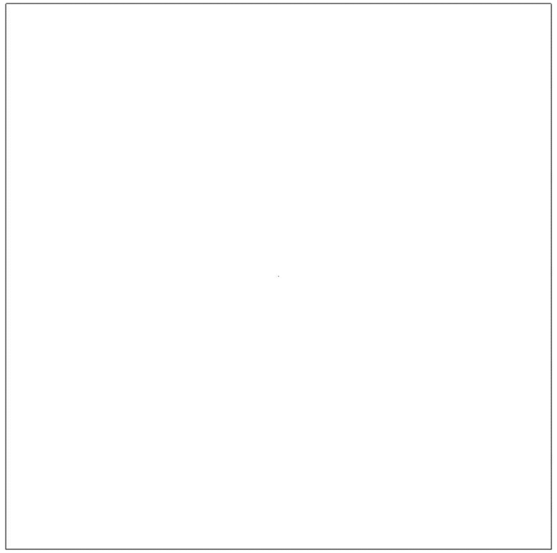

Exp/Exp

Numerical applications considering explicit/implicit and explicit/explicit analyses

Three heterogeneous models are also analysed:

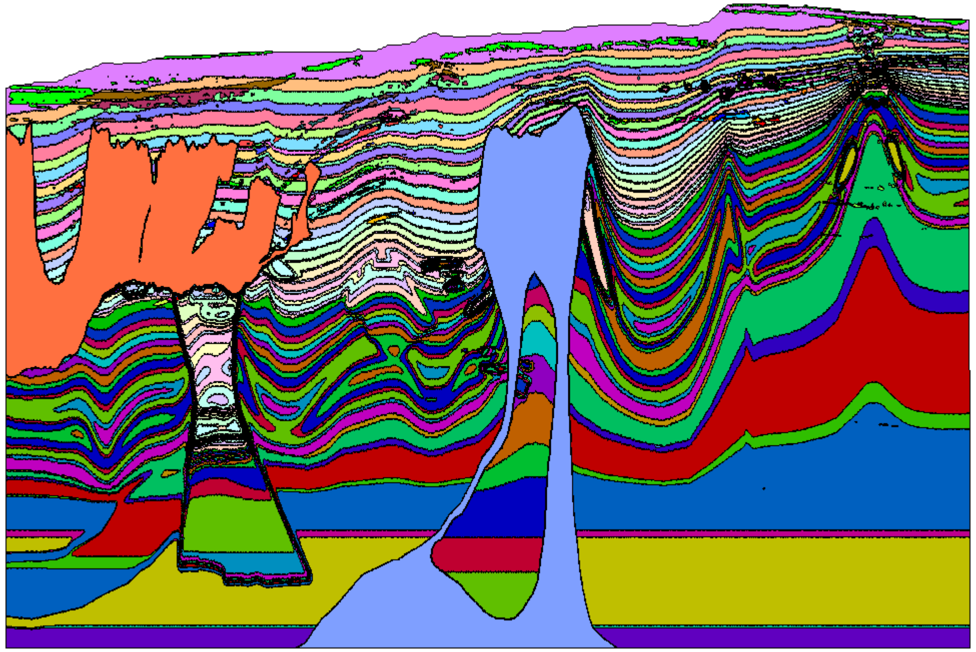

Model 1 (Elastodynamic model, discretized by 2.57M elements)

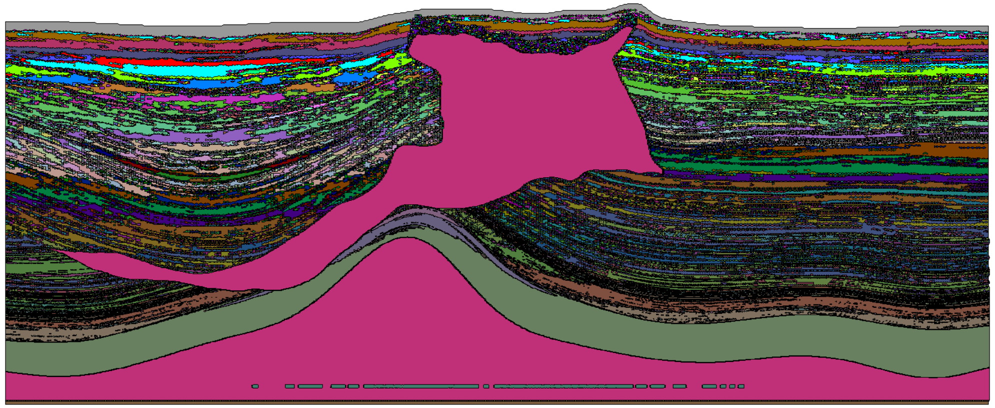

Model 2 (Elastodynamic model, discretized by 0.72M elements)

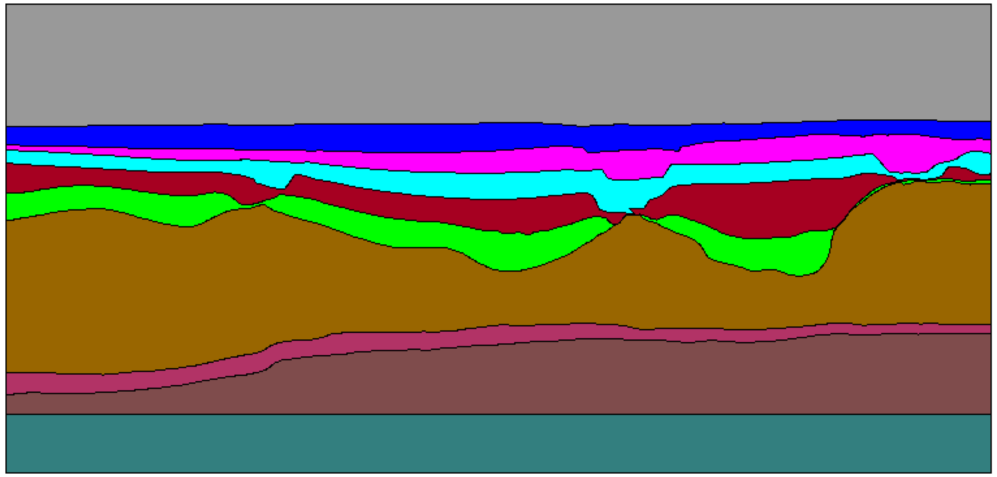

Model 3 (acoustic model, discretized by 4.86M elements)

Numerical applications considering explicit/implicit and explicit/explicit analyses

Model	Method	Δt (max) (s)	Relative value	CPU time (s)	Relative value
1	CD	0.003241549	1.109548407	11322.8	2.152869149
	EGα	0.002921503	1	12283.3	2.335494543
	NB	0.006069848	2.07764565	14773.1	2.808894551
	Exp	0.003241549	1.109548407	11737.68	2.231752671
	Exp/Exp	0.103729568	35.50554903	5883.3	1.118625699
	Imp/Exp	0.004248888	1.454350075	5259.4	1

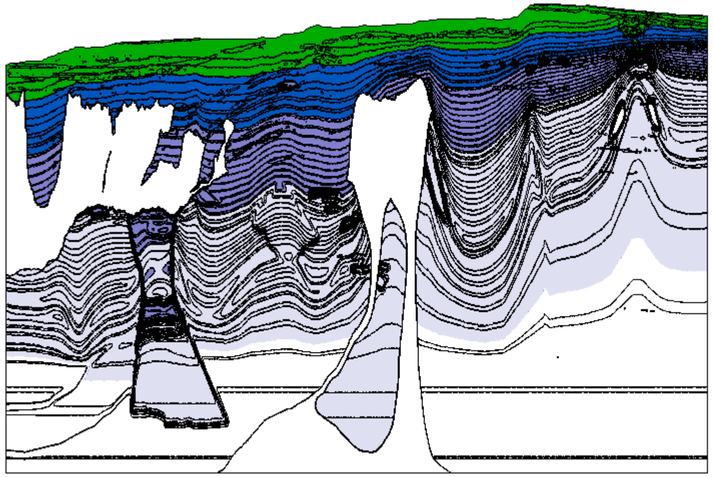

Method	Type	Percentage of elements (%)
Exp/Exp	$\Delta t1$ = 0.003241549	71.323290617
	$\Delta t2$ = 0.006483098	17.877215636
	$\Delta t3$ = 0.012966196	4.130985733
	$\Delta t4$ = 0.025932392	3.431895840
	$\Delta t5$ = 0.051864784	3.231484373
	$\Delta t6$ = 0.103729568	0.005360880
Imp/Exp	Explicit	86.472245400
	Implicit	13.527754599

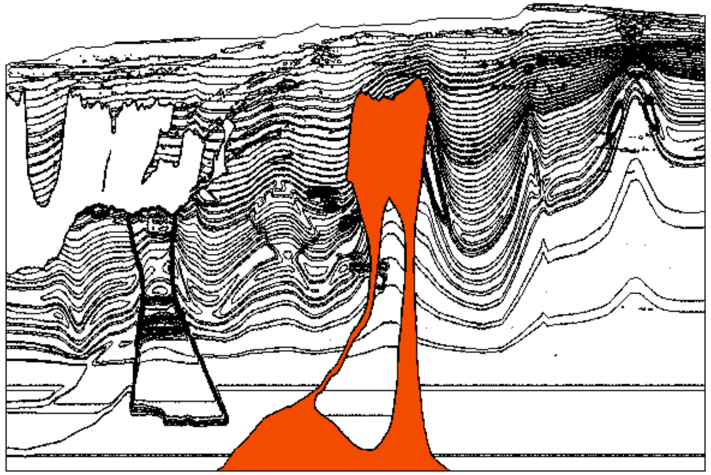

Numerical applications considering explicit/implicit and explicit/explicit analyses

Model	Method	Δt (max) (s)	Relative value	CPU time (s)	Relative value
2	CD	0.002425544	1.109548485	8661.5	1.98558067
	EGα	0.002186064	1	8991.6	2.061253496
	NB	0.004541866	2.077645647	9511.1	2.18034478
	Exp	0.002425544	1.109548485	8654.5	1.983975975
	Exp/Exp	0.019404352	8.876387883	4362.2	1
	Imp/Exp	0.003423479	1.566046831	5436.3	1.246228967

Method	Type	Percentage of elements (%)
Exp/Exp	Δt_1 = 0.002425544	76.907126791
	Δt_2 = 0.004851088	10.543423241
	Δt_3 = 0.009702176	8.077792450
	Δt_4 = 0.019404352	4.472215288
Imp/Exp	Explicit	83.225288263
	Implicit	16.774711736

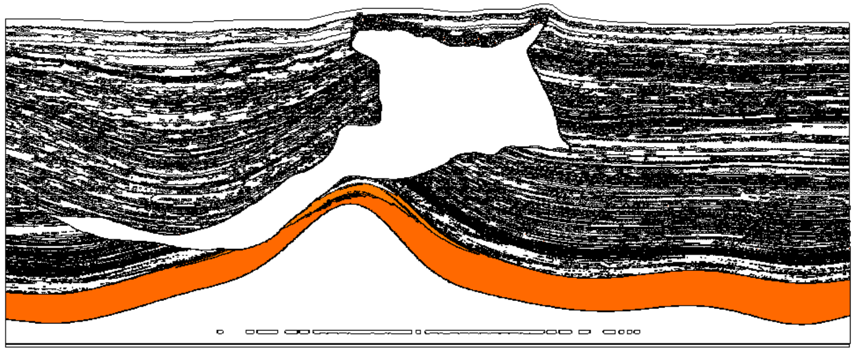

Numerical applications considering explicit/implicit and explicit/explicit analyses

Model	Method	Δt (max) (s)	Relative value	CPU time (s)	Relative value
3	CD	0.00064051	1.109548202	5233.7	1.68129397
	EGα	0.000577271	1	5462.8	1.754890938
	NB	0.00119936	2.077637713	5683.6	1.825821581
	Exp	0.00064051	1.109548202	5261.2	1.690128176
	Exp/Exp	0.00256204	4.438192807	3112.9	1
	Imp/Exp	0.00086751	1.502777725	4282.5	1.375726814

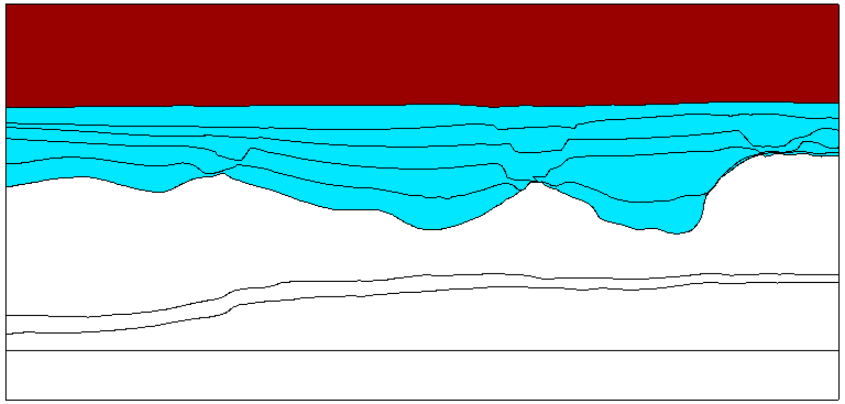

Method	Type	Percentage of elements (%)
Exp/Exp	Δt_1 = 0.00064051	51.879546377
	Δt_2 = 0.00128102	22.653851150
	Δt_3 = 0.00256204	25.466664144
Imp/Exp	Explicit	71.465666675
	Implicit	28.534333324

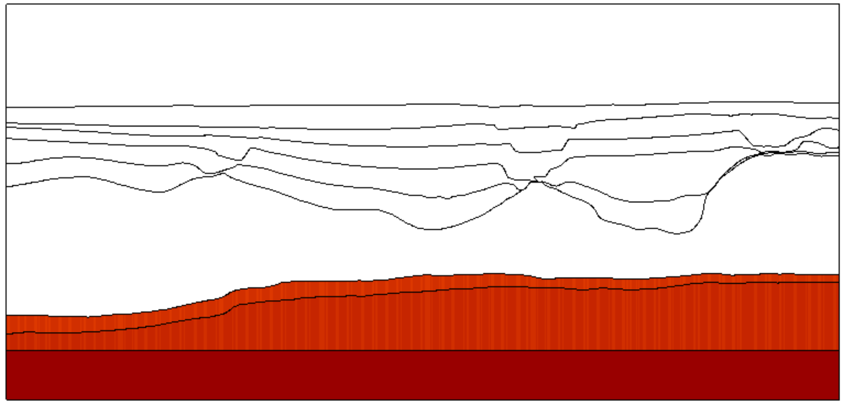

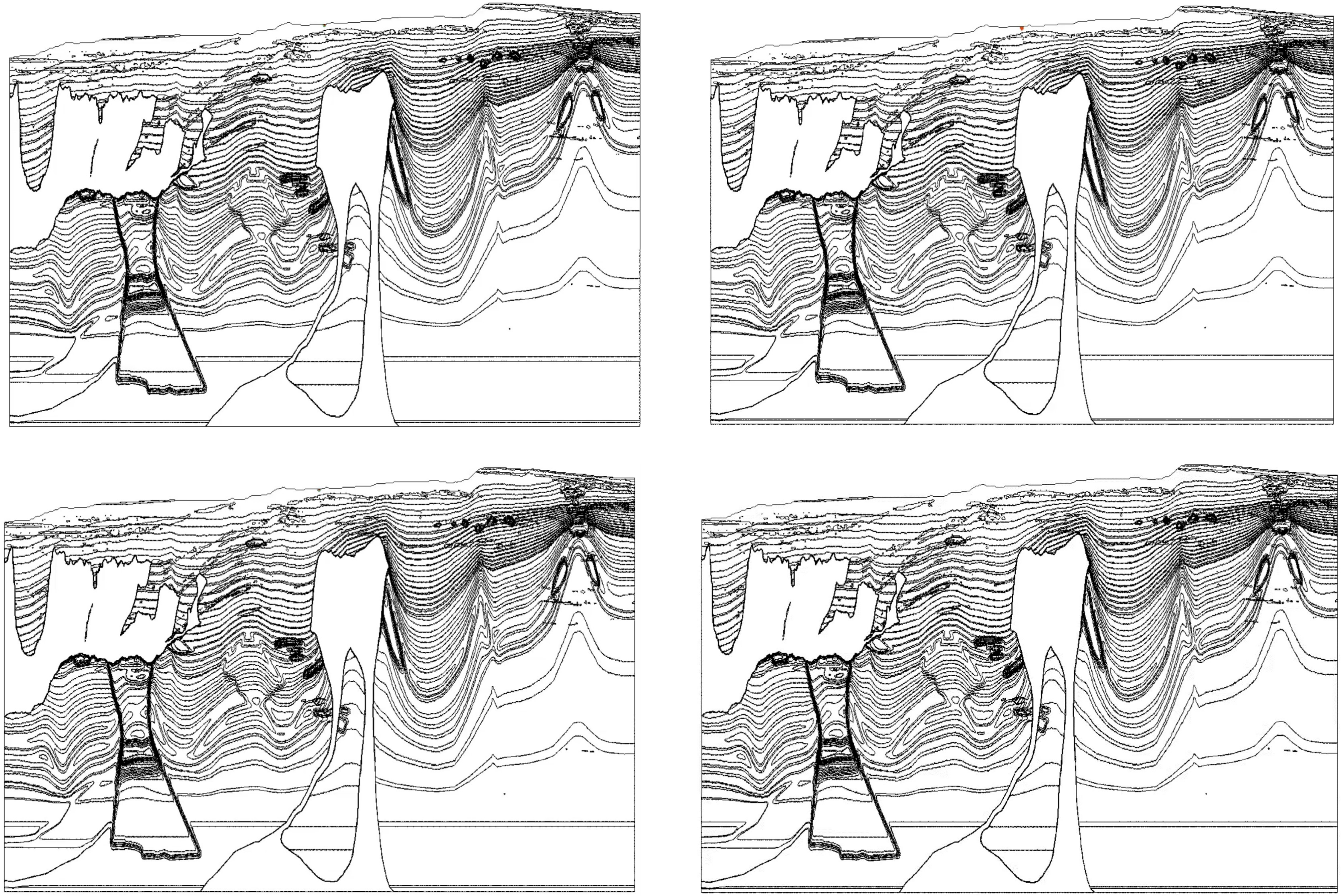

Explicit/explicit analysis

Explicit/implicit analysis

Computed solution

Time integration parameters

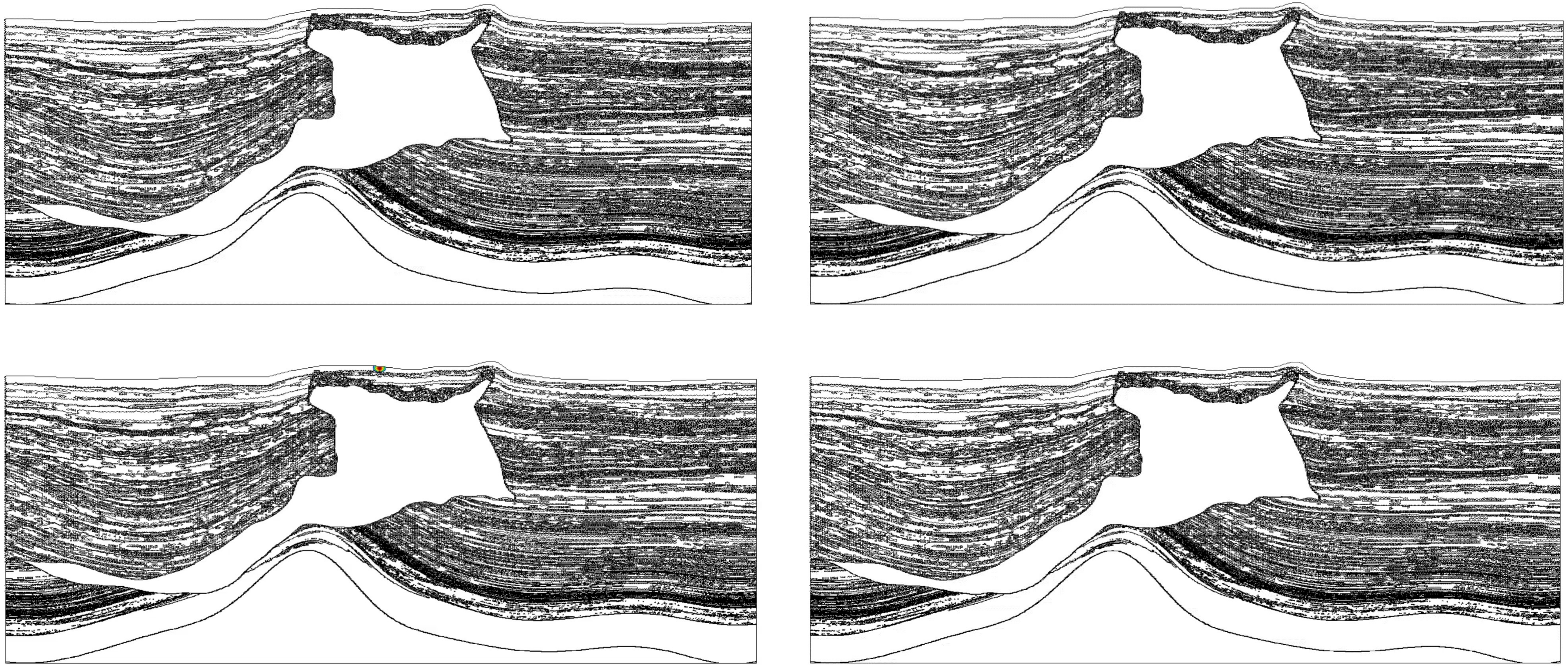

Explicit/explicit analysis

Explicit/implicit analysis

Computed solution

Time integration parameters

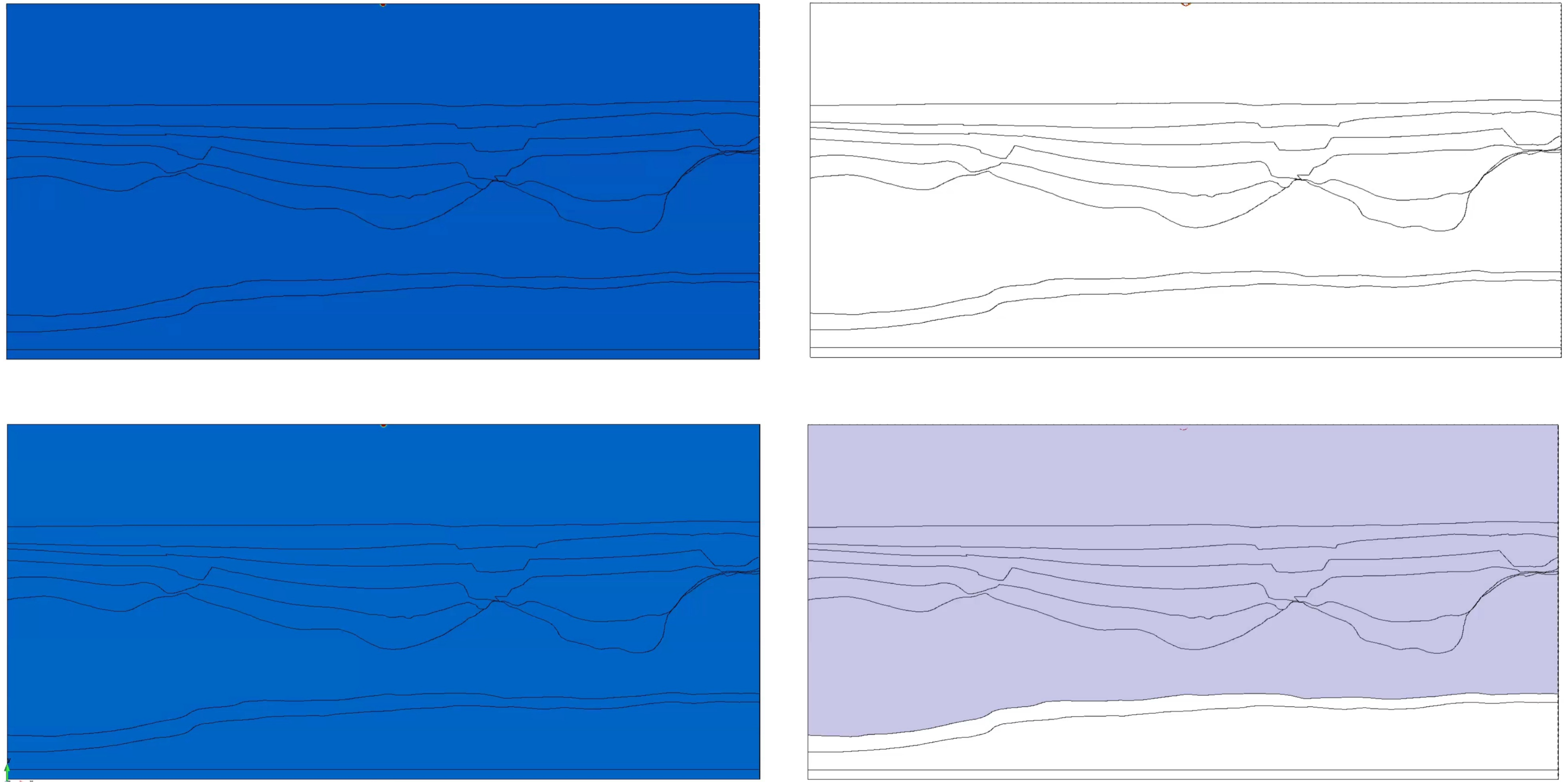

Explicit/explicit analysis

Explicit/implicit analysis

Computed solution

Time integration parameters

Discussion considering explicit/implicit and explicit/explicit analyses

- The discussed explicit/explicit formulation usually provides better accuracy, since it stands as a more versatile approach and, consequently, it usually allows better adaptability for the parameters of the method;
- The described explicit/implicit approach is highly straightforward and considerably easier to implement, but it requires more memory resources (since it deals with a non-diagonal effective matrix);
- The efficiency of each discussed adaptive approach depends on the features of the discretized model; however, both referred explicit/implicit and explicit/explicit techniques are regularly more effective than standard time integration procedures.

Enhanced explicit/implicit and explicit/explicit adaptive techniques

The previously presented ideas may be extended, improved and/or generalized providing enhanced explicit/implicit or explicit/explicit formulations.

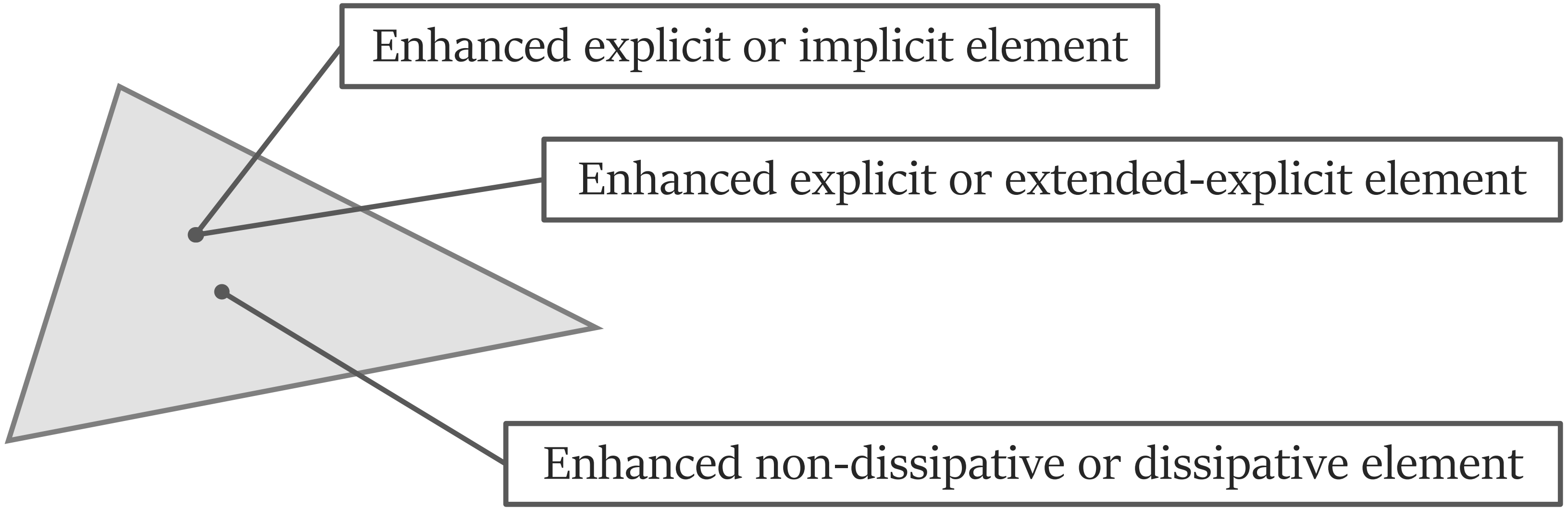

Enhanced explicit/implicit and explicit/explicit adaptive techniques

For instance, by modifying the previously presented time-marching framework:

$$(\mathbf{M}+\tfrac{1}{2}\Delta t\mathbf{C}+\tfrac{1}{2}\gamma\Delta t^2\mathbf{K})\dot{\mathbf{U}}^{n+1}=\overline{\mathbf{F}}+(\mathbf{M}-\tfrac{1}{2}\Delta t\mathbf{C})\dot{\mathbf{U}}^{n}-\Delta t\mathbf{K}(\mathbf{U}^{n}+\tfrac{1}{2}\alpha\Delta t\dot{\mathbf{U}}^{n})$$

$$\mathbf{U}^{n+1}=\mathbf{U}^{n}+\tfrac{1}{2}\Delta t(\dot{\mathbf{U}}^{n}+\dot{\mathbf{U}}^{n+1})$$

The following recurrence relationships may be obtained:

Enhanced explicit/implicit framework:

$$\mathbf{V}=\dot{\mathbf{U}}^{n}+\mathbf{E}^{-1}(\overline{\mathbf{F}}-\Delta t(\mathbf{C}\dot{\mathbf{U}}^{n}+\mathbf{K}(\mathbf{U}^{n}+\tfrac{1}{2}\Delta t\dot{\mathbf{U}}^{n})))\qquad \mathbf{E}=\mathbf{M}+\tfrac{1}{2}\Delta t\mathbf{C}+\alpha'_0\mathbf{K}$$

$$\dot{\mathbf{U}}^{n+1}=\mathbf{V}-\mathbf{M}^{-1}\mathbf{K}(\alpha'_1\dot{\mathbf{U}}^{n}+\alpha'_2\mathbf{V})$$

$$\mathbf{U}^{n+1}=\mathbf{U}^{n}+\tfrac{1}{2}\Delta t(\dot{\mathbf{U}}^{n}+\dot{\mathbf{U}}^{n+1})$$

Guarantees stability

1 extra equation

+1 extra parameter

Introduce numerical damping

Enhanced explicit/explicit framework:

$$\mathbf{V}=\dot{\mathbf{U}}^{n}+\mathbf{E}^{-1}(\overline{\mathbf{F}}-\Delta t(\mathbf{C}\dot{\mathbf{U}}^{n}+\mathbf{K}(\mathbf{U}^{n}+\tfrac{1}{2}\Delta t\dot{\mathbf{U}}^{n})))\qquad \mathbf{E}=\mathbf{M}+\tfrac{1}{2}\Delta t\mathbf{C}$$

$$\dot{\mathbf{U}}^{n+1}=\mathbf{V}-\mathbf{E}^{-1}\mathbf{K}(\alpha'_1\dot{\mathbf{U}}^{n}+\alpha'_2\mathbf{V})$$

$$\mathbf{U}^{n+1}=\mathbf{U}^{n}+\tfrac{1}{2}\Delta t(\dot{\mathbf{U}}^{n}+\dot{\mathbf{U}}^{n+1})$$

1 extra equation

+1 extra parameter

Provide extended stability limits

Introduce numerical damping

Enhanced explicit/implicit and explicit/explicit adaptive techniques

For instance, by modifying the previously presented time-marching framework:

$$(\mathbf{M}+\tfrac{1}{2}\Delta t\mathbf{C}+\tfrac{1}{2}\gamma\Delta t^2\mathbf{K})\dot{\mathbf{U}}^{n+1}=\overline{\mathbf{F}}+(\mathbf{M}-\tfrac{1}{2}\Delta t\mathbf{C})\dot{\mathbf{U}}^{n}-\Delta t\mathbf{K}(\mathbf{U}^{n}+\tfrac{1}{2}\alpha\Delta t\dot{\mathbf{U}}^{n})$$

$$\mathbf{U}^{n+1}=\mathbf{U}^{n}+\tfrac{1}{2}\Delta t(\dot{\mathbf{U}}^{n}+\dot{\mathbf{U}}^{n+1})$$

The following recurrence relationships may be obtained:

Enhanced explicit/implicit framework:

$$\mathbf{V}=\dot{\mathbf{U}}^{n}+\mathbf{E}^{-1}(\overline{\mathbf{F}}-\Delta t(\mathbf{C}\dot{\mathbf{U}}^{n}+\mathbf{K}(\mathbf{U}^{n}+\tfrac{1}{2}\Delta t\dot{\mathbf{U}}^{n}))) \qquad \mathbf{E}=\mathbf{M}+\tfrac{1}{2}\Delta t\mathbf{C}+\alpha'_0\mathbf{K}$$

$$\dot{\mathbf{U}}^{n+1}=\mathbf{V}-\mathbf{M}^{-1}\mathbf{K}(\alpha'_1\dot{\mathbf{U}}^{n}+\alpha'_2\mathbf{V})$$

$$\mathbf{U}^{n+1}=\mathbf{U}^{n}+\tfrac{1}{2}\Delta t(\dot{\mathbf{U}}^{n}+\dot{\mathbf{U}}^{n+1})$$

Computed only if necessary

(i.e., if numerical damping is locally necessary)

Provide enhanced accuracy

Enhanced explicit/explicit framework:

$$\mathbf{V}=\dot{\mathbf{U}}^{n}+\mathbf{E}^{-1}(\overline{\mathbf{F}}-\Delta t(\mathbf{C}\dot{\mathbf{U}}^{n}+\mathbf{K}(\mathbf{U}^{n}+\tfrac{1}{2}\Delta t\dot{\mathbf{U}}^{n}))) \qquad \mathbf{E}=\mathbf{M}+\tfrac{1}{2}\Delta t\mathbf{C}$$

$$\dot{\mathbf{U}}^{n+1}=\mathbf{V}-\mathbf{E}^{-1}\mathbf{K}(\alpha'_1\dot{\mathbf{U}}^{n}+\alpha'_2\mathbf{V})$$

$$\mathbf{U}^{n+1}=\mathbf{U}^{n}+\tfrac{1}{2}\Delta t(\dot{\mathbf{U}}^{n}+\dot{\mathbf{U}}^{n+1})$$

Computed only if necessary

(i.e., if numerical damping and/or extended stability limits are locally necessary)

Enhanced explicit/implicit and explicit/explicit adaptive techniques

For instance, by modifying the previously presented time-marching framework:

$$(\mathbf{M}+\tfrac{1}{2}\Delta t\mathbf{C}+\tfrac{1}{2}\gamma\Delta t^2\mathbf{K})\dot{\mathbf{U}}^{n+1}=\overline{\mathbf{F}}+(\mathbf{M}-\tfrac{1}{2}\Delta t\mathbf{C})\dot{\mathbf{U}}^{n}-\Delta t\mathbf{K}(\mathbf{U}^{n}+\tfrac{1}{2}\alpha\Delta t\dot{\mathbf{U}}^{n})$$

$$\mathbf{U}^{n+1}=\mathbf{U}^{n}+\tfrac{1}{2}\Delta t(\dot{\mathbf{U}}^{n}+\dot{\mathbf{U}}^{n+1})$$

The following recurrence relationships may be obtained:

Enhanced explicit/implicit framework:

For a non-dissipative formulation:
= 0, for explicit elements ($0 < \Omega_e^{\max} \leq 2$)
≠ 0, for extended-explicit elements ($2 < \Omega_e^{\max} \leq 4$)

Enhanced explicit/explicit framework:

$$\mathbf{V}=\dot{\mathbf{U}}^{n}+\mathbf{E}^{-1}(\overline{\mathbf{F}}-\Delta t(\mathbf{C}\dot{\mathbf{U}}^{n}+\mathbf{K}(\mathbf{U}^{n}+\tfrac{1}{2}\Delta t\dot{\mathbf{U}}^{n}))) \qquad \mathbf{E}=\mathbf{M}+\tfrac{1}{2}\Delta t\mathbf{C}$$

$$\dot{\mathbf{U}}^{n+1}=\mathbf{V}-\mathbf{E}^{-1}\mathbf{K}(\alpha'_1\dot{\mathbf{U}}^{n}+\alpha'_2\mathbf{V})$$

$$\mathbf{U}^{n+1}=\mathbf{U}^{n}+\tfrac{1}{2}\Delta t(\dot{\mathbf{U}}^{n}+\dot{\mathbf{U}}^{n+1})$$

Computed only if necessary

(i.e., if numerical damping and/or extended stability limits are locally necessary)

Enhanced explicit/implicit time integration

Solution algorithm for each time step of the analysis.

1. Compute vector $\overline{\mathbf{F}}$ by time integrating the force vector: $\overline{\mathbf{F}} = \int_{t^n}^{t^{n+1}} \mathbf{F}(\tau) d\tau$;
2. Compute the velocity vector:
   2.1 Solve: $\mathbf{E}\Delta\dot{\mathbf{U}} = \overline{\mathbf{F}} - \Delta t(\mathbf{C}\dot{\mathbf{U}}^n + \mathbf{K}(\mathbf{U}^n + \frac{1}{2}\Delta t\dot{\mathbf{U}}^n))$;
   (where $\mathbf{E}$ is defined by the assembling of $\mathbf{M}_e + \frac{1}{2}\Delta t\mathbf{C}_e + \alpha'^e_0\mathbf{K}_e$)
   2.2. Compute: $\dot{\mathbf{U}}^{n+1} = \dot{\mathbf{U}}^n + \Delta\dot{\mathbf{U}}$;
3. Update the computed velocity vector:
   3.1 Compute ϕ_η for each degree of freedom η of the model:
   If $(\dot{U}^{n+1}_\eta \dot{U}^n_\eta < 0)$, $\phi_\eta = 1$; otherwise, $\phi_\eta = 0$;
   3.2 Initialize vector $\mathbf{V} = \mathbf{0}$ and, for each element e of the spatial discretization:
   If $[\sum \phi_\eta]_e > 0$, assemble $\mathbf{K}_e(\alpha'^e_1\dot{\mathbf{U}}^n_e + \alpha'^e_2\dot{\mathbf{U}}^{n+1}_e)$ into $\mathbf{V}$;
   3.3 Update: $\dot{\mathbf{U}}^{n+1} = \dot{\mathbf{U}}^{n+1} - \mathbf{M}^{-1}\mathbf{V}$;
4. Compute the displacement vector: $\mathbf{U}^{n+1} = \mathbf{U}^n + \frac{1}{2}\Delta t(\dot{\mathbf{U}}^n + \dot{\mathbf{U}}^{n+1})$;

Adaptive parameters ($\alpha'^e_i = \frac{1}{2}\Delta t^2\alpha^e_i$).

Explicit ($\Omega^{\max}_e \leq 2$)	$\alpha^e_0 = 0$
	$\alpha^e_1 = 2(1 - \Omega^{\max}_e\xi_e)\Omega^{\max -4}_e$
	$\alpha^e_2 = 2(\Omega^{\max 2}_e - \Omega^{\max}_e\xi_e - 1)\Omega^{\max -4}_e$
Implicit	$\alpha^e_0 = \frac{1}{2} - 2\Omega^{\max -2}_e$
	$\alpha^e_1 = (\frac{1}{2}\Omega^{\max}_e - 2\xi_e)\Omega^{\max -3}_e$
	$\alpha^e_4 = (3\Omega^{\max}_e/2 - 2\xi_e)\Omega^{\max -3}_e$

Enhanced explicit/implicit time integration

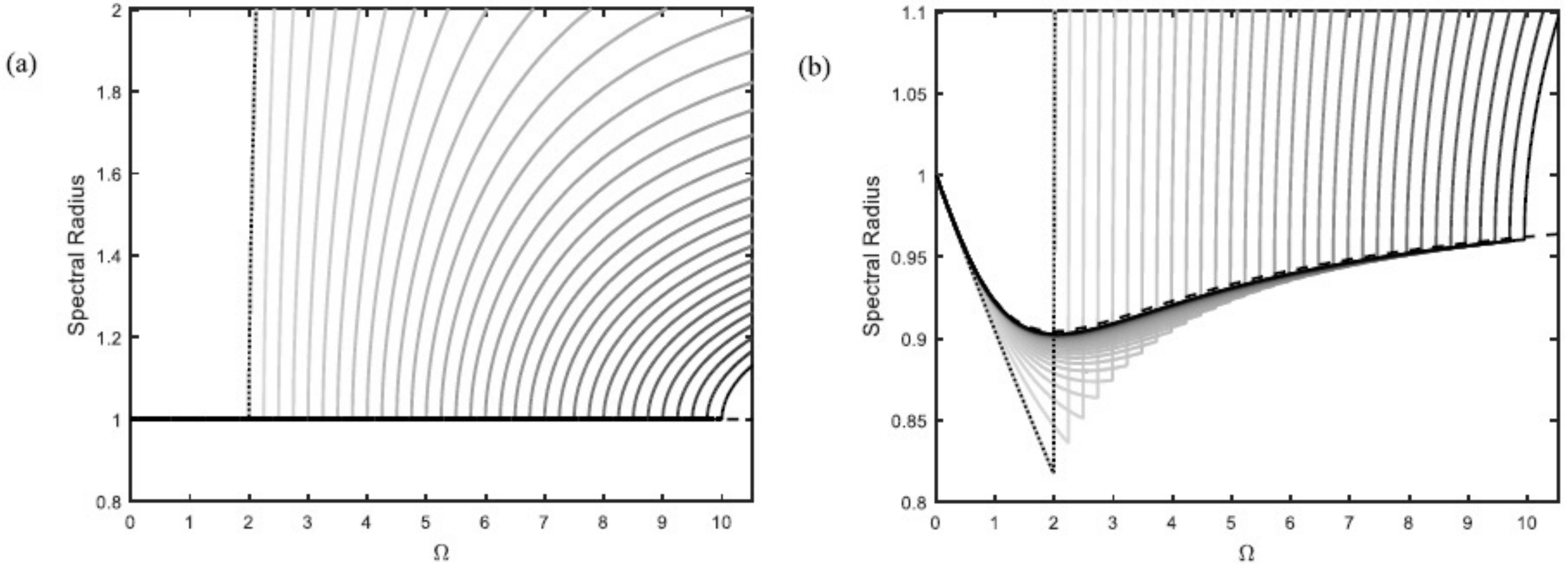

Spectral radii for $\Omega_e^{\max}(\equiv \Omega_c) = 1, 1.25, \ldots, 10$ (lighter to darker grey colour), considering explicit–implicit analyses without updating the computed velocity values (non-dissipative approach): (a) $\xi = 0.0$; (b) $\xi = 0.1$. Results for the CD and the TR are depicted as black dotted and dashed lines, respectively, for reference.

Enhanced explicit/implicit time integration

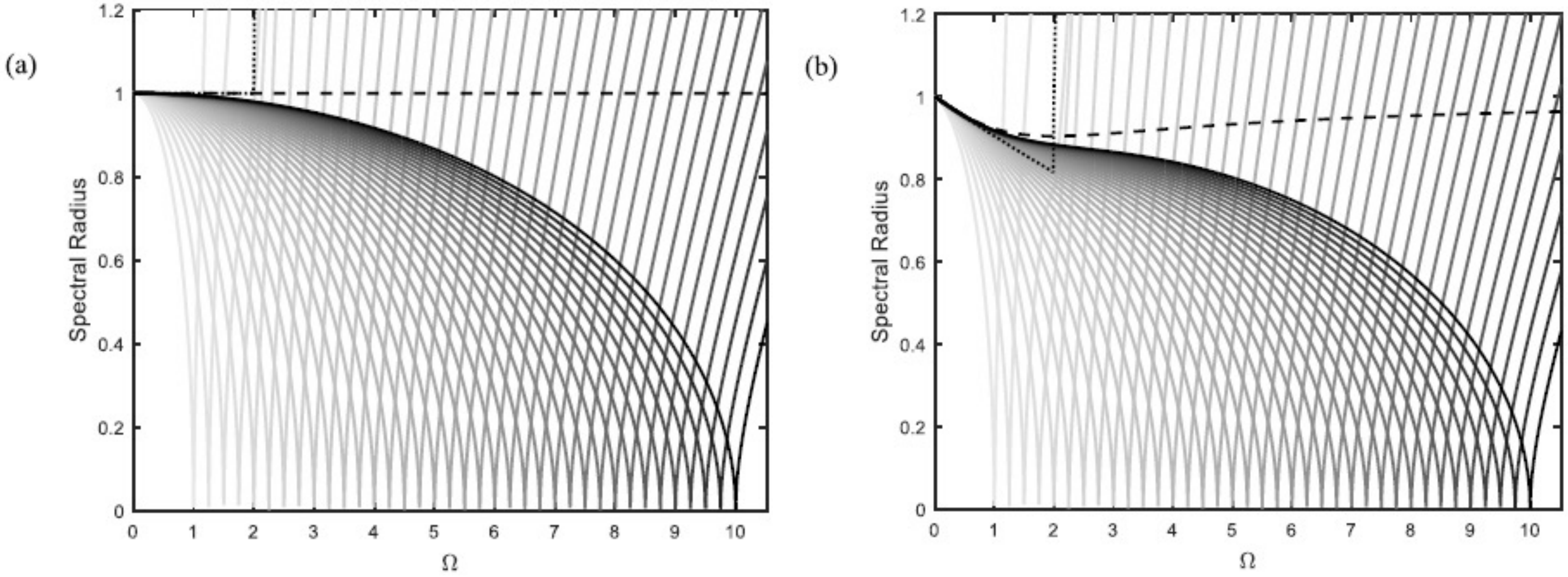

Spectral radii for $\Omega_e^{\max}(\equiv \Omega_b) = 1, 1.25, \ldots, 10$ (lighter to darker grey colour), considering explicit–implicit analyses updating the computed velocity values (dissipative approach): (a) $\xi = 0.0$; (b) $\xi = 0.1$. Results for the CD and the TR are depicted as black dotted and dashed lines, respectively, for reference.

Enhanced explicit/implicit time integration

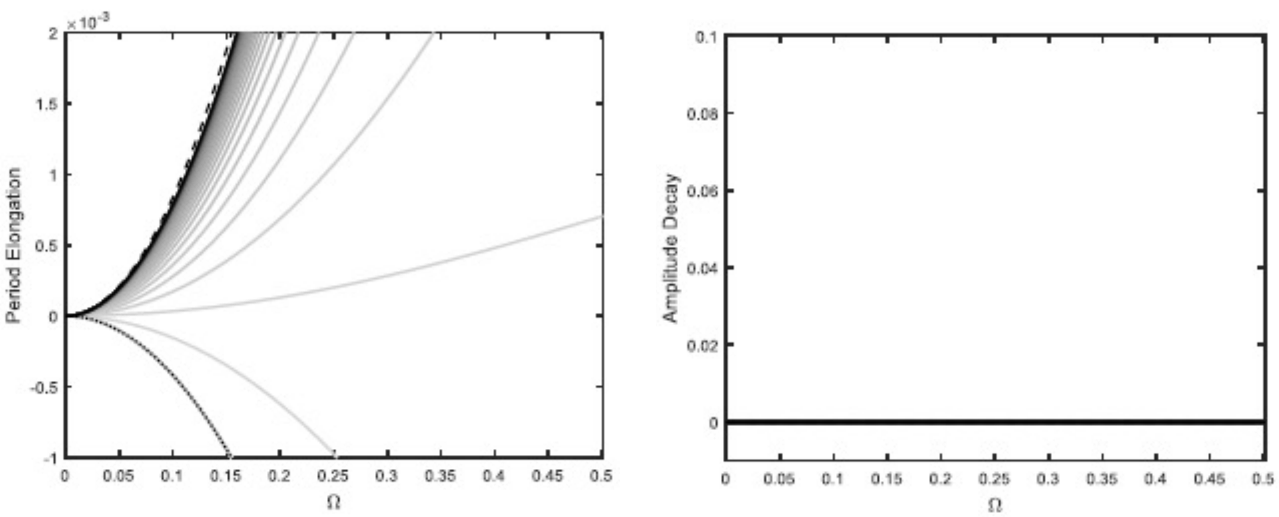

Period elongation and amplitude decay errors for the non-dissipative approach

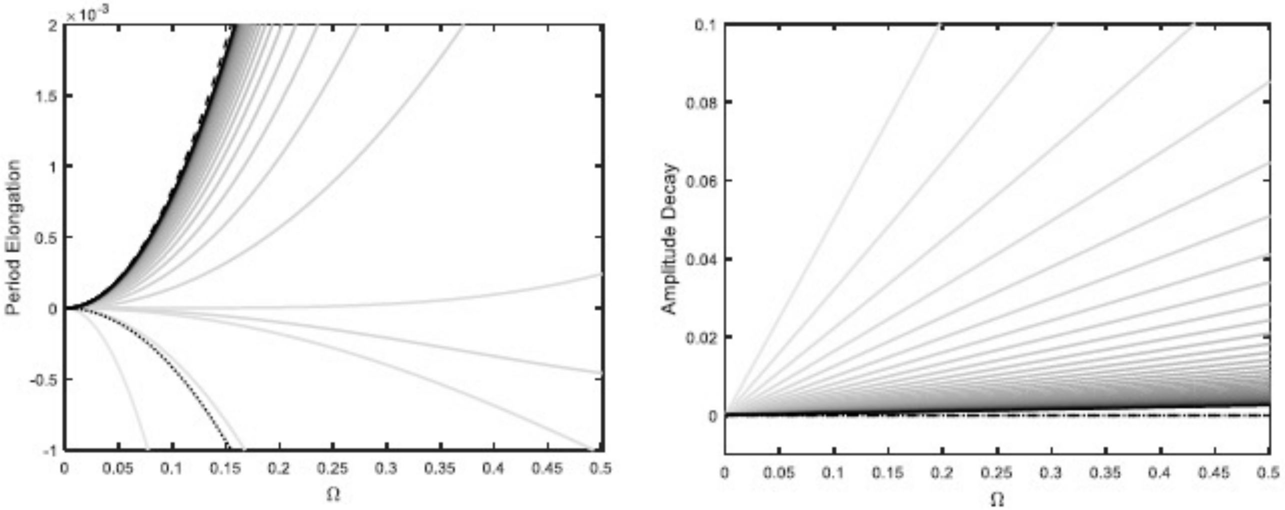

Period elongation and amplitude decay errors for the dissipative approach

Enhanced explicit/implicit time integration

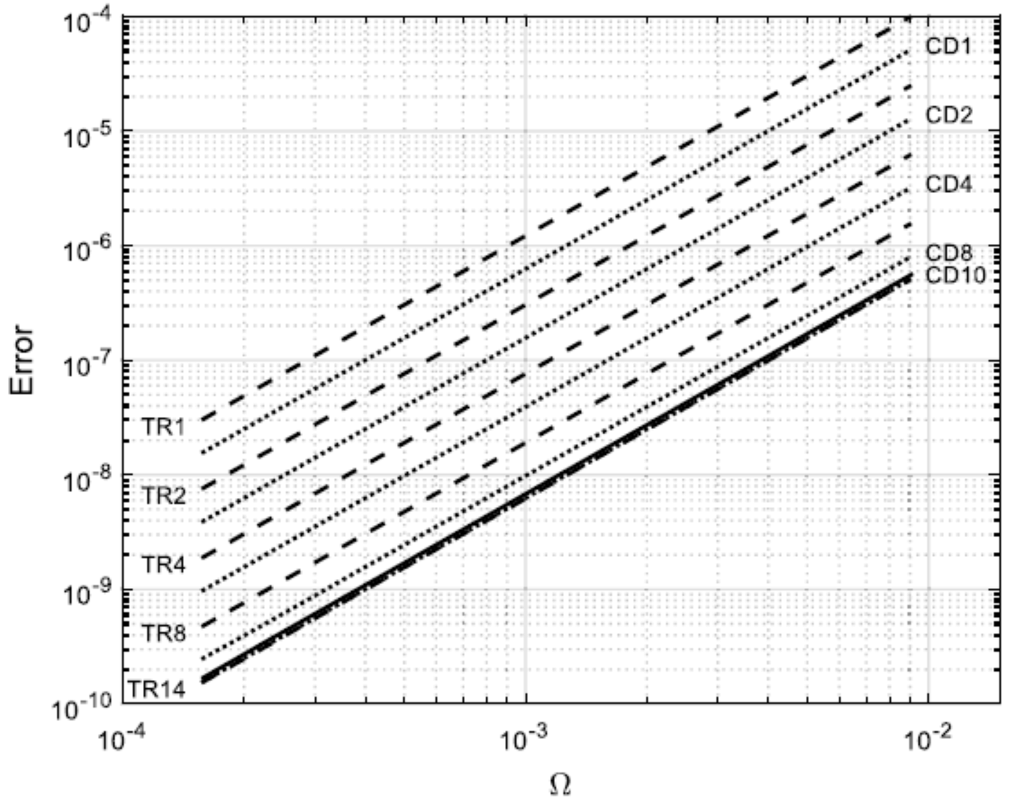

Convergence analysis considering the n-substep CD (dotted lines, results for $n = 1, 2, 4, 8$ and 10 are depicted), the n-substep TR (dashed lines, results for $n = 1, 2, 4, 8$ and 14 are depicted), and the new single-step technique without updating the computed velocity values (non-dissipative approach) for $\Omega_e^{max} = 2.46$ (solid line).

Enhanced explicit/explicit time integration

Solution algorithm for each time step of the analysis.

1. Compute vector $\overline{\mathbf{F}}$ by time integrating the force vector: $\overline{\mathbf{F}} = \int_{t^n}^{t^{n+1}} \mathbf{F}(\tau)d\tau$;
2. Compute vector $\mathbf{V}$: $\mathbf{V} = \dot{\mathbf{U}}^n + \mathbf{E}^{-1}(\overline{\mathbf{F}} - \Delta t\mathbf{C}\dot{\mathbf{U}}^n - \Delta t\mathbf{K}(\mathbf{U}^n + \frac{1}{2}\Delta t\dot{\mathbf{U}}^n))$;
3. Initialize vector $\mathbf{\Lambda} = \mathbf{0}$ and, for each element e of the spatial discretization:
   3.1. If $[\sum \phi_\eta]_e > 0$, $\alpha'_1 = \widetilde{\alpha}_1^e$ and $\alpha'_2 = \widetilde{\alpha}_2^e$; otherwise, $\alpha'_1 = \overline{\alpha}_1^e$ and $\alpha'_2 = \overline{\alpha}_2^e$;
   3.2. If ($\alpha'_1 \neq 0$ or $\alpha'_2 \neq 0$), assemble $\mathbf{K}_e(\alpha'_1\dot{\mathbf{U}}_e^n + \alpha'_2\mathbf{V}_e)$ into $\mathbf{\Lambda}$;
4. Compute the velocity vector: $\dot{\mathbf{U}}^{n+1} = \mathbf{V} - \mathbf{E}^{-1}\mathbf{\Lambda}$;
5. Compute the displacement vector: $\mathbf{U}^{n+1} = \mathbf{U}^n + \frac{1}{2}\Delta t(\dot{\mathbf{U}}^n + \dot{\mathbf{U}}^{n+1})$;
6. For each degree of freedom η of the model, update the oscillatory parameter ϕ_η:
   If ($\dot{U}_\eta^{n+1}\dot{U}_\eta^n < 0$), $\phi_\eta = 1$; otherwise, $\phi_\eta = 0$;

Enhanced explicit/explicit time integration

Adaptive non-dissipative parameters $\overline{\alpha}_1^e$ and $\overline{\alpha}_2^e$.

$0 < \Omega_e^{\max} \le 2$	$\overline{\alpha}_1^e = 0$ $\overline{\alpha}_2^e = 0$
$2 < \Omega_e^{\max} \le 2\sqrt{2}$	$\overline{\alpha}_1^e = \Delta t^2(-\Omega_e^{\max^3}\xi_e - \Omega_e^{\max^2}(4\xi_e^2 + 1) + 4)\Omega_e^{\max^{-4}}$ $\overline{\alpha}_2^e = \Delta t^2(\Omega_e^{\max^3}\xi_e - \Omega_e^{\max^2}(4\xi_e^2 - 1) - 8\Omega_e^{\max}\xi_e - 4)\Omega_e^{\max^{-4}}$
$2\sqrt{2} < \Omega_e^{\max} \le 4$	$\overline{\alpha}_1^e = \frac{1}{16}\Delta t^2(-4\xi_e - 1)$ $\overline{\alpha}_2^e = \frac{1}{16}\Delta t^2(4\xi_e + 1)$

Adaptive dissipative parameters $\widetilde{\alpha}_1^e$ and $\widetilde{\alpha}_2^e$.

$0 < \Omega_e^{\max} \le 1$	$\widetilde{\alpha}_1^e = \Delta t^2(-\xi_e^2 + 1)$ $\widetilde{\alpha}_2^e = \Delta t^2(-\xi_e^2 - \xi_e)$
$1 < \Omega_e^{\max} \le 3$	$\widetilde{\alpha}_1^e = \Delta t^2(-\Omega_e^{\max^2}\xi_e^2 + 1)\Omega_e^{\max^{-4}}$ $\widetilde{\alpha}_2^e = \Delta t^2(\Omega_e^{\max^3}\xi_e - \Omega_e^{\max^2}(\xi_e^2 - 1) - 2\Omega_e^{\max}\xi_e - 1)\Omega_e^{\max^{-4}}$
$3 < \Omega_e^{\max} \le 4$	$\widetilde{\alpha}_1^e = -\Delta t^2(\Omega_e^{\max^5}(\xi_e^3 - 2\xi_e^2 + \xi_e)$ $+\Omega_e^{\max^4}(\xi_e^4 - 8\xi_e^3 + 14\xi_e^2 - 8\xi_e + 1)$ $-\Omega_e^{\max^3}(6\xi_e^4 - 23\xi_e^3 + 32\xi_e^2 - 21\xi_e + 6)$ $+\Omega_e^{\max^2}(9\xi_e^4 - 24\xi_e^3 + 24\xi_e^2 - 16\xi_e + 8)$ $+\Omega_e^{\max}(6\xi_e^2 - 14\xi_e + 8) - (9\xi_e^2 - 24\xi_e + 16))\Omega_e^{\max^{-4}}$ $\widetilde{\alpha}_2^e = -\Delta t^2(\Omega_e^{\max^4}(\xi_e^4 - 2\xi_e^3 + \xi_e^2)$ $-\Omega_e^{\max^3}(6\xi_e^4 - 16\xi_e^3 + 12\xi_e^2 - \xi_e)$ $+\Omega_e^{\max^2}(9\xi_e^4 - 36\xi_e^3 + 45\xi_e^2 - 18\xi_e)$ $+\Omega_e^{\max}(18\xi_e^3 - 54\xi_e^2 + 46\xi_e - 8) + (9\xi_e^2 - 24\xi_e + 16))\Omega_e^{\max^{-4}}$

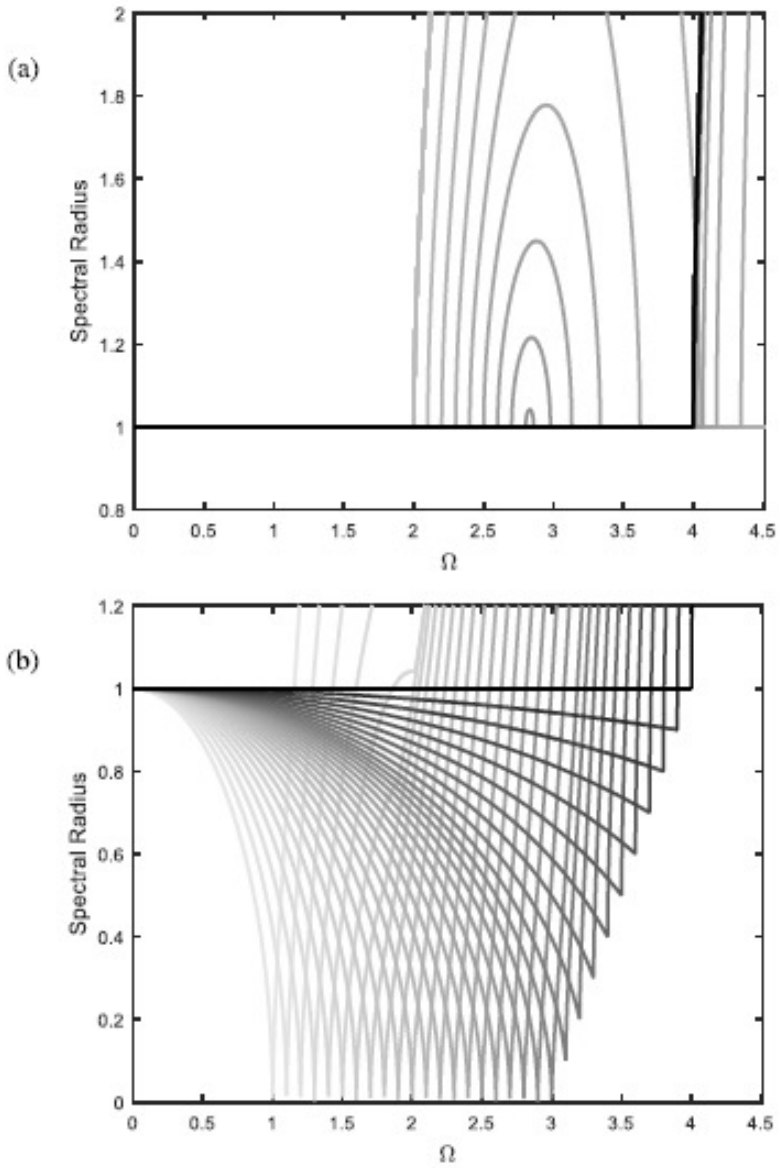

Spectral radii for $\Omega_e^{\max} = 1.0, 1.1, \ldots, 4.0$ (lighter to darker grey colour): (a) non-dissipative formulation (b) dissipative formulation

Enhanced explicit/explicit time integration

Method	Ω_{max}	Operations
New	4	1+
CD	2	1
EGα ($\rho_b = 0.3665$)	1.803[a]	1
NB ($p = 0.54$)	3.745[a]	2
RK	2.828[a]	4

[a]For undamped models.

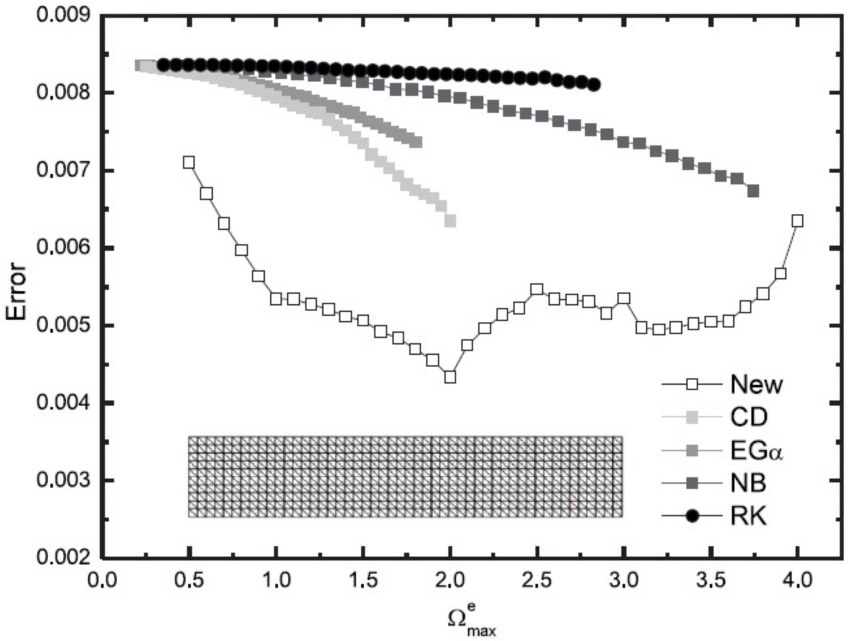

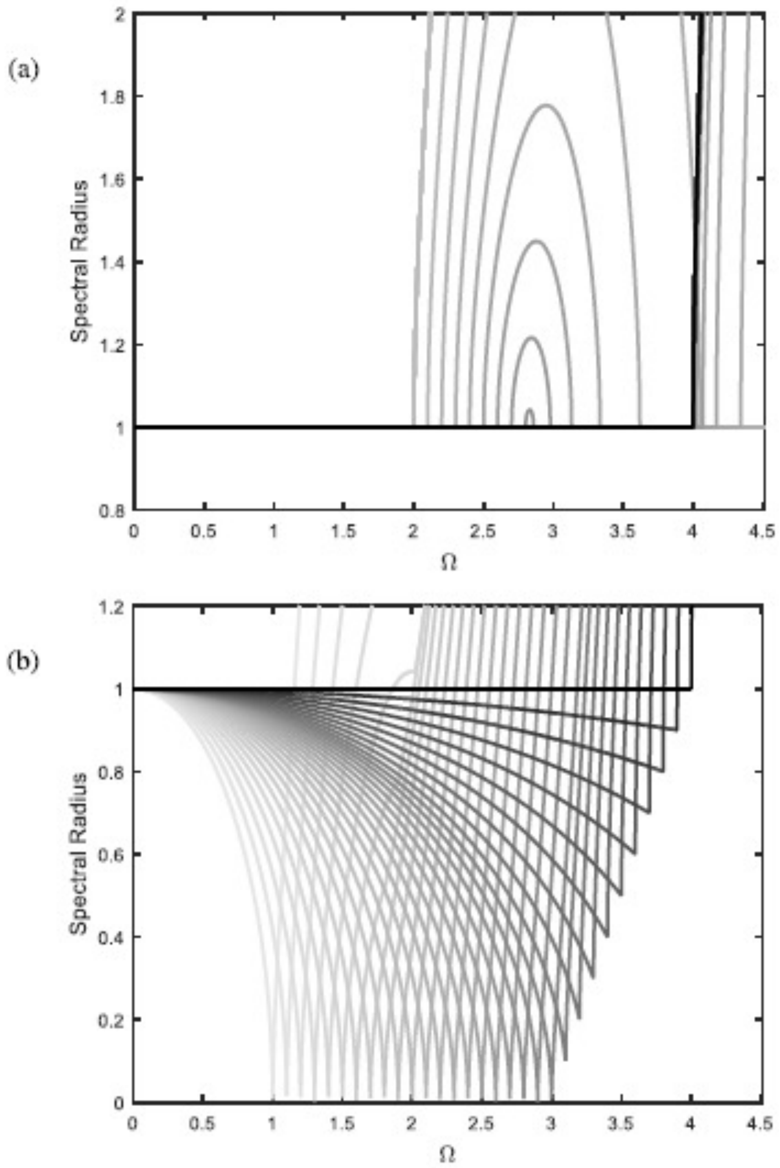

Spectral radii for $\Omega_e^{max} = 1.0, 1.1, \ldots, 4.0$ (lighter to darker grey colour): (a) non-dissipative formulation (b) dissipative formulation

Enhanced explicit/explicit time integration

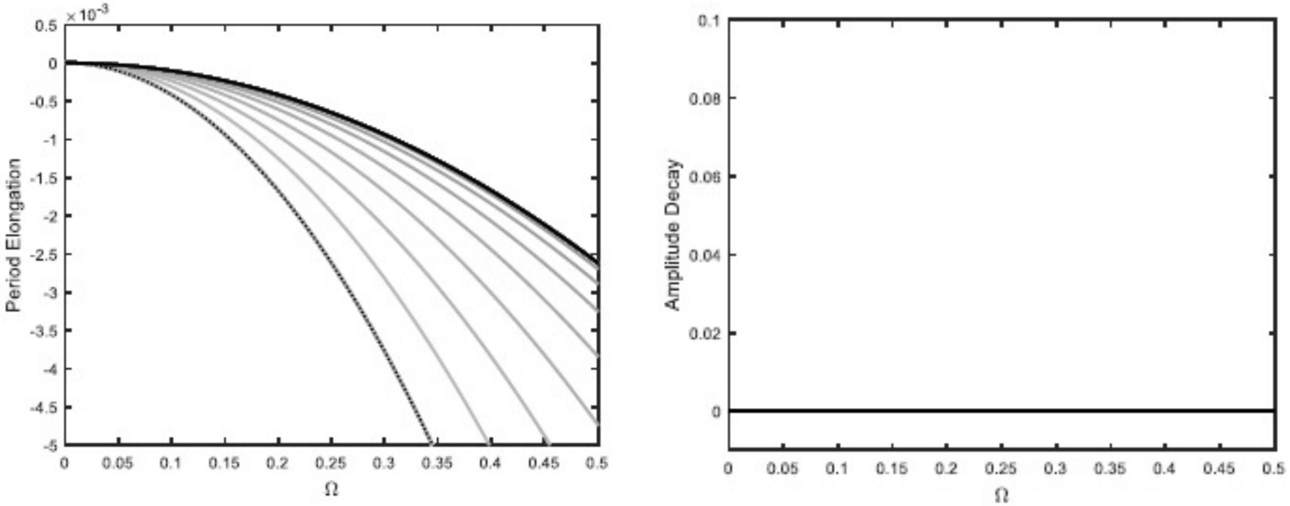

Period elongation and amplitude decay errors for the non-dissipative approach

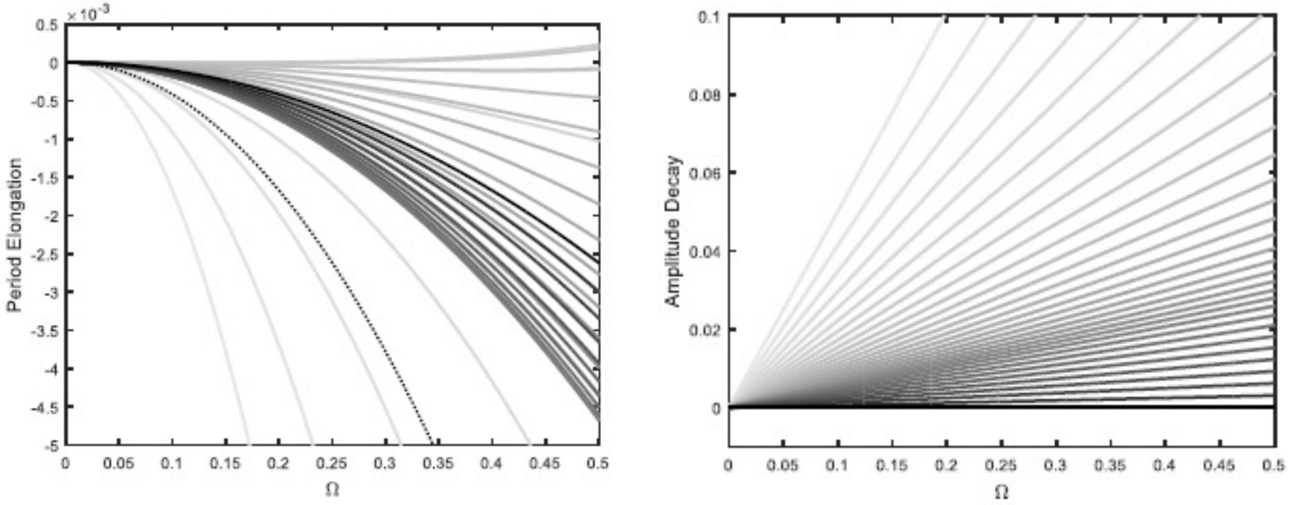

Period elongation and amplitude decay errors for the dissipative approach

Enhanced explicit/explicit time integration

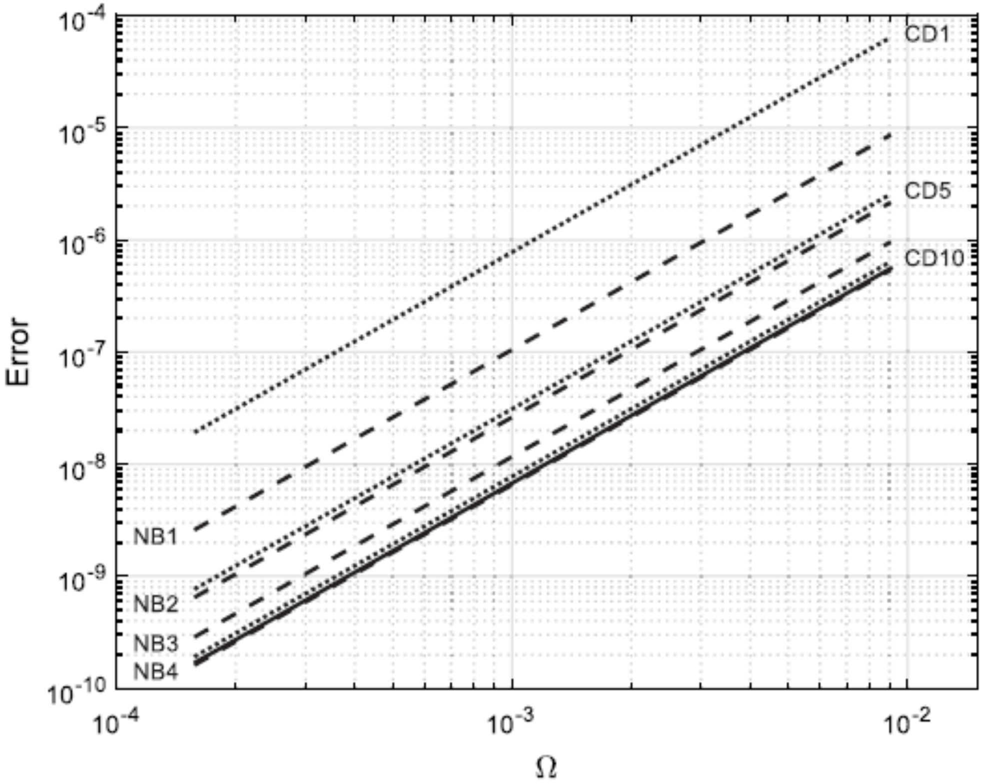

Convergence analysis considering the n-substep CD (dotted lines, results for $n = 1$, 5 and 10 are depicted), the n-substep NB (dashed lines, results for $n = 1$, 2, 3 and 4 are depicted), and the discussed technique

Numerical applications considering enhanced approaches

A rod and a membrane are here analysed, for which analytical answers are known:

$$u_A(x,t) = \frac{8AL}{E\pi^2} \sum_{n=1}^{\infty} \frac{(-1)^{n-1}}{(2n-1)^2} \sin\left(\frac{2n-1}{2L}\pi x\right) \left(1 - \cos\left(\frac{2n-1}{2L}\pi c t\right)\right)$$

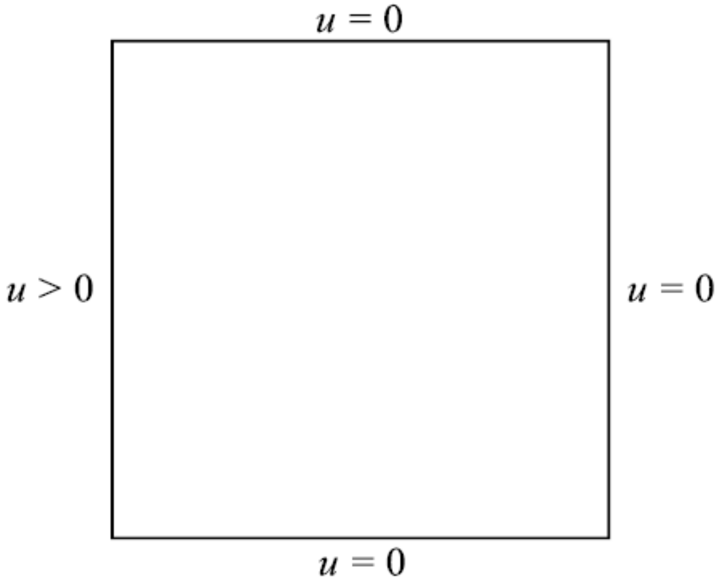

$$u_A(x,y,t) = \frac{2A}{\pi} \sum_{l=1}^{\infty} \frac{\cos(l\pi)-1}{l \sin\text{h}(l\pi L_x/L_y)} \sin\text{h}\left(\frac{l\pi(x-L_x)}{L_y}\right) \sin\left(\frac{l\pi y}{L_y}\right) + \\ + \frac{4A}{\pi^2} e^{-\frac{\varsigma t}{2\rho}} \sum_m^{\infty} \sum_n^{\infty} \frac{n L_y^2(\cos(m\pi)-1)}{m(L_x^2 m^2 + L_y^2 n^2)} f_{mn}(t) \sin\left(\frac{n\pi x}{L_x}\right) \sin\left(\frac{m\pi y}{L_y}\right)$$

Numerical applications

Adopted discretizations and computed errors for the enhanced explicit/implicit approach:

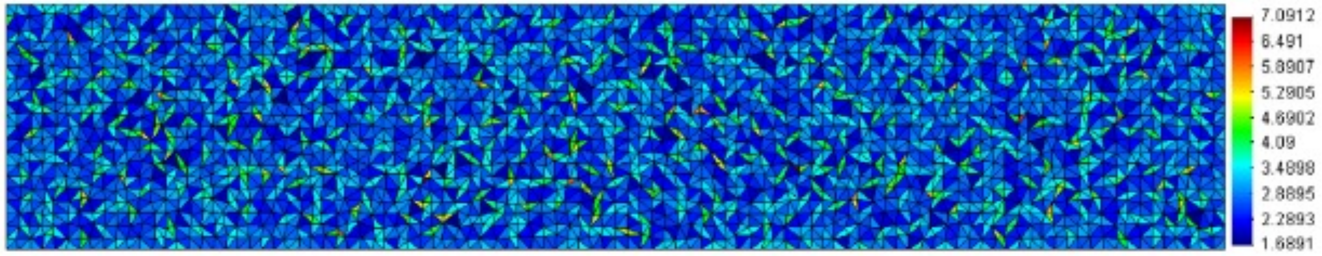

Adopted mesh (4k elements) for the rod and computed Ω_e^{max} values for Δt = 10^{-3}s.

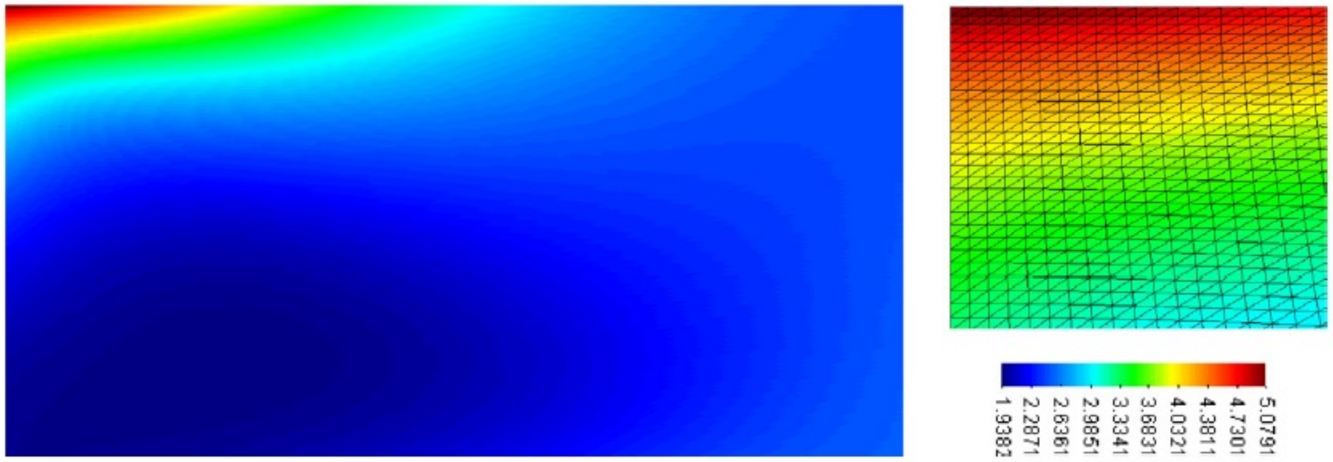

Adopted mesh (20k elements) for the membrane (in zoom) and computed Ω_e^{max} values for Δt =$5\cdot 10^{-4}$s.

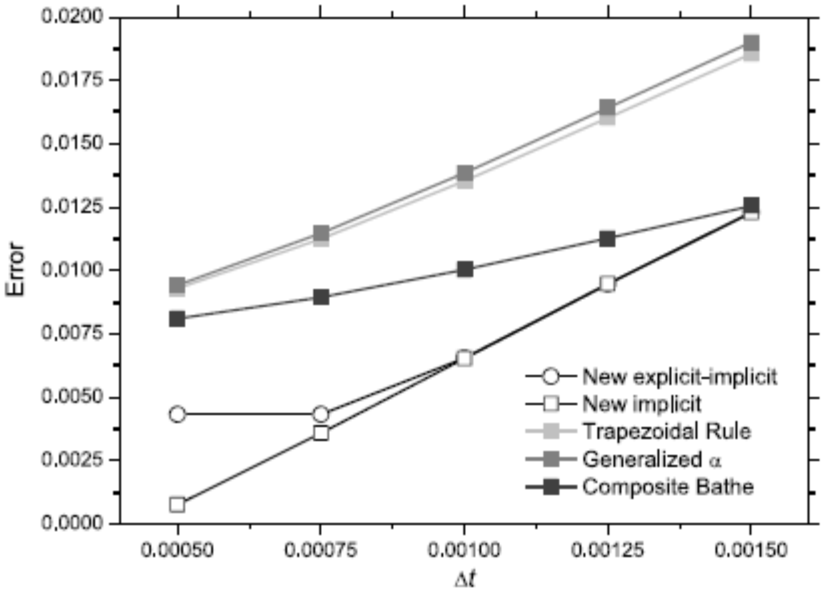

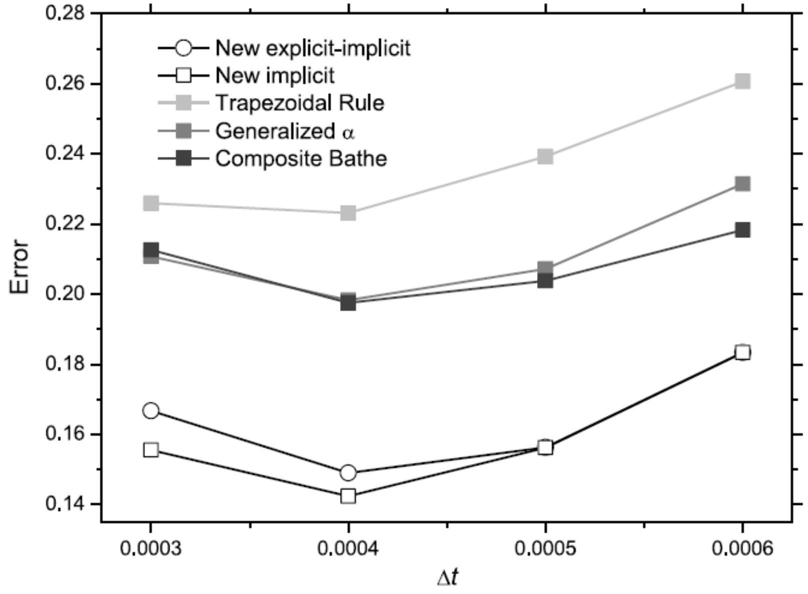

Numerical applications

Computed results for the enhanced explicit/implicit approach:

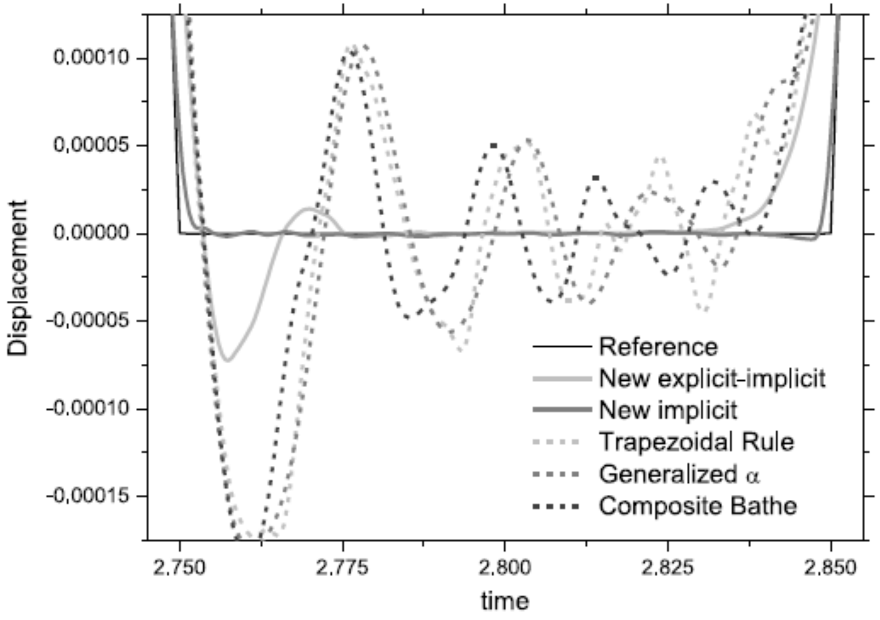

Zoomed view of the axial displacements at the middle of the rod

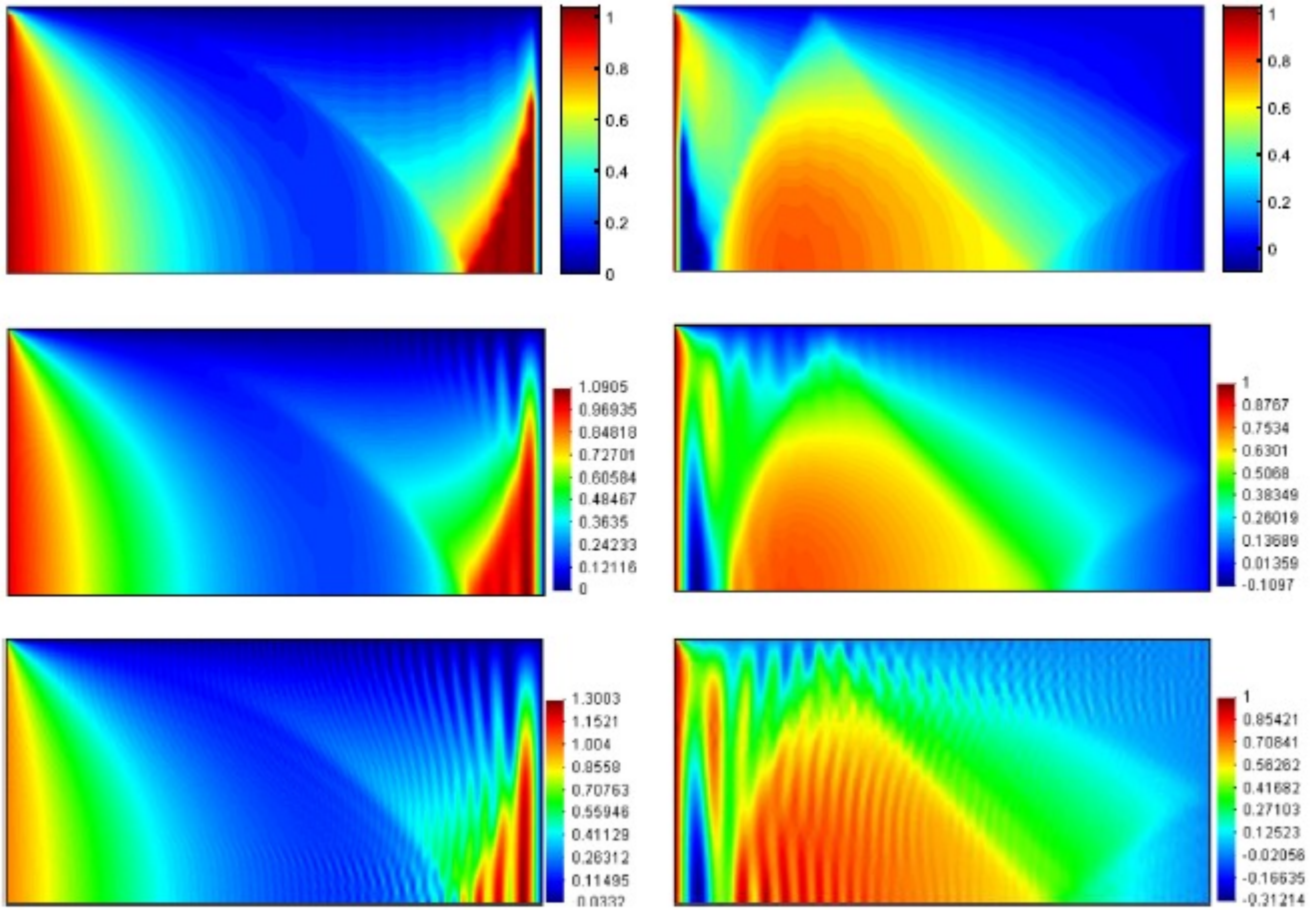

Computed results along the membrane, considering a mesh with 80k elements and $\Delta t = 2{\cdot}10^{-4}$ s: reference response (top); new explicit–implicit (middle); composite Bathe (bottom); at t = 0.1 s (left); and t = 0.2 s (right).

Numerical applications

Adopted discretizations and computed errors for the enhanced explicit/explicit approach:

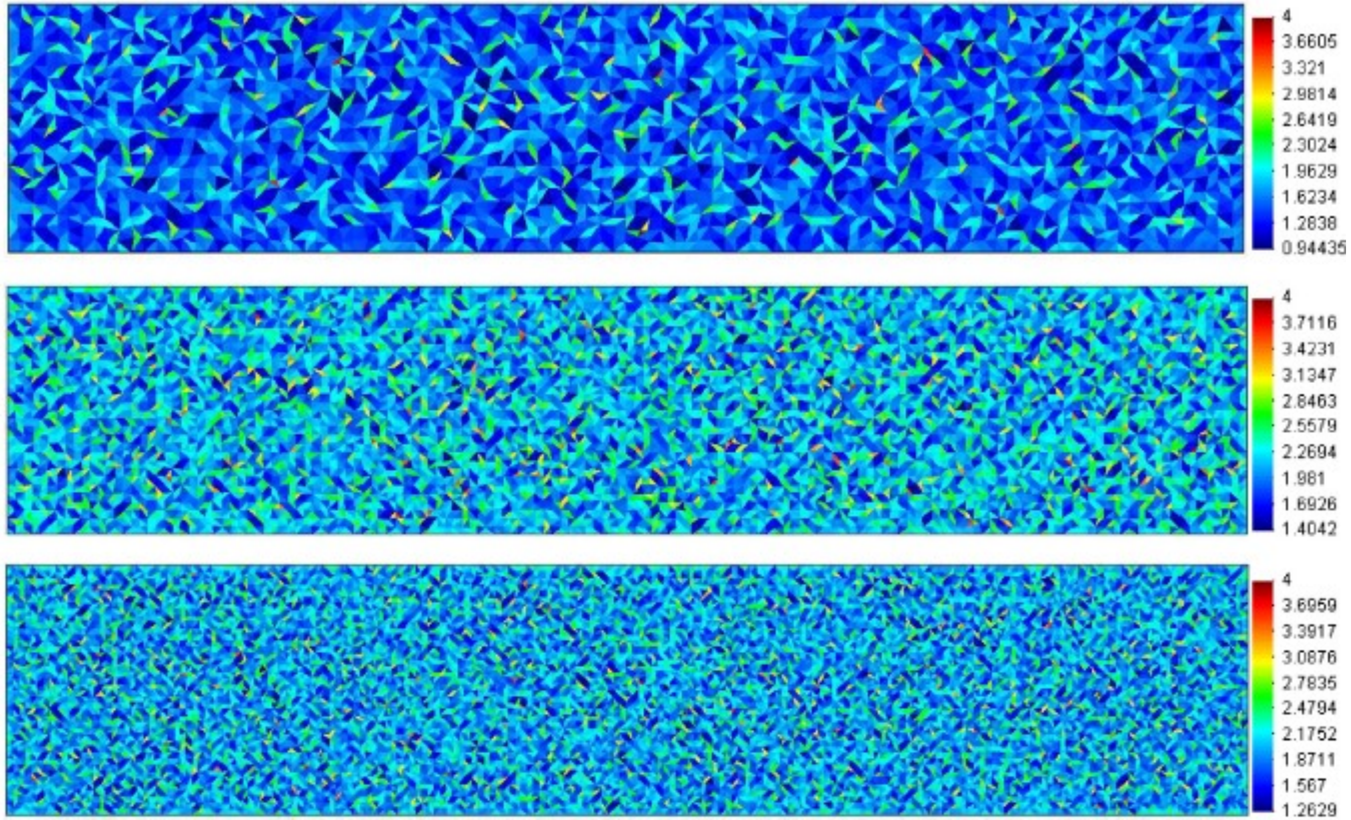

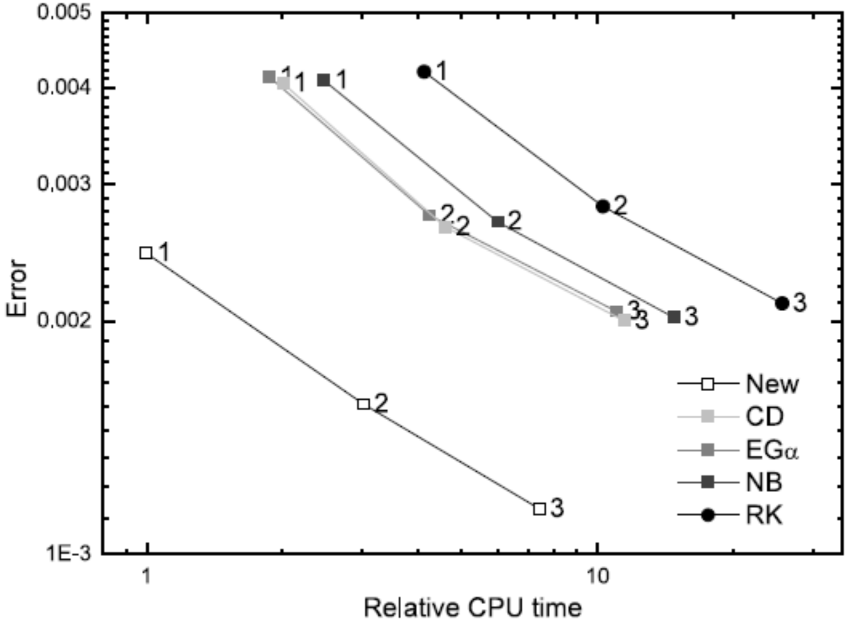

Adopted meshes for the rod analysis and computed Ω_e^{max} values:
discretization 1 (4k elements); discretization 2 (9k elements); discretization 3 (16k elements)

Numerical applications

Adopted discretizations and computed errors for the enhanced explicit/explicit approach:

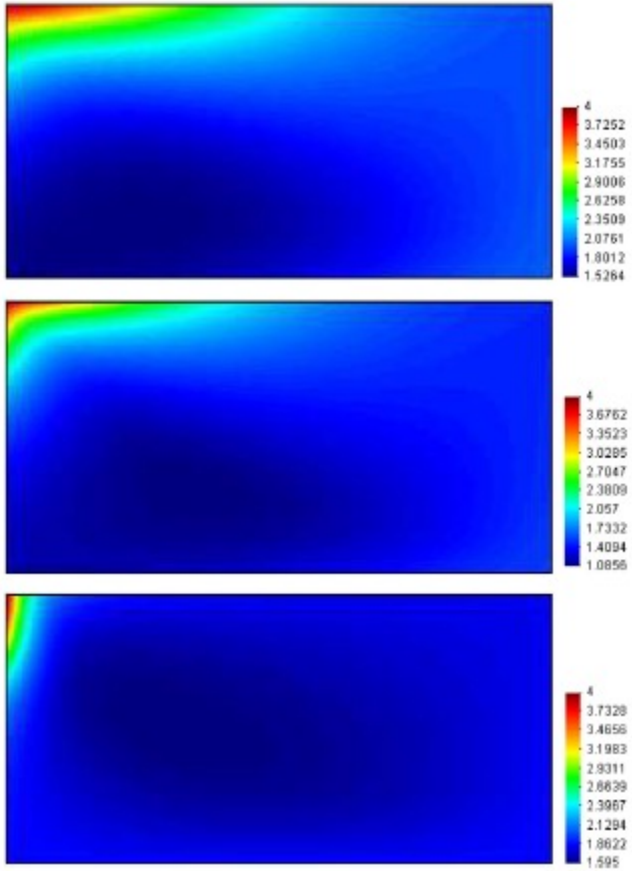

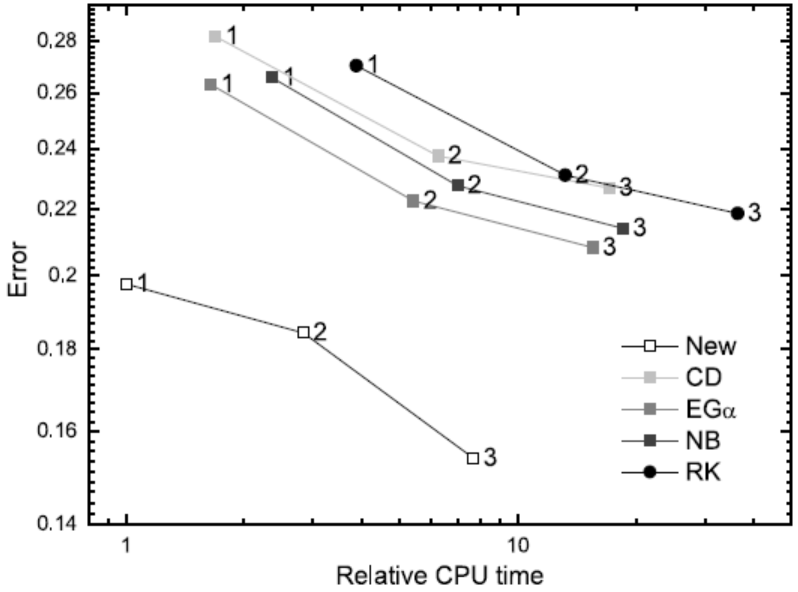

Ω_e^{max} values for discretization 1 (20k elements); discretization 2 (40k elements); and discretization 3 (80k elements)

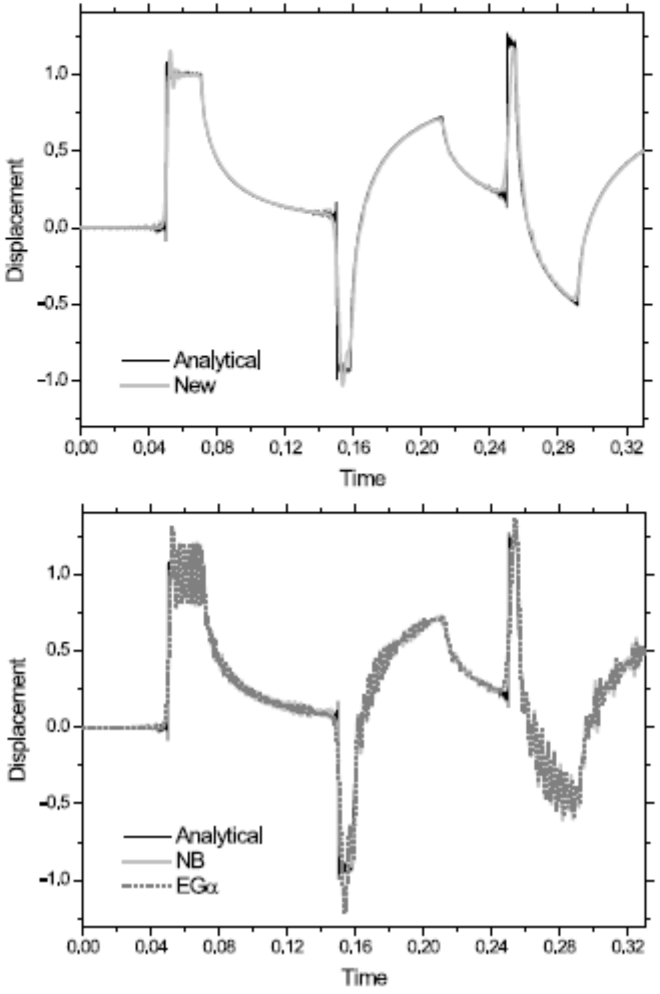

Time-history results at the middle of the membrane (discretization 3)

Numerical applications

Computed results for the enhanced explicit/explicit approach:

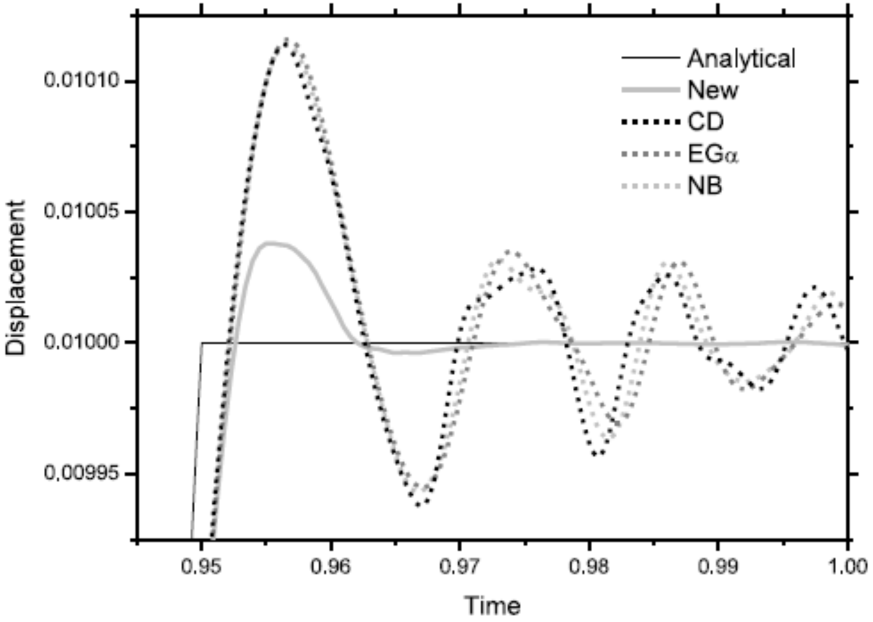

Zoomed view of the axial displacements at the middle of the rod (discretization 1)

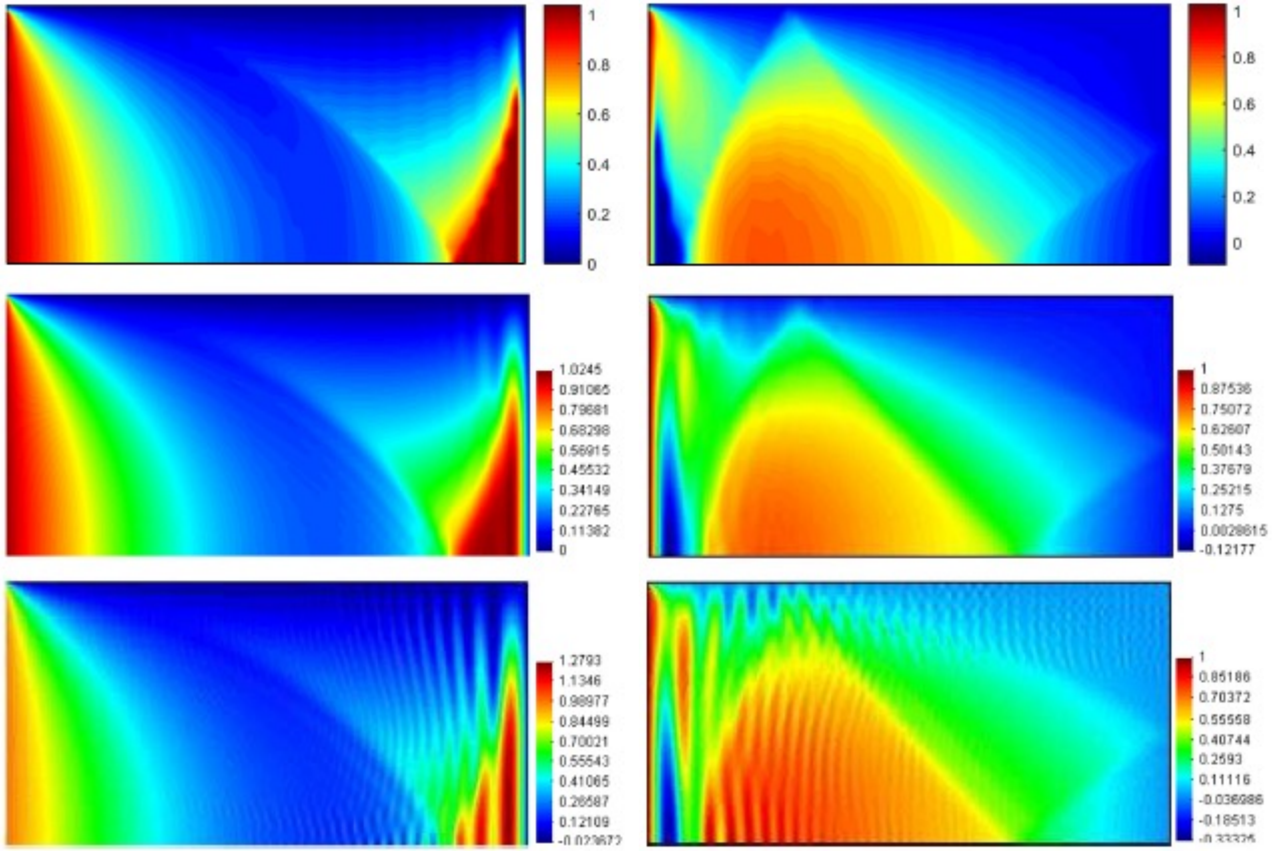

Computed results along the membrane: reference response (top); new explicit/explicit (middle); NB (bottom); t = 0.1 s and discretization 2 (left); t = 0.2 s and discretization 3 (right).

Alternative time integration procedures

Several other adaptive time integration procedures may be elaborated, providing different numerical properties and computational performances, which may be more suitable and/or better explored, according to the features of the model.

One last adaptive time integration procedure is discussed here, which not only enables stable analyses and reduced solver efforts (as in the referred explicit/implicit techniques), but also allows to avoid iterative computations (as, for instance, in nonlinear analyses, decoupled solutions of multiphysic applications etc.). This procedure is here referred to as an adaptive semi-explicit/explicit approach.

Adaptive semi-explicit/explicit time integration procedure

Consider the following nonlinear system of equations:
(where the nonlinear relations of the model are represented within vector **P**)

$$\mathbf{M}\ddot{\mathbf{U}}(t) + \mathbf{C}\dot{\mathbf{U}}(t) + \mathbf{P}(t) = \mathbf{F}(t)$$

By introducing a dissipative time integration parameter α, this system can be rewritten, at a given time instant *n*, as:

$$\mathbf{M}\ddot{\mathbf{U}}^n + \mathbf{C}\dot{\mathbf{U}}^n + (1+\alpha)\mathbf{P}^n - \alpha\mathbf{P}^{n-1} = \mathbf{F}^n$$

which, after considering the standard central difference method to approximate its time derivatives (as described on the right), may generate the following, locally-written, recurrence relationship, once a modified mass matrix is considered (as in selective mass scaling techniques):

$$\ddot{\mathbf{U}}^n = \frac{1}{\Delta t^2}(\mathbf{U}^{n+1} - 2\mathbf{U}^n + \mathbf{U}^{n-1})$$

$$\dot{\mathbf{U}}^n = \frac{1}{2\Delta t}(\mathbf{U}^{n+1} - \mathbf{U}^{n-1})$$

$$(\overline{\mathbf{M}}_e + \frac{1}{2}\Delta t\mathbf{C}_e)\mathbf{U}_e^{n+1} = \Delta t^2(\mathbf{F}_e^n - (1+\alpha_e^n)\mathbf{P}_e^n + \alpha_e^n\mathbf{P}_e^{n-1}) + \overline{\mathbf{M}}_e(2\mathbf{U}_e^n - \mathbf{U}_e^{n-1}) + \frac{1}{2}\Delta t\mathbf{C}_e\mathbf{U}_e^{n-1}$$

This modified mass matrix is here properly defined as:
(where $\mathbf{K}_e^\tau$ stands for the tangent nonlinear stiffness matrix of the model)

$$\overline{\mathbf{M}}_e = \mathbf{M}_e + \Delta t^2 a_e^\tau \mathbf{K}_e^\tau$$

Adaptive semi-explicit/explicit time integration procedure

In this case, similarly to the discussed explicit/implicit approach, the parameters of the semi-explicit/explicit procedure may be adaptively computed as follows:

$$\text{If } \Omega_e^{\max} \leq 2,\ a_e^{\tau} = 0$$

$$\text{If } \Omega_e^{\max} > 2,\ a_e^{\tau} = \frac{1}{4}\tanh\left(\frac{1}{4}\Omega_e^{\max}\right)$$

$$\varphi_e^{n+1} = \sum_{i=1}^{\eta_e} \left| \left|u_i^{n+1} - u_i^{n-1}\right| - \left|u_i^{n+1} - u_i^{n}\right| - \left|u_i^{n} - u_i^{n-1}\right| \right|$$

$$\text{If}\left(\underset{j=n-m}{\overset{n}{or}}\left(\varphi_e^{j} = 0\right)\right),\quad \alpha_e^{n} = 0$$

$$\text{If}\left(\underset{j=n-m}{\overset{n}{and}}\left(\varphi_e^{j} \neq 0\right)\right),\quad \alpha_e^{n} = \frac{2}{\Omega_e^{\max}}\left(\left(1 + \frac{\varsigma_e \Delta t}{2\rho_e} + a_e \Omega_e^{\max^2}\right)^{1/2} - \frac{\varsigma_e \Delta t}{2\rho_e \Omega_e^{\max}}\right) - 1$$

Adaptive semi-explicit/explicit time integration procedure

For a nonlinear model, the following updating criterion for the local tangent matrices $\mathbf{K}^{\tau}_{e}$ may be established, based on stability aspects, avoiding their continuous (and computationally demanding) updating for each time step:

$$\text{If } [(\frac{1}{2}\alpha_e^n + \frac{1}{4})\mu_e^{n^2} - a_e^{\tau}]\Omega_e^{\max^2} > 1, \text{ update } \mathbf{K}_e^{\tau}$$

where μ^{n}_{e} stands for the instantaneous degree of nonlinearity of the element (for $\mu = 1$, linear behaviour is reproduced).

Adaptive semi-explicit/explicit time integration procedure

As highlighted, this formulation may become very effective to analyse multiphysic applications, allowing decoupling their governing equations. The numerical solutions of two coupled problems are discussed next, both of them considering solid/fluid interactions. In the first model, the referred coupling occurs through a common interface between the different subdomains of the model, whereas, in the second case, it takes place through the governing PDEs of the problem.

PDEs for some coupled wave propagation models:
(with index notation)

Acoustic/elastodynamic models

$$(Kp_{,i})_{,i} - \rho\ddot{p} - \xi\dot{p} + S = 0$$

$$\sigma_{ij,j} - \rho\ddot{u}_i - \rho\zeta\dot{u}_i + \rho b_i = 0$$

interface: $\ddot{u}_n - (1/\rho)q = 0$

$\tau_n + p = 0$

+ boundary and initial conditions

Porodynamic models

$$\sigma_{ij,j} - \rho_m\ddot{u}_i - \varsigma\dot{u}_i + \rho_m b_i = 0$$

$$\alpha\dot{\varepsilon}_{ii} - (\kappa_{ij}p_{,j})_{,i} + (1/Q)\dot{p} + a = 0$$

where: $\sigma'_{ij} = \sigma_{ij} + \alpha\delta_{ij}p$

$\varepsilon_{ij} = (u_{i,j} + u_{j,i})/2$

+ boundary and initial conditions

Adaptive semi-explicit/explicit time integration procedure

Coupled acoustic/elastodynamic models

The following matrix equation is obtained, once the FEM is applied to spatially discretize the acoustic/elastodynamic subdomains of the model: $\mathbf{M}\ddot{\mathbf{X}}(t) + \mathbf{C}\dot{\mathbf{X}}(t) + \mathbf{K}\mathbf{X}(t) = \mathbf{F}(t) + \mathbf{R}(t)$

Solid subdomains:

$$\mathbf{M}_{se} = \int_{\Pi_e} \mathbf{N}_s^T \rho_s \mathbf{N}_s \, d\Pi$$

$$\mathbf{C}_{se} = \int_{\Pi_e} \mathbf{N}_s^T \varsigma_s \mathbf{N}_s \, d\Pi$$

$$\mathbf{K}_{se} = \int_{\Pi_e} \mathbf{B}_s^T \mathbf{D}_s \mathbf{B}_s \, d\Pi$$

$$\mathbf{F}_{se} = \int_{\Gamma_{2e}} \mathbf{N}_s^T \bar{\boldsymbol{\tau}} \, d\Gamma + \int_{\Pi_e} \mathbf{N}_s^T \mathbf{b} \, d\Pi \;\; \Pi$$

$$(\mathbf{R}_{ie})_s = \int_{\Gamma_{ie}} \mathbf{N}_s^T \bar{\boldsymbol{\tau}} \, d\Gamma = \int_{\Gamma_{ie}} \mathbf{N}_s^T \mathbf{n}_f \mathbf{N}_f \, d\Gamma \, \mathbf{P}_{ie} = \mathbf{Q}_{ie}^T \mathbf{P}_{ie} = -\kappa_f \rho_f \, \mathbf{Q}_{ie} \ddot{\mathbf{U}}_{ie} = -\mathbf{Q}'_{ie} \ddot{\mathbf{U}}_{ie}$$

Adaptive semi-explicit/explicit time integration procedure

Coupled acoustic/elastodynamic models

The following matrix equation is obtained, once the FEM is applied to spatially discretize the acoustic/elastodynamic subdomains of the model: $\mathbf{M}\ddot{\mathbf{X}}(t) + \mathbf{C}\dot{\mathbf{X}}(t) + \mathbf{K}\mathbf{X}(t) = \mathbf{F}(t) + \mathbf{R}(t)$

Solution procedure (for each subdomain):

$$(\overline{\mathbf{M}}_e + \frac{1}{2}\Delta t\mathbf{C}_e)\mathbf{X}_e^{n+1} = \Delta t^2(\mathbf{F}_e^n + \mathbf{R}_{ie}^n - \mathbf{K}_e((1+\alpha_e^n)\mathbf{X}^n - \alpha_e^n\mathbf{X}^{n-1})) + \overline{\mathbf{M}}_e(2\mathbf{X}_e^n - \mathbf{X}_e^{n-1}) + \frac{1}{2}\Delta t\mathbf{C}_e\mathbf{X}_e^{n-1}$$

where $\overline{\mathbf{M}}_e = \mathbf{M}_e + a_e\Delta t^2\mathbf{K}_e + b_e\Delta t^2\mathbf{W}_{ie}$

$$(\mathbf{W}_{ie})_f = \mathbf{Q}'_{ie}(\mathbf{M}_{se}^{-1})_i\mathbf{Q}_{ie}^T$$
$$(\mathbf{W}_{ie})_s = \mathbf{Q}_{ie}^T(\mathbf{M}_{fe}^{-1})_i\mathbf{Q}'_{ie}$$

if $\Omega_e^{\max} < 2,\ a_e = 0$

if $\Omega_e^{\max} \geq 2,\ a_e = \frac{1}{4}\tanh(\frac{1}{4}\Omega_e^{\max})$

if $\Gamma_e \cap \Gamma_i = \varnothing,\ b_e = 0$

if $\Gamma_e \cap \Gamma_i \neq \varnothing,\ b_e = \frac{1}{4}$

Adaptive semi-explicit/explicit time integration procedure

Coupled acoustic/elastodynamic models

The following matrix equation is obtained, once the FEM is applied to spatially discretize the acoustic/elastodynamic subdomains of the model: $\mathbf{M}\ddot{\mathbf{X}}(t) + \mathbf{C}\dot{\mathbf{X}}(t) + \mathbf{K}\mathbf{X}(t) = \mathbf{F}(t) + \mathbf{R}(t)$

Solution procedure:

$$(\overline{\mathbf{M}}_{se} + \frac{1}{2}\Delta t\mathbf{C}_{se})\mathbf{U}_e^{n+1} = \Delta t^2\mathbf{Q}_{ie}^T\mathbf{P}_{ie}^n$$
$$+\Delta t^2(\mathbf{F}_{se}^n - \mathbf{K}_{se}((1+\alpha_{se}^n)\mathbf{U}_e^n - \alpha_{se}^n\mathbf{U}_e^{n-1})) + \overline{\mathbf{M}}_{se}(2\mathbf{U}_e^n - \mathbf{U}_e^{n-1}) + \frac{1}{2}\Delta t\mathbf{C}_{se}\mathbf{U}_e^{n-1}$$
$$(\overline{\mathbf{M}}_{fe} + \frac{1}{2}\Delta t\mathbf{C}_{fe})\mathbf{P}_e^{n+1} = \mathbf{Q}_{ie}'(\mathbf{U}_{ie}^{n+1} - 2\mathbf{U}_{ie}^n + \mathbf{U}_{ie}^{n-1})$$
$$+\Delta t^2(\mathbf{F}_{fe}^n - \mathbf{K}_{fe}((1+\alpha_{fe}^n)\mathbf{P}_e^n - \alpha_{fe}^n\mathbf{P}_e^{n-1})) + \overline{\mathbf{M}}_{fe}(2\mathbf{P}_e^n - \mathbf{P}_e^{n-1}) + \frac{1}{2}\Delta t\mathbf{C}_{fe}\mathbf{P}_e^{n-1}$$

Adaptive semi-explicit/explicit time integration procedure

Coupled acoustic/elastodynamic models

Stability analysis, considering an equivalent group of scalar equations:

$$m_s\ddot{u} + c_s\dot{u} + k_s u - q_s p - f_s = 0$$
$$m_f\ddot{p} + c_f\dot{p} + k_f p + q_f\ddot{u} - f_f = 0$$

Recursive relationship:

$$\begin{bmatrix} u^{n+1} \\ u^n \\ p^{n+1} \\ p^n \end{bmatrix} = \begin{bmatrix} A_{11} & A_{12} & A_{13} & A_{14} \\ A_{21} & A_{22} & A_{23} & A_{24} \\ A_{31} & A_{32} & A_{33} & A_{34} \\ A_{41} & A_{42} & A_{43} & A_{44} \end{bmatrix} \begin{bmatrix} u^n \\ u^{n-1} \\ p^n \\ p^{n-1} \end{bmatrix} + \begin{bmatrix} L_1 \\ L_2 \\ L_3 \\ L_4 \end{bmatrix} = \mathbf{A} \begin{bmatrix} u^n \\ u^{n-1} \\ p^n \\ p^{n-1} \end{bmatrix} + \mathbf{L}$$

where:

$$A_{11} = (2m_f m_s + 2a_s m_f k_s \Delta t^2 - (1+\alpha_s) m_f k_s \Delta t^2 + 2b_s q_f q_s \Delta t^2)/\Lambda_s$$
$$A_{12} = (-m_f m_s + \frac{1}{2} m_f c_s \Delta t - (a_s - \alpha_s) m_f k_s \Delta t^2 - b_s q_f q_s \Delta t^2)/\Lambda_s$$
$$A_{13} = m_f q_s \Delta t^2 / \Lambda_s$$
$$A_{14} = 0$$
$$A_{21} = 1$$
$$A_{22} = 0$$
$$A_{23} = 0$$
$$A_{24} = 0$$
$$A_{31} = q_f m_f m_s (c_s \Delta t + (1+\alpha_s) k_s \Delta t^2)/\mathrm{A}$$
$$A_{32} = -q_f m_f m_s (c_s \Delta t + \alpha_s k_s \Delta t^2)/\mathrm{A}$$

$$\begin{aligned} A_{33} = {} & (2m_f^2 m_s^2 + m_f^2 m_s c_s \Delta t + (2b_s + 2b_f - 1) q_f q_s m_f m_s \Delta t^2 \\ & + 2a_s m_f^2 m_s k_s \Delta t^2 + (2a_f - \alpha_f - 1) m_f m_s^2 k_f \Delta t^2 \\ & + \frac{1}{2}(2a_f - \alpha_f - 1) m_f m_s c_s k_f \Delta t^3 + b_f q_f q_s m_f c_s \Delta t^3 \\ & + (2a_f - \alpha_f - 1) a_s m_f m_s k_s k_f \Delta t^4 + (2a_f - \alpha_f - 1) b_s m_s q_f q_s k_f \Delta t^4 \\ & + 2b_f a_s m_f q_f q_s k_s \Delta t^4 + 2b_f b_s q_f^2 q_s^2 \Delta t^4)/\mathrm{A} \end{aligned}$$
$$A_{34} = (-m_s m_f + \frac{1}{2} m_s c_f \Delta t - (a_f - \alpha_f) m_s k_f \Delta t^2 - b_f q_s q_f \Delta t^2)/\Lambda_f$$
$$A_{41} = 0$$
$$A_{42} = 0$$
$$A_{43} = 1$$
$$A_{44} = 0$$

and:

$$\Lambda_s = m_f \chi_s + b_s q_f q_s \Delta t^2 \qquad \chi_j = m_j + \tfrac{1}{2} c_j \Delta t + a_j k_j \Delta t^2$$
$$\Lambda_f = m_s \chi_f + b_f q_s q_f \Delta t^2 \qquad \mathrm{A} = \Lambda_s \Lambda_f$$

Adaptive semi-explicit/explicit time integration procedure

Coupled acoustic/elastodynamic models

The roots λ of the characteristic polynomial $p_{\mathbf{A}}(\lambda)$ of the amplification matrix **A** determine the stability properties of the method. In order to ensure stability, the modulus of all these roots must be less or equal to one (when the modulus is unity, the root must be a simple one). If λ is replaced by (z +1)/(z −1), the equivalent requirement for stability is that all roots z of the polynomial $(z-1)^4\, p_{\mathbf{A}}((z+1)/(z-1))$ fulfil the condition $\mathrm{Re}(z) \leq 0$ (where roots with a vanishing real part have to be simple ones) and the well-known Routh–Hurwitz criterion can be applied.

Modified characteristic equation of the amplification matrix: $a_0 z^4 + a_1 z^3 + a_2 z^2 + a_3 z + a_4 = 0$

where, by adopting $b_s = b_f = ¼$ and, for simplicity, $a_s = a_f = ¼$:

$$a_4 = m_f m_s k_f k_s \Delta t^4$$
$$a_3 = 2m_f m_s(c_s k_f + c_f k_s)\Delta t^3$$
$$a_2 = q_f q_s(m_s k_f + m_f k_s)\Delta t^4 + 4m_f m_s(q_f q_s + c_f c_s + m_s k_f + m_f k_s)\Delta t^2$$
$$a_1 = 2q_f q_s(m_s c_f + m_f c_s)\Delta t^3 + 8m_f m_s(m_s c_f + m_f c_s)\Delta t$$
$$a_0 = q_f^2 q_s^2 \Delta t^4 + 4m_f m_s q_f q_s \Delta t^2 + 16 m_f^2 m_s^2$$

$$\begin{aligned} a_1a_2 - a_0a_3 = {} & 2q_f^2 q_s^2(m_f^2 c_s k_s + m_s^2 c_f k_f)\Delta t^7 \\ & +8q_f q_s m_f m_s((q_f q_s + c_f c_s)(m_s c_f + m_f c_s) \\ & +2(m_f^2 c_s k_s + m_s^2 c_f k_f) + m_f m_s(c_s k_f + c_f k_s))\Delta t^5 \\ & +32 m_f^2 m_s^2((q_f q_s + c_f c_s)(m_s c_f + m_f c_s) + (m_f^2 c_s k_s + m_s^2 c_f k_f))\Delta t^3 \end{aligned}$$

$$\begin{aligned} a_1a_2a_3 - a_0a_3^2 - a_4a_1^2 = {} & 4q_f^2 q_s^2 m_f m_s c_f c_s(m_f k_s - m_s k_f)^2 \Delta t^{10} \\ & +16 q_f q_s m_f^2 m_s^2((c_f c_s + q_f q_s)(m_f c_s + m_s c_f)(c_s k_f + c_f k_s) \\ & +2c_f c_s(m_f^2 k_s^2 + m_s^2 k_f^2) + m_f m_s(c_f k_s - c_s k_f)^2)\Delta t^8 \\ & +64 m_f^3 m_s^3((c_f c_s + q_f q_s)(m_f c_s + m_s c_f)(c_s k_f + c_f k_s) + c_f c_s(m_f k_s - m_s k_f)^2)\Delta t^6 \end{aligned}$$

Since $a_i > 0$ $(i = 0, \ldots, 4)$, $(a_1a_2 - a_0a_3) > 0$ and $(a_1a_2a_3 - a_0a_3^2 - a_4a_1^2) > 0$, stability is observed, according to the Routh–Hurwitz criterion.

For physically undamped models, stability is still observed following the Routh–Hurwitz criterion, once, in this case: $a_0 > 0$, $a_2 > 0$, $a_4 > 0$ and $(a_2^2 - 4a_0a_4) > 0$

Adaptive semi-explicit/explicit time integration procedure

Coupled porodynamic models

The following matrix equations are obtained, once the FEM is applied to spatially discretize the porodynamic model:

$$\mathbf{M}\ddot{\mathbf{U}}(t) + \mathbf{C}\dot{\mathbf{U}}(t) + \mathbf{R}(\mathbf{U}(t)) - \mathbf{Q}\mathbf{P}(t) - \mathbf{F}_u(t) = \mathbf{0}$$
$$\mathbf{Q}^T\dot{\mathbf{U}}(t) + \mathbf{H}\mathbf{P}(t) + \mathbf{S}\dot{\mathbf{P}}(t) - \mathbf{F}_p(t) = \mathbf{0}$$

where

$$\mathbf{M} = \int_\Omega \mathbf{N}_u^T \rho_m \mathbf{N}_u \mathrm{d}\Omega$$

$$\mathbf{C} = \int_\Omega \mathbf{N}_u^T \varsigma \mathbf{N}_u \mathrm{d}\Omega \qquad \mathbf{F}_u(t) = \int_{\Gamma_\tau} \mathbf{N}_u^T \boldsymbol{\tau}(t)\mathrm{d}\Gamma + \int_\Omega \mathbf{N}_u^T \mathbf{b}(t)\mathrm{d}\Omega$$

$$\mathbf{H} = \int_\Omega \nabla\mathbf{N}_p^T \boldsymbol{\kappa} \nabla\mathbf{N}_p \mathrm{d}\Omega \qquad \mathbf{F}_p(t) = \int_{\Gamma_q} \mathbf{N}_p^T q(t)\mathrm{d}\Gamma + \int_\Omega \mathbf{N}_p^T a(t)\mathrm{d}\Omega$$

$$\mathbf{S} = \int_\Omega \mathbf{N}_p^T \frac{1}{Q} \mathbf{N}_p \mathrm{d}\Omega$$

$$\mathbf{Q} = \int_\Omega \mathbf{B}^T \alpha \mathbf{m} \mathbf{N}_p \mathrm{d}\Omega$$

for linear analysis:

$$\mathbf{R}(\mathbf{U}(t)) = \mathbf{K}\mathbf{U}(t) \qquad \mathbf{K} = \int_\Omega \mathbf{B}^T \mathbf{D} \mathbf{B}\, \mathrm{d}\Omega$$

Adaptive semi-explicit/explicit time integration procedure

Coupled porodynamic models

The following matrix equations are obtained, once the FEM is applied to spatially discretize the porodynamic model:

Central Difference Method

$$\ddot{\mathbf{U}}^n = \frac{1}{\Delta t^2}(\mathbf{U}^{n+1} - 2\mathbf{U}^n + \mathbf{U}^{n-1})$$

$$\dot{\mathbf{U}}^n = \frac{1}{2\Delta t}(\mathbf{U}^{n+1} - \mathbf{U}^{n-1})$$

$$\mathbf{M}\ddot{\mathbf{U}}(t) + \mathbf{C}\dot{\mathbf{U}}(t) + \mathbf{R}(\mathbf{U}(t)) - \mathbf{Q}\mathbf{P}(t) - \mathbf{F}_u(t) = \mathbf{0}$$

$$\mathbf{Q}^T\dot{\mathbf{U}}(t) + \mathbf{H}\mathbf{P}(t) + \mathbf{S}\dot{\mathbf{P}}(t) - \mathbf{F}_p(t) = \mathbf{0}$$

Forward Difference Method

$$\dot{\mathbf{U}}^n = \frac{1}{\Delta t}(\mathbf{U}^{n+1} - \mathbf{U}^n)$$

$$\dot{\mathbf{P}}^n = \frac{1}{\Delta t}(\mathbf{P}^{n+1} - \mathbf{P}^n)$$

Solution procedure:

$$(\bar{\mathbf{M}}_e + \tfrac{1}{2}\Delta t\mathbf{C}_e)\mathbf{U}_e^{n+1} = \Delta t^2(\mathbf{F}_{ue}^n - \mathbf{R}_e^n + \mathbf{Q}_e\mathbf{P}_e^n) + \bar{\mathbf{M}}_e(2\mathbf{U}_e^n - \mathbf{U}_e^{n-1}) + \tfrac{1}{2}\Delta t\mathbf{C}_e\mathbf{U}_e^{n-1}$$

$$\bar{\mathbf{S}}_e\mathbf{P}_e^{n+1} = \Delta t(\mathbf{F}_{pe}^n - \mathbf{H}_e\mathbf{P}_e^n) - \mathbf{Q}_e^T(\mathbf{U}_e^{n+1} - \mathbf{U}_e^n) + \bar{\mathbf{S}}_e\mathbf{P}_e^n$$

Adaptive semi-explicit/explicit time integration procedure

Coupled porodynamic models

Solution procedure: $(\bar{\mathbf{M}}_e + \frac{1}{2}\Delta t \mathbf{C}_e)\mathbf{U}_e^{n+1} = \Delta t^2(\mathbf{F}_{ue}^n - \mathbf{R}_e^n + \mathbf{Q}_e\mathbf{P}_e^n) + \bar{\mathbf{M}}_e(2\mathbf{U}_e^n - \mathbf{U}_e^{n-1}) + \frac{1}{2}\Delta t \mathbf{C}_e \mathbf{U}_e^{n-1}$

$$\bar{\mathbf{S}}_e \mathbf{P}_e^{n+1} = \Delta t(\mathbf{F}_{pe}^n - \mathbf{H}_e\mathbf{P}_e^n) - \mathbf{Q}_e^T(\mathbf{U}_e^{n+1} - \mathbf{U}_e^n) + \bar{\mathbf{S}}_e\mathbf{P}_e^n$$

Method 1 – The coupled stabilization matrix is introduced into the solid phase:

$$\bar{\mathbf{S}}_e = \mathbf{S}_e + a_e^p \Delta t \mathbf{H}_e \qquad \bar{\mathbf{M}}_e = \mathbf{M}_e + a_e^u \Delta t^2 \bar{\mathbf{K}}_e \qquad \bar{\mathbf{K}}_e = \mathbf{K}_e^\tau + \mathbf{W}_e^u$$

if $\lambda_e^{\max}\Delta t < 2,\ a_e^p = 0$ if $\bar{\omega}_e^{\max}\Delta t < 2,\ a_e^u = 0$

if $\lambda_e^{\max}\Delta t \geq 2,\ a_e^p = 1$ if $\bar{\omega}_e^{\max}\Delta t \geq 2,\ a_e^u = \frac{1}{4}$

$$\mathbf{W}_e^u = \int_{\Omega_e} \mathbf{B}^T\left[(\alpha\mathbf{m})Q(\alpha\mathbf{m})^T\right]\mathbf{B}\,d\Omega$$

Method 2 – The coupled stabilization matrix is introduced into the fluid phase:

$$\bar{\mathbf{M}}_e = \mathbf{M}_e + a_e^u \Delta t^2 \mathbf{K}_e^\tau \qquad \bar{\mathbf{S}}_e = \mathbf{S}_e + a_e^p \Delta t \bar{\mathbf{H}}_e \qquad \bar{\mathbf{H}}_e = \mathbf{H}_e + \mathbf{W}_e^p$$

if $\omega_e^{\max}\Delta t < 2,\ a_e^u = 0$ if $\bar{\lambda}_e^{\max}\Delta t < 2$ (and $\bar{\lambda}_e^{\max} \neq 0$), $a_e^p = 0$

if $\omega_e^{\max}\Delta t \geq 2,\ a_e^u = \frac{1}{4}$ if $\bar{\lambda}_e^{\max}\Delta t \geq 2$ (or $\bar{\lambda}_e^{\max} = 0$), $a_e^p = 1$

$$\mathbf{W}_e^p = \Delta t \int_{\Omega_e} \nabla\mathbf{N}_p^T \frac{\alpha^2}{\rho_m} \nabla\mathbf{N}_p\,d\Omega$$

Adaptive semi-explicit/explicit time integration procedure

Coupled porodynamic models

Stability analysis, considering an equivalent group of scalar equations:

$$m\ddot{u} + c\dot{u} + \eta k u - qp - f_u = 0$$

$$q\dot{u} + hp + s\dot{p} - f_p = 0$$

Recursive relationship:

$$\begin{bmatrix} u^{n+1} \\ u^{n} \\ p^{n+1} \end{bmatrix} = \begin{bmatrix} A_{11} & A_{12} & A_{13} \\ A_{21} & A_{22} & A_{23} \\ A_{31} & A_{32} & A_{33} \end{bmatrix} \begin{bmatrix} u^{n} \\ u^{n-1} \\ p^{n} \end{bmatrix} + \begin{bmatrix} L_1 \\ L_2 \\ L_3 \end{bmatrix} = \mathbf{A} \begin{bmatrix} u^{n} \\ u^{n-1} \\ p^{n} \end{bmatrix} + \mathbf{L}$$

Method 1:

$$A_{11} = 2(2ms + (2a^u - \eta)ks\Delta t^2 + 2a^u q^2 \Delta t^2)/\Lambda$$

$$A_{12} = -(2ms - cs\Delta t + 2a^u ks\Delta t^2 + 2a^u q^2 \Delta t^2)/\Lambda$$

$$A_{13} = 2qs\Delta t^2/\Lambda$$

$$A_{21} = 1 \qquad A_{22} = 0 \qquad A_{23} = 0$$

$$A_{31} = -q(2ms - cs\Delta t + 2(a^u - \eta)ks\Delta t^2 + 2a^u q^2 \Delta t^2)/\mathrm{A}$$

$$A_{32} = q(2ms - cs\Delta t + 2a^u ks\Delta t^2 + 2a^u q^2 \Delta t^2)/\mathrm{A}$$

$$\begin{aligned} A_{33} = {} & (2ms^2 + (cs + 2(a^p - 1)mh)s\Delta t \\ & + (2a^u ks + (a^p - 1)ch + 2(a^u - 1)q^2)s\Delta t^2 \\ & + 2a^u((a^p - 1)ks + 2(a^p - 1)q^2)h\Delta t^3)/\mathrm{A} \end{aligned}$$

where:

$$\Lambda = 2ms + cs\Delta t + 2a^u ks\Delta t^2 + 2a^u q^2 \Delta t^2$$

$$\mathrm{A} = \Lambda\,(s + a^p h\Delta t)$$

Method 2:

$$A_{11} = 2(2m + (2a^u - \eta)k\Delta t^2)/\Lambda$$

$$A_{12} = -(2m - c\Delta t + 2a^u k\Delta t^2)/\Lambda$$

$$A_{13} = 2q\Delta t^2/\Lambda$$

$$A_{21} = 1 \qquad A_{22} = 0 \qquad A_{23} = 0$$

$$A_{31} = -qm(2m - c\Delta t + 2(a^u - \eta)k\Delta t^2)/\mathrm{A}$$

$$A_{32} = qm(2m - c\Delta t + 2a^u k\Delta t^2)/\mathrm{A}$$

$$\begin{aligned} A_{33} = {} & (2sm^2 + (cs + 2(a^p - 1)mh)m\Delta t \\ & + (2a^u ks + (a^p - 1)ch + 2(a^u - 1)q^2)m\Delta t^2 \\ & + (2a^u(a^p - 1)mkh + a^p cq^2)\Delta t^3 + 2a^u a^p kq^2 \Delta t^4)/\mathrm{A} \end{aligned}$$

where:

$$\Lambda = 2m + c\Delta t + 2a^u k\Delta t^2$$

$$\mathrm{A} = \Lambda\,(ms + a^p mh\Delta t + a^p q^2 \Delta t^2)$$

Adaptive semi-explicit/explicit time integration procedure

Coupled porodynamic models

The roots λ of the characteristic polynomial $p_{\mathbf{A}}(\lambda)$ of the amplification matrix **A** determine the stability properties of the method. In order to ensure stability, the modulus of all these roots must be less or equal to one (when the modulus is unity, the root must be a simple one). If λ is replaced by $(z+1)/(z-1)$, the equivalent requirement for stability is that all roots z of the polynomial $(z-1)^3\, p_{\mathbf{A}}((z+1)/(z-1))$ fulfil the condition $\mathrm{Re}(z) \leq 0$ (where roots with a vanishing real part have to be simple ones) and the well-known Routh–Hurwitz criterion can be applied.

Modified characteristic equation of the amplification matrix: $a_0 z^3 + a_1 z^2 + a_2 z + a_3 = 0$

where, by adopting $a^u = 1/4$ and $a^p = 1$:

Method 1:

$$a_0 = ((1-\eta)ks + q^2)mh\Delta t^3 + 2(1-\eta)kms^2\Delta t^2 + 4shm^2\Delta t + 8m^2s^2$$

$$a_1 = ((1-\eta)ks + q^2)mh\Delta t^3 + 2mcsh\Delta t^2 + (4cs + 4mh)ms\Delta t$$

$$a_2 = m\eta ksh\Delta t^3 + 2(ch + \eta ks + q^2)ms\Delta t^2$$

$$a_3 = m\eta ksh\Delta t^3$$

$$a_1a_2 - a_0a_3 = 2(cksh + (ch + ks + q^2)q^2)mshq^2\Delta t^5 + 4(ch + 2\eta ks + q^2)chm^2s^2\Delta t^4 + 8(shc^2 + mch^2 + c\eta ks^2 + (cs + mh)q^2)m^2s^2\Delta t^3$$

Method 2:

$$a_0 = 2(1-\eta)ksq^2\Delta t^4 + (1-\eta)ksmh\Delta t^3 + 2((1-\eta)ks + 3q^2)ms\Delta t^2 + 4shm^2\Delta t + 8m^2s^2$$

$$a_1 = ((1-\eta)kmh + 4cq^2)s\Delta t^3 + 2mcsh\Delta t^2 + (4cs + 4mh)ms\Delta t$$

$$a_2 = 2\eta ksq^2\Delta t^4 + m\eta ksh\Delta t^3 + 2(ch + \eta ks + q^2)ms\Delta t^2$$

$$a_3 = m\eta ksh\Delta t^3$$

$$a_1a_2 - a_0a_3 = 8c\eta ks^2q^4\Delta t^7 + mc\eta khs^2q^2\Delta t^6 + 2(mckh^2 + (mkh + 4hc^2 + 8c\eta ks + 4cq^2)q^2)ms^2\Delta t^5 + 4(ch + 2\eta ks + q^2)chm^2s^2\Delta t^4 + 8(shc^2 + mch^2 + c\eta ks^2 + (cs + mh)q^2)m^2s^2\Delta t^3$$

Since $a_i > 0 \ (i = 0, \ldots, 3)$ and $(a_1a_2 - a_0a_3) > 0$,

the proposed methods are stable for linear analyses ($\eta = 1$) according to the Routh–Hurwitz criterion. In addition, stability is expected for nonlinear analyses if the tangent stiffness matrix of the model is recurrently updated ($\eta \equiv 1$) or if the tangent matrix is not updated and reduced stiffness develops due to the nonlinear behaviour ($0 < \eta \leq 1$), which is a usual configuration considering several common applications regarding porous models.

Numerical applications considering semi-explicit/explicit analyses

Lamb's problem (axisymmetric solution):

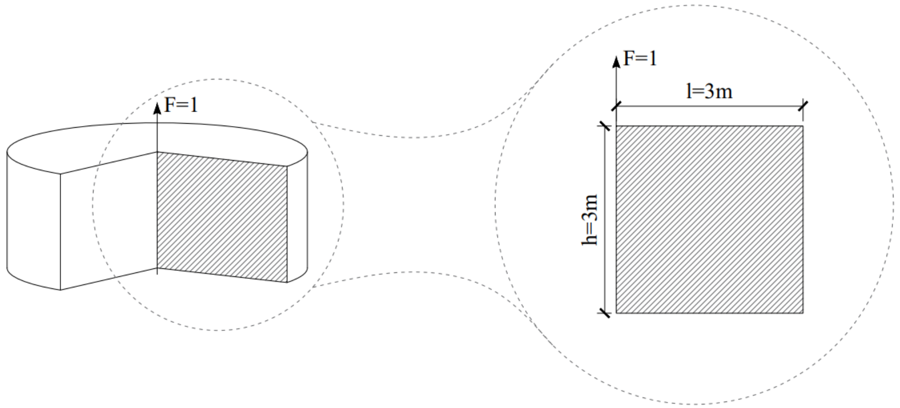

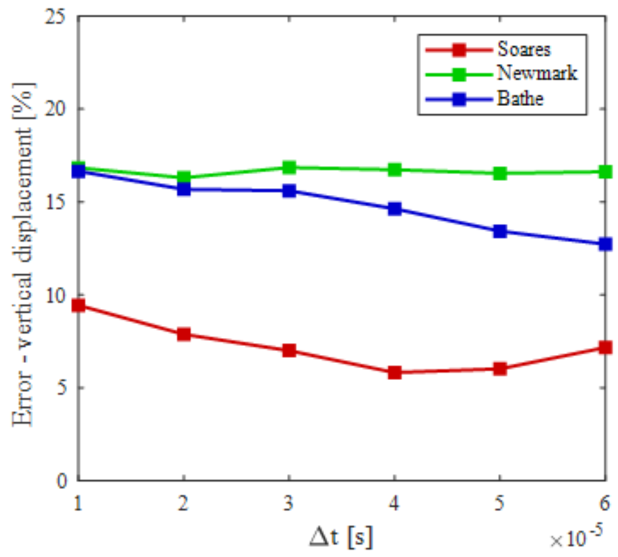

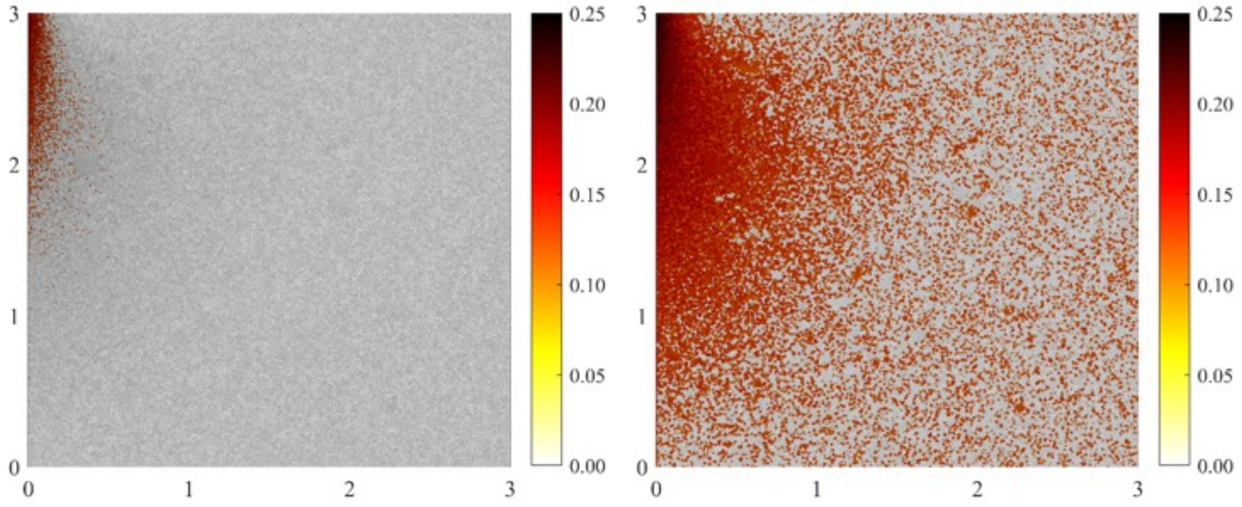

Computed a_e values along the discretized model (semi-explicit elements are colored and explicit elements are white): Δt = 3.10^{-5} s (left); Δt = 5.10^{-5} s (right).

Adopted time-steps and corresponding domain decomposition.

Time-step (10^{-5}s)	Explicit elements	Semi-explicit elements
1	128557 (100%)	0 (0%)
2	127904 (99.49%)	653 (0.51%)
3	121503 (94.51%)	7054 (5.49%)
4	103388 (80.42%)	25169 (19.58%)
5	57968 (45.09%)	70589 (54.91%)

Numerical applications considering semi-explicit/explicit analyses

Lamb's problem (axisymmetric solution):

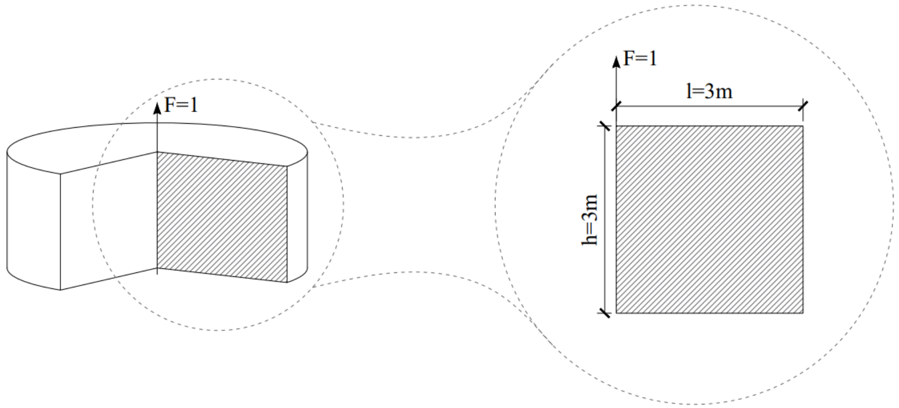

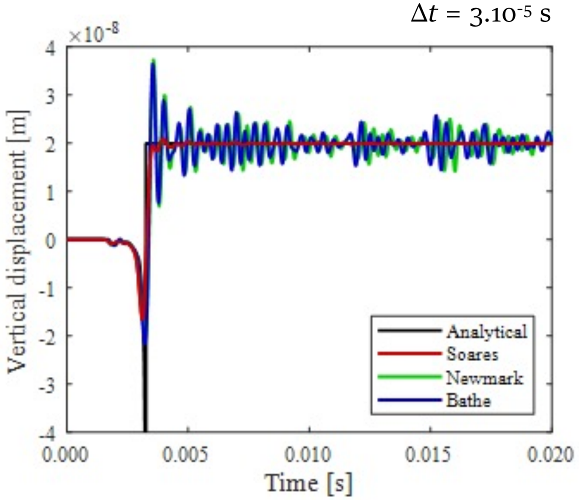

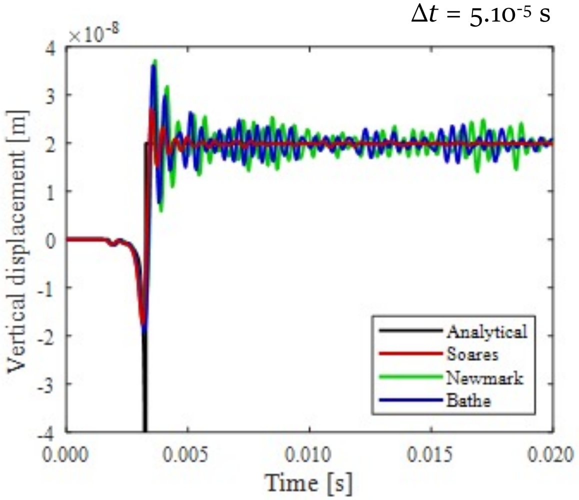

CPU times and relative error results for the selected techniques and time-step values

Δt (10^{-5} s)	Method	δ_{vert} (%)	δ_{hor} (%)	CPU time (s)
1	Soares	9.44 (1.00)	16.50 (1.00)	1905 (1.00)
	Newmark	16.83 (1.78)	26.08 (1.58)	5457 (2.86)
	Bathe	16.65 (1.76)	25.98 (1.57)	11437 (6.00)
2	Soares	7.87 (1.00)	18.57 (1.00)	957 (1.00)
	Newmark	16.30 (2.07)	26.49 (1.43)	2535 (2.65)
	Bathe	15.67 (1.99)	25.92 (1.40)	5370 (5.61)
3	Soares	7.00 (1.00)	17.92 (1.00)	769 (1.00)
	Newmark	16.85 (2.41)	26.00 (1.45)	1768 (2.30)
	Bathe	15.60 (2.23)	24.50 (1.37)	3869 (5.03)
4	Soares	5.81 (1.00)	18.90 (1.00)	645 (1.00)
	Newmark	16.73 (2.88)	26.91 (1.42)	1120 (1.74)
	Bathe	14.63 (2.52)	24.06 (1.27)	2468 (3.83)
5	Soares	6.02 (1.00)	20.36 (1.00)	789 (1.00)
	Newmark	16.54 (2.75)	27.48 (1.35)	887 (1.12)
	Bathe	13.43 (2.23)	23.61 (1.16)	1899 (2.41)

Numerical applications considering semi-explicit/explicit analyses

Coupled soil/structure model:

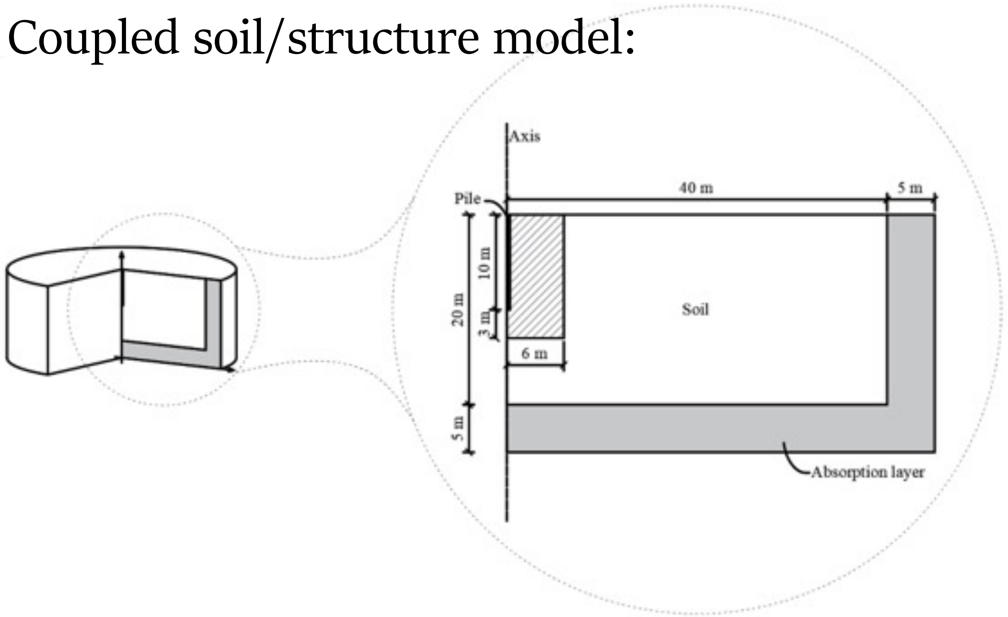

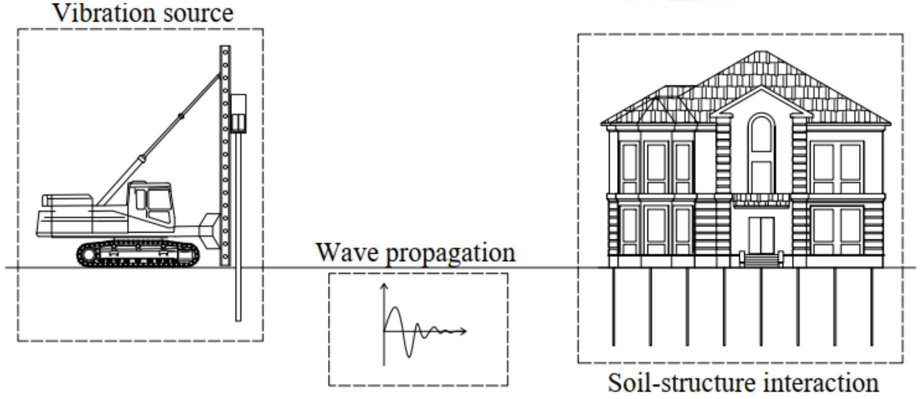

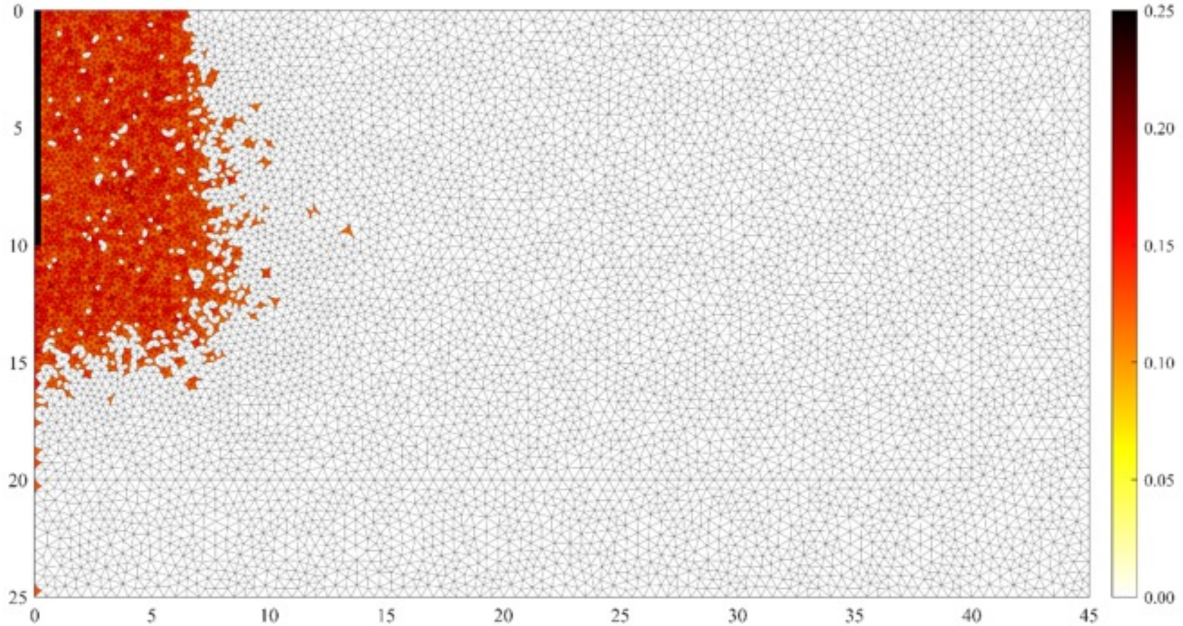

Numerical soil-structure coupled model for a pile penetration depth of 10 [m]

Number of modified elements for each penetration depth

	$h_1 = 2\ [m]$	$h_2 = 5\ [m]$	$h_3 = 10\ [m]$
Modified	2181 (15.2%)	3113 (20.5%)	4337 (27.1%)
Unmodified	12204 (84.8%)	12104 (79.5%)	11680 (72.9%)

Numerical applications considering semi-explicit/explicit analyses

Coupled soil/structure model:

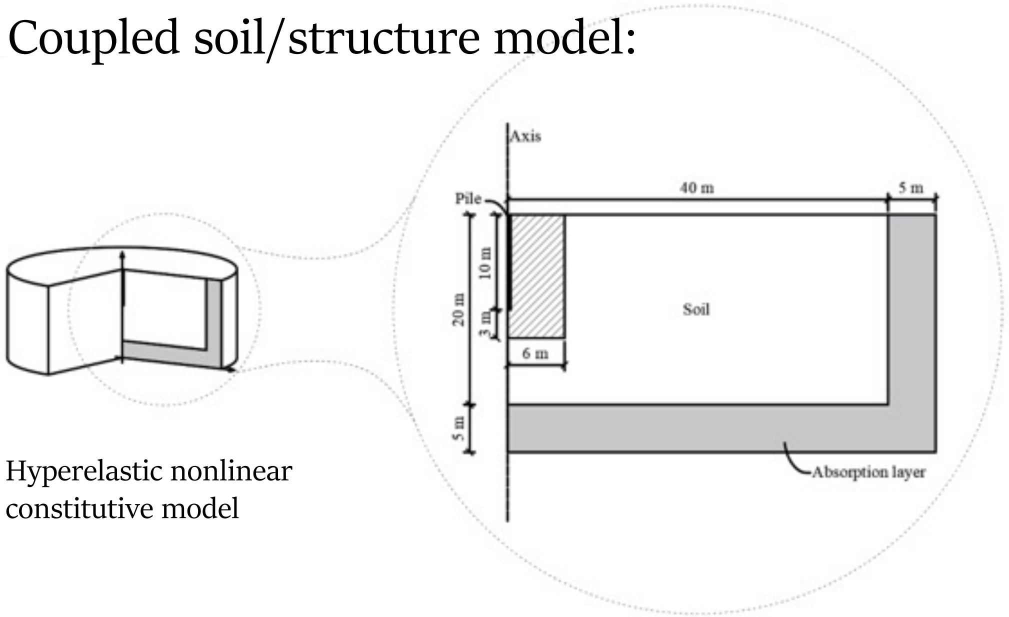

Hyperelastic nonlinear
constitutive model

CPU times (in seconds) for the studied scenarios.

		$h_1 = 2\ [m]$	$h_2 = 5\ [m]$	$h_3 = 10\ [m]$
Linear	New	59.8 (1.00)	67.8 (1.00)	76.6 (1.00)
	Newmark	76.4 (1.28)	82.0 (1.21)	89.3 (1.17)
Nonlinear	New	79.6 (1.00)	84.5 (1.00)	93.9 (1.00)
	Newmark	450.3 (5.66)	480.5 (5.68)	445.9 (4.75)

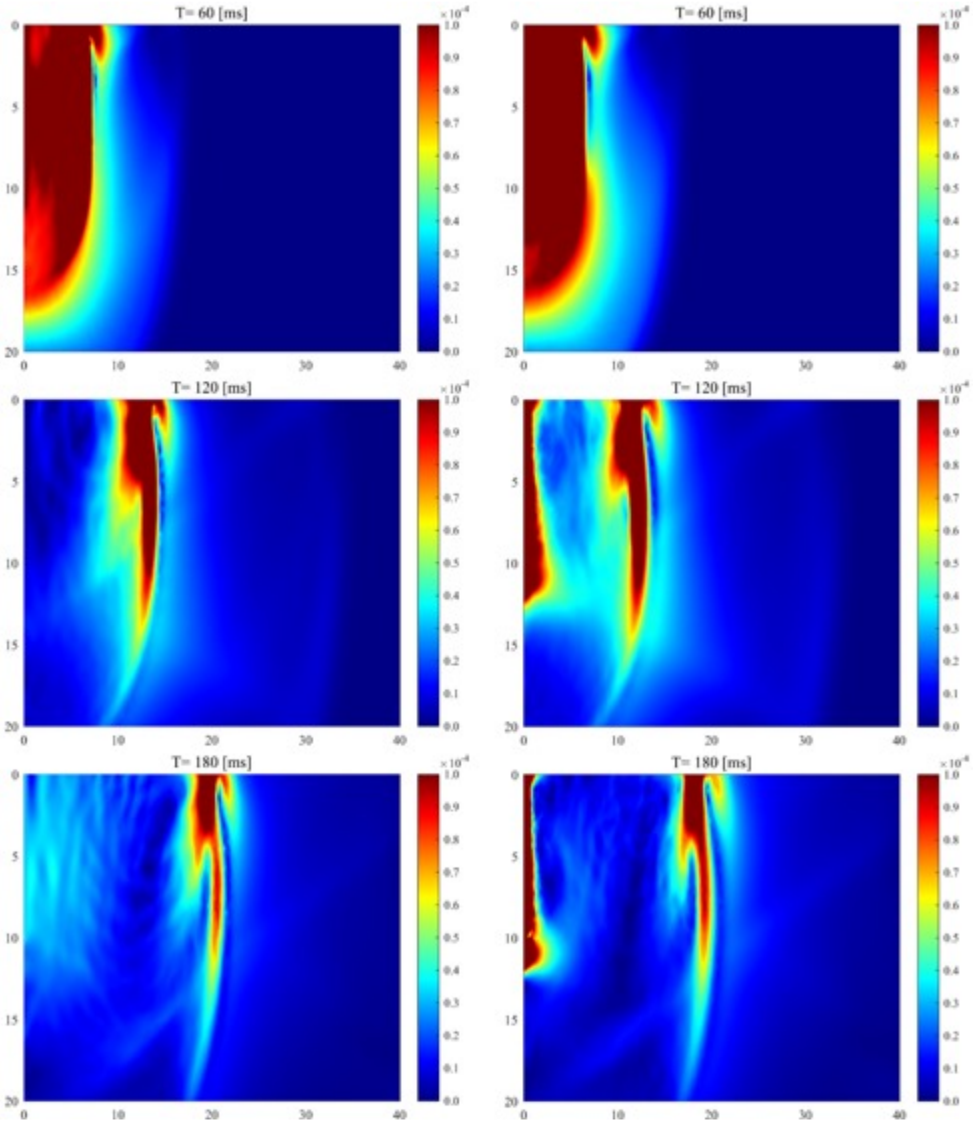

Snapshots for the norms of the displacements considering linear (left) and nonlinear (right) analyses

Numerical applications considering semi-explicit/explicit analyses

Coupled acoustic/elastodynamic model:

Amount of unmodified and modified elements for the coupled water–riser model.

	$a_e = 0$	$a_e \neq 0$	$b_e = 0$	$b_e \neq 0$
Subdomain 1	4 989	0	4 571	418
Subdomain 2	48 900	2	46 938	1964
Subdomain 3	66 294	0	64 726	1568
Subdomain 4	53	3 712	2 851	914
Subdomain 5	1 292	12 024	10 280	3036

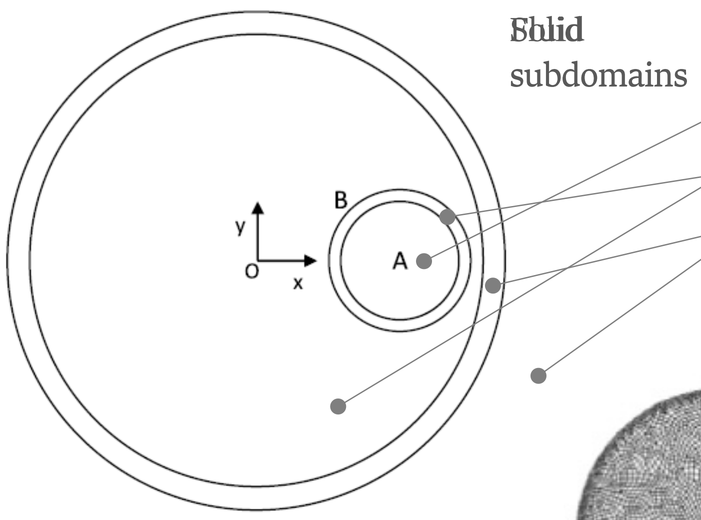

Sketch of the coupled water–riser model

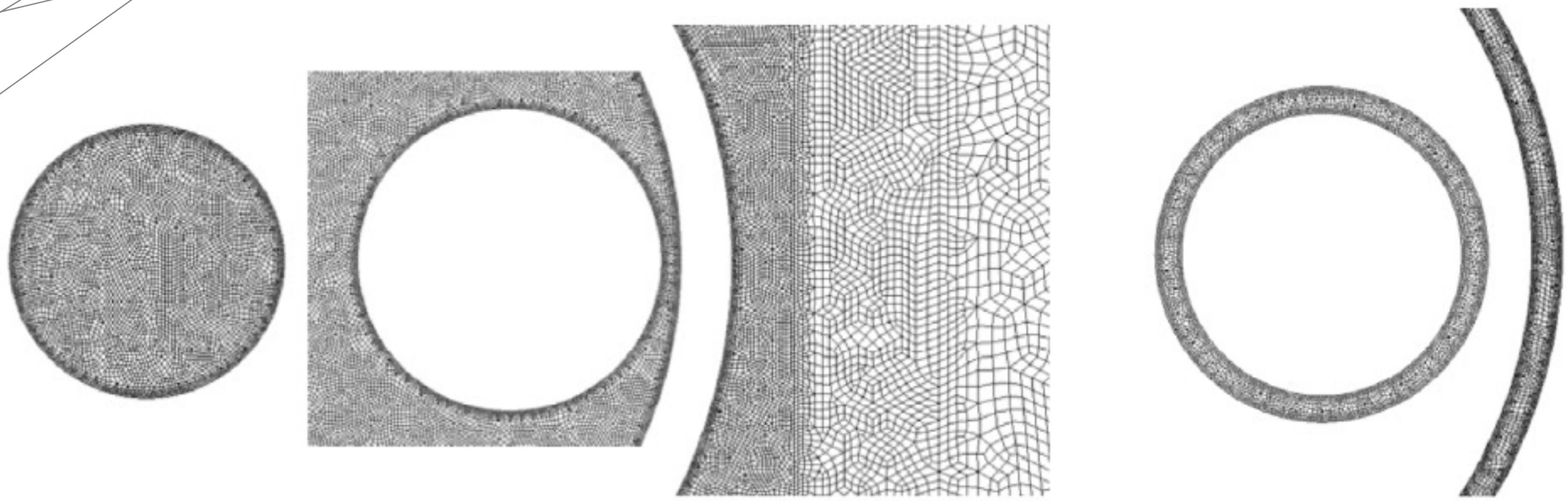

Partial views of the adopted spatial discretizations: fluid subdomains (left); solid subdomains (right)

Numerical applications considering semi-explicit/explicit analyses

Coupled acoustic/elastodynamic model:

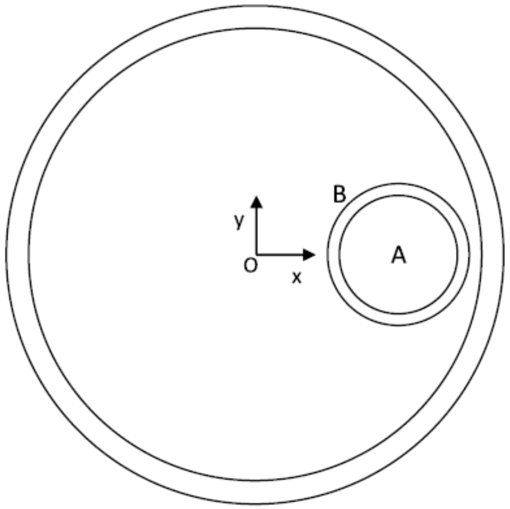

Amount of unmodified and modified elements for the coupled water–riser model.

	$a_e = 0$	$a_e \neq 0$	$b_e = 0$	$b_e \neq 0$
Subdomain 1	4 989	0	4 571	418
Subdomain 2	48 900	2	46 938	1964
Subdomain 3	66 294	0	64 726	1568
Subdomain 4	53	3 712	2 851	914
Subdomain 5	1 292	12 024	10 280	3036

The CPU time of the new technique was approximately 14% of that of the standard CDM; i.e., solution was evaluated by the new approach more than 7 times faster than by the CDM.

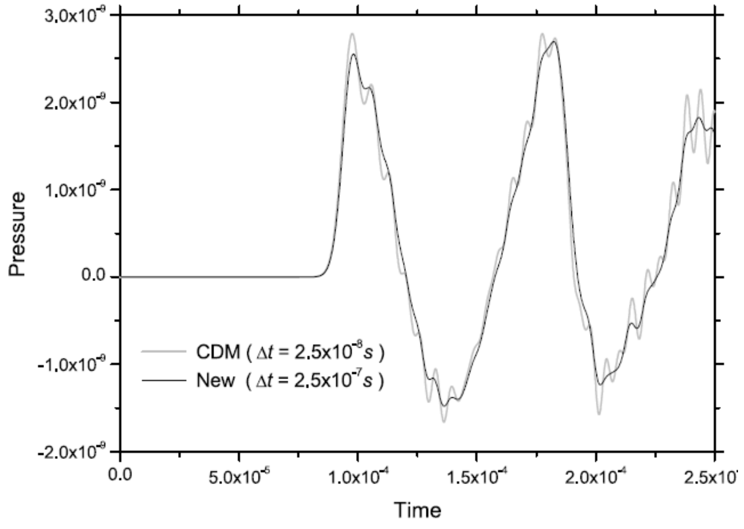

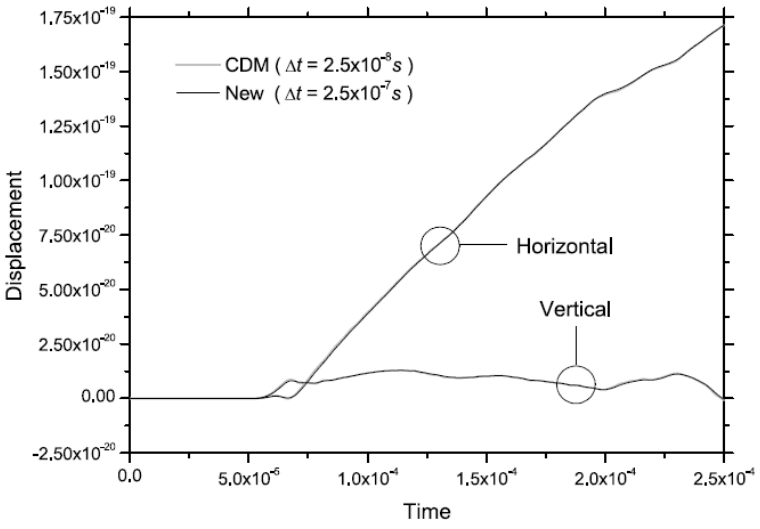

Computed hydrodynamic pressures at point A (left) and displacements at point B (right).

Numerical applications considering semi-explicit/explicit analyses

Coupled acoustic/elastodynamic model:

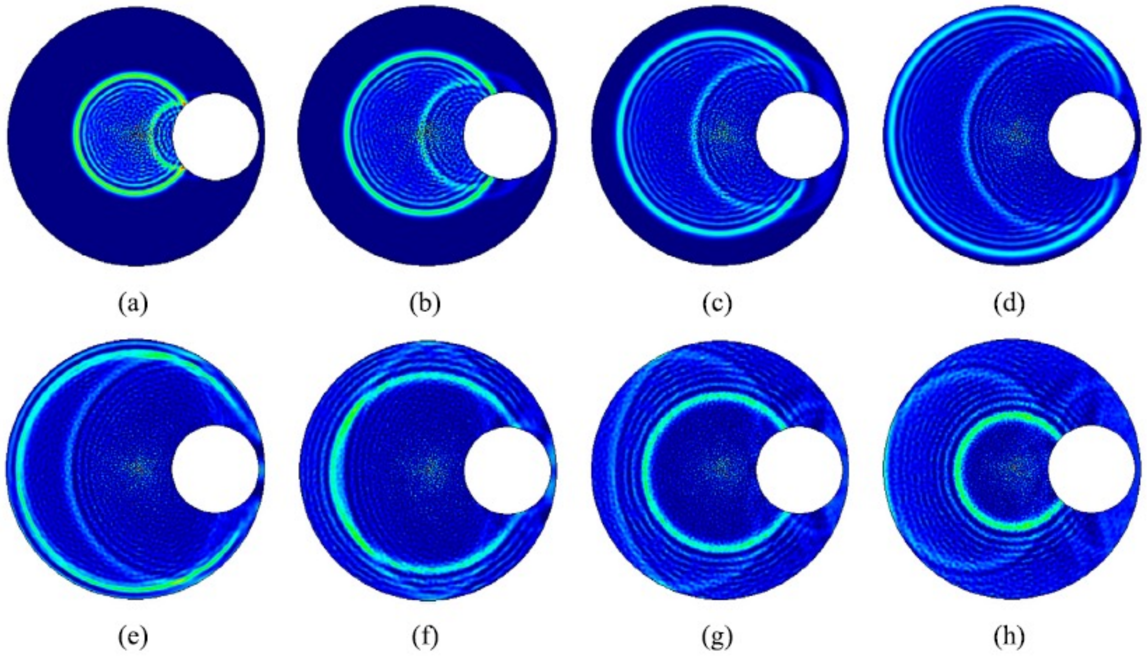

Computed hydrodynamic pressures (subdomain 2) considering the standard CDM with $\Delta t = 2.5\text{x}10^{-8}$ s: (a) $t = 0.75\text{x}10^{-4}$ s; (b) $t = 1.00\text{x}10^{-4}$ s; (c) $t = 1.25\text{x}10^{-4}$ s; (d) $t = 1.50\text{x}10^{-4}$ s; (e) $t = 1.75\text{x}10^{-4}$ s; (f) $t = 2.00\text{x}10^{-4}$ s; (g) $t = 2.25\text{x}10^{-4}$ s; (h) $t = 2.50\text{x}10^{-4}$ s.

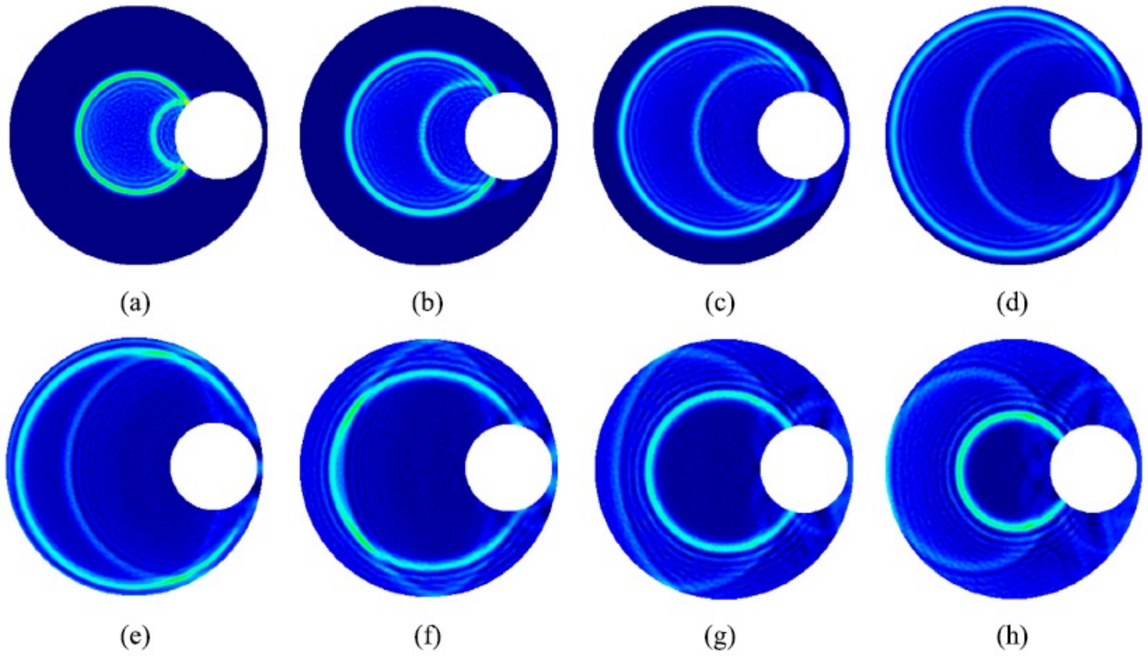

Computed hydrodynamic pressures (subdomain 2) considering the new approach with $\Delta t = 2.5\text{x}10^{-7}$ s: (a) $t = 0.75\text{x}10^{-4}$ s; (b) $t = 1.00\text{x}10^{-4}$ s; (c) $t = 1.25\text{x}10^{-4}$ s; (d) $t = 1.50\text{x}10^{-4}$ s; (e) $t = 1.75\text{x}10^{-4}$ s; (f) $t = 2.00\text{x}10^{-4}$ s; (g) $t = 2.25\text{x}10^{-4}$ s; (h) $t = 2.50\text{x}10^{-4}$ s.

Numerical applications considering semi-explicit/explicit analyses

Coupled porodynamic model:

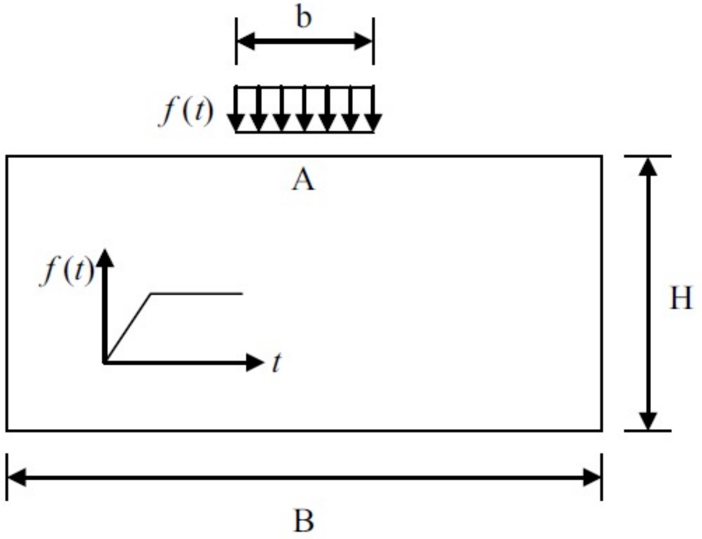

Sketch of the soil strip.
Two elastoplastic models are considered (Model 1 and Model 2).

Method	Model	Percentage of CPU time (new/standard) (%)
1	1	9.66
	2	0.98
2	1	5.01
	2	0.52

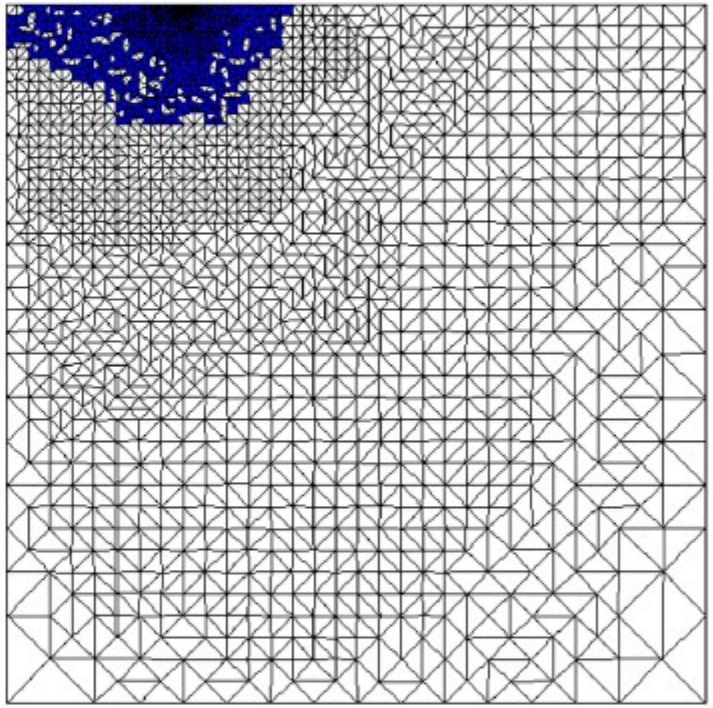

Modified elements along the mesh
(considering the solid phase of method 2)

Numerical applications considering semi-explicit/explicit analyses

Coupled porodynamic model:

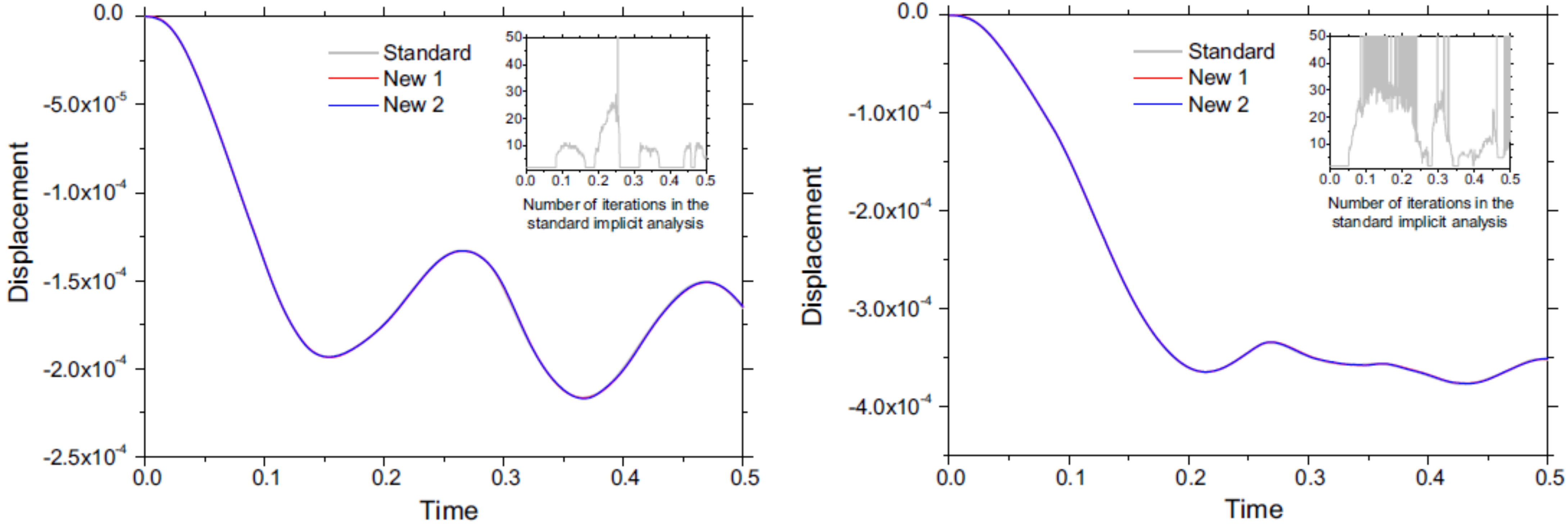

Time history results for the vertical displacements at point A of the soil strip for model 1 (left) and model 2 (right).

Numerical applications considering semi-explicit/explicit analyses

Coupled porodynamic model:

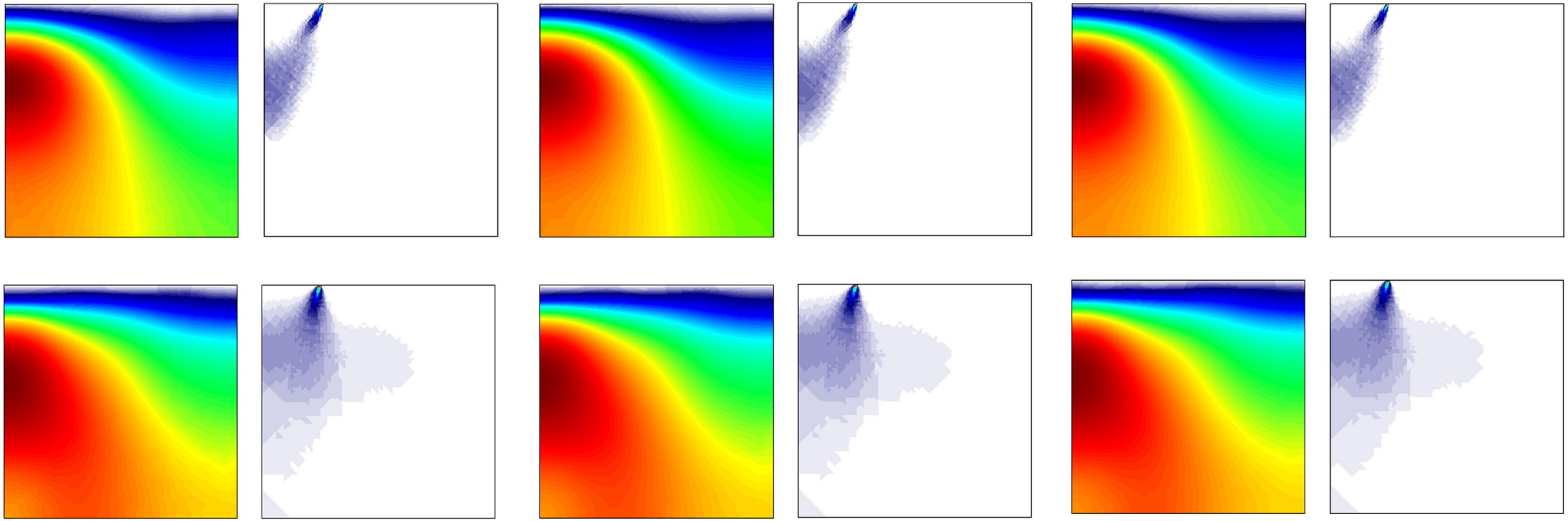

Computed pore-pressures and equivalent plastic strains along the discretised domain at time instant t = 0.5 s, for model 1 (top) and model 2 (bottom): new method 1 (left); new method 2 (middle); and standard procedure (right).

Conclusions

Several adaptive time integration procedures have been briefly presented and discussed, reporting the main aspects of their formulations and illustrating their basic performances.

Conclusions

The main features of the discussed adaptive time integration procedures may be summarized as follows:

- They stand as simple, easy to implement and to apply, single-step procedures;
- Most of the discussed techniques describe truly self-starting formulations;
- They are locally defined and they may self-adjust according to the properties of the discretized model, as well as to the behavior of the computed responses;
- They consider a link between the adopted temporal and spatial discretization procedures, allowing their errors to be better counterbalanced and enhanced accuracy provided;
- They self-adapt to enable stable analyses;
- They provide advanced controllable algorithmic dissipation in higher modes by considering adaptive calculations associated to a proper “tracking” of the higher-frequency range of the model;

Conclusions

The main features of the discussed adaptive time integration procedures may be summarized as follows:

- They consider single-solver frameworks based on reduced, or nonexistent (in case of explicit approaches), systems of equations;
- They may become equivalent to or always more accurate than classical time integration procedures (such as the CD, the TR etc.), considering specific configurations;
- They enable mixed analyses by just employing a single group of recurrence relationships, avoiding elaborated coupling procedures and/or interface treatments;
- They may become very effective to analyse complex models, such as those regarding nonlinear multiphysic applications;
- They are extremely versatile and entirely automated, requiring no decision nor effort from the user.

Conclusions

As one can observe, these adaptive techniques may stand as very effective procedures to numerically analyse space-time PDEs, providing the main positive features that are required from a competitive time integration method.

References

Soares, D.; An enhanced explicit-implicit time-marching formulation based on fully-adaptive time-integration parameters. COMPUTER METHODS IN APPLIED MECHANICS AND ENGINEERING, v. 403, p. 115711, 2023.

Soares, D.; An improved adaptive formulation for explicit analyses of wave propagation models considering locally-defined self-adjustable time-integration parameters. COMPUTER METHODS IN APPLIED MECHANICS AND ENGINEERING, v. 399, p. 115324, 2022.

Soares, D.; Godinho, L.; Nonlinear porodynamic analysis by adaptive semi-explicit/explicit time marching formulations. ACTA GEOTECHNICA, v.16, p. 1879–1894, 2021

Sofiste, T. V. ; Godinho, L. ; Alves-Costa, P. ; Soares, D.; Colaco, A.; Numerical modelling for prediction of ground-borne vibrations induced by pile driving. ENGINEERING STRUCTURES, v. 242, p. 112533, 2021.

Pinto, L. R. ; Soares, D.; Mansur W.J.; Elastodynamic wave propagation modelling in geological structures considering fully-adaptive explicit time-marching procedures. SOIL DYNAMICS AND EARTHQUAKE ENGINEERING, v. 150, p. 106962, 2021.

Soares, D.; A stabilized explicit approach to efficiently analyse wave propagation through coupled fluid-structure models. COMPUTER METHODS IN APPLIED MECHANICS AND ENGINEERING, v. 356, p. 528-547, 2019.

Soares, D.; An adaptive semi-explicit/explicit time marching technique for nonlinear dynamics. COMPUTER METHODS IN APPLIED MECHANICS AND ENGINEERING, v. 354, p. 637-662, 2019.

Soares, D.; A model/solution-adaptive explicit-implicit time marching technique for wave propagation analysis. INTERNATIONAL JOURNAL FOR NUMERICAL METHODS IN ENGINEERING, v. 119, p. 590-617, 2019.

Soares, D. A simple and effective single-step time marching technique based on adaptive time integrators. INTERNATIONAL JOURNAL FOR NUMERICAL METHODS IN ENGINEERING, v. 109, p. 1344-1368, 2017.

Soares, D.; A simple and effective new family of time marching procedures for dynamics. COMPUTER METHODS IN APPLIED MECHANICS AND ENGINEERING, v. 283, p. 1138-1166, 2015.

References

Comparative techniques:

Noh, G.; Bathe, K.J.; An explicit time integration scheme for the analysis of wave propagations. COMPUTERS & STRUCTURES, v. 129, p. 178-193, 2013.

Bathe, K.J.; Baig, M.M.I.; On a composite implicit time integration procedure for nonlinear dynamics. COMPUTERS & STRUCTURES, v. 83, p.2513-2524, 2005.

Hulbert, G.M.; Chung, J.; Explicit time integration algorithms for structural dynamics with optimal numerical dissipation. COMPUTER METHODS IN APPLIED MECHANICS AND ENGINEERING, v. 137, p. 175-188, 1996.

Chung J., Hulbert J.M.; A time integration method for structural dynamics with improved numerical dissipation: the generalized α method. JOURNAL OF APPLIED MECHANICS, v. 30, p. 371–375, 1993.

Newmark N.M.; A method of computation for structural dynamics. JOURNAL ENGINEERING MECHANICS DIVISION, ASCE, v. 85, p. 67–94, 1959.

Thank you for your attention.